Theoretical study of the interaction of agonists with the 5-HT_{2A} receptor

Dissertation

zur Erlangung des Doktorgrades
der Naturwissenschaften (Dr. rer. nat)
der Fakultät für Chemie und Pharmazie
der Universität Regensburg

vorgelegt von
Maria Elena Silva
aus Buccinasco

Regensburg 2008

Die vorliegende Arbeit wurde in der Zeit von Oktober 2004 bis August 2008 an der Fakultät für Chemie und Pharmazie der Universität Regensburg in der Arbeitsgruppe von Prof. Dr. A. Buschauer unter der Leitung von Prof. Dr. S. Dove angefertigt

Die Arbeit wurde angeleitet von:	Prof. Dr. S. Dove
Promotiongesucht eingereicht am:	28. Juli 2008
Promotionkolloquium am	26. August 2008
Prüfungsausschuß:	Vorsitzender: Prof. Dr. A. Buschauer 1. Gutachter: Prof. Dr. S. Dove 2. Gutachter: Prof. Dr. S. Elz 3. Prüfer: Prof. Dr. H.-A. Wagenknecht

Contents

Chapter 1
Introduction

1.1 G protein coupled receptors

G protein coupled receptors (GPCRs), also known as seven transmembrane (7TM) receptors, represent the largest protein superfamily of cell surface receptors involved in signal transduction. GPCRs are activated by an external signal in the form of a ligand or, in the case of rhodopsin, a photon. Both induce a conformational change in the receptor and, by this, the intracellular transduction of the signal via the G protein and second transmitters to subsequent pathways modulating cellular responses.
GPCRs are found only in eukaryotes, including yeast, plants and choanoflagellates (King et al., 2003). They are extremely versatile receptors. About 800 different GPCRs in human respond to a wide variety of activating ligands: biogenic amines, purines and nucleic acid derivatives, lipids, peptides and proteins, organic odorants and pheromones, tastants, ions like calcium and protons, and even to photons (Jacoby et al., 2006). Just as diverse are the modulated physiological processes: neurotransmission, secretion, cellular metabolism, differentiation and growth, inflammatory and immune responses, taste and odor. Therefore, GPCRs represent the major target class (30% of all targets investigated so far) for the design of new drugs for pharmacological intervention. Around 30% of all marketed drugs act on GPCRs as agonists or antagonists, activating and blocking the receptor, respectively (Hebert and Bouvier, 1998). On the other hand, 40 to 50% of the current drug target are GPCRs (Drews, 2000; Jacoby et al., 2006). In the human genome project (Consortium, 2004) more than 800 genes (about 2% of the genome) have been identified that belong to the GPCR superfamily (Fredriksson and Schiöth, 2005),

most being orphan receptors having no as yet identified ligand. In conclusion, this class of proteins is historically the most successful therapeutic target family (Hopkins and Groom, 2002).

To classify a protein as GPCR depends on two essential requirements: the first concerns the presence of seven sequence stretches of about 25 to 30 amino acids with a relatively high degree of hydrophobicity. These sequences form seven α-helices, the so-called transmembrane (TM) domain, that span the plasma membrane in a counter-clockwise order when viewed from the extracellular side. The presence of extracellular and/or intra-TM ligand binding sites and sufficient conformational flexibility to swith from inactive to active states enable signal transduction from outside to inside the cell. The second principal requirement is the capability of the receptor to interact with a particular heterotrimeric G protein. However, the term 7TM receptor is more technically correct because the coupling with a G protein has not been demonstrated for a number of GPCRs whose genes have recently been sequenced (Fredriksson and Schiöth, 2003), and not all receptors that activate a G protein are members of the GPCR superfamily (e.g. receptors for epidermal growth factor, insulin, insulin-like growth factor-I and II) (Iismaa et al., 1995; Kuemmerle and Murthy, 2001).

1.1.1 GPCR classification

Several approaches have been used to classify this superfamily, some of these are based on the native ligands, on phylogenetic analysis of the amino acid sequences, on clustering of the genes in the human genome and on physiological and structural features. One of the most frequently used systems used clans or classes to group the GPCRs. Following this classification the GPCRs can be grouped into six classes based on sequence homology and functional similarity: A, B, C, D, E and F. Subclasses are assigned by roman numbers (Attwood and Findlay, 1994; Foord et al., 2005; http://www.ebi.ac.uk/interpro/ISearch?query=gpcr; Kolakowski, 1994). These classes try to cover all GPCRs in vertebrates and invertebrates (Table 1.1).

Table 1.1: Classification of GPCRs in vertebrates and invertebrates

Class A	(Rhodopsin-like)
I	*Chemokine receptor, GPR137B*
II	*Chemokine , Interleukin-8, Adrenomedullin receptors, Duffy blood group, chemokine receptorG, Protein-coupled Receptor 30*
III	*Angiotensin II , Bradykinin receptor , GPR15, 25*
IV	*Opioid , Somatostatin , neuropeptide, orphan , DEZ orphan receptors, GPR1*
V	*Galanin , Cysteinyl leukotriene, Leukotriene B4 , Relaxin , KiSS1-derived peptide , Melanin-concentrating hormone 1Urotensin-II receptors*
VI	*GPR40-related , P2 purinoceptor, GPR31, 81, 82, 109B, Oxoglutarate (alpha-ketoglutarate) receptor 1, Succinate receptor 1*
VII	*P2 purinoceptor, Protease-activated receptor, Epstein-Barr virus induced gene 2 (lymphocyte-specific G protein-coupled receptor), GPR4, 17, 18, 20, 23, 35, 55, 65, 68, 132, Coagulation factor II receptor*
VIII	*P2 purinoceptor, GPR34, 87, 171, Platelet-activating factor receptor*
IX	*Cannabinoid , Lysophosphatidic acid , Sphingosine 1-phosphate, Melanocortin/ACTH receptors, GPR3, 6, 12*
X	*Opsins*
XI	*Eicosanoid receptor*
XII	*Cholecystokinin , Neuropeptide FF , Orexin, Vasopressin r, Gonadotrophin releasing hormone receptors, GPR22, 103, 176*
XIII	*Melatonin, Neurokinin, Neuropeptide Y, Prolactin-releasing peptide, Prokineticin receptors, 1GPR19, 50, 75, 83*
XIV	*Bombesin, Endothelin , Neuromedin U, Neurotensin r, Thyrotropin-releasing hormone, Growth hormone secretagogue, Motilin receptors,GPR39*
XV	*5-Hydroxytryptamine (5-$HT_{2,6}$), Adrenergic, Dopamine, OctopamineTrace amine, Histamine H_2 receptors*
XVI	*Histamine $H_{1,3,4}$, Adenosine, Muscarinic acetylcholine receptors, GPR21, 45, 52, 61, 62, 63, 78, 84, 85, 88, 101, 161, 173*
XVII	*5-Hydroxytryptamine (5-$HT_{1,4,5A,7}$) receptor*
XVIII	*Anaphylatoxin, Formyl peptide receptors, MAS1 oncogene, GPR1, 32, 44, 77*
XIX	*Glycoprotein hormone receptor, Leucine-rich repeat-containing G protein-coupled receptor 4*
Class B	(Secretin receptor family)
I	*Adenylate cyclase-activating type 1, pituitary, Calcitonin, Corticotropin-releasing hormone, Glucagon receptor-related, Growth hormone releasing hormone, Parathyroid hormone, Secretin, Vasoactive intestinal peptide receptors*
II	*Brain-specific angiogenesis inhibitor, CD97 antigen, EMR hormone, Gastric inhibitory polypeptide, GPR56 orphan, Latrophilin, Diuretic hormone receptors*
Class C	(Metabotropic glutamate/pherormone)
I	*$mGluR_1 mGluR_5$*
II	*$mGluR_2 mGluR_3$*
III	*$mGluR_4 mGluR_6 mGluR_7 mGluR_8$*
Class D	(Fungal mating pherormone receptor)
Class E	(Cyclic AMP receptor)
Class F	(Frizzled/Smoothened)

Some families in this A-F classification do not exist in human. For example, clans D and E are fungal pheromone and cAMP receptors, and clan F contains archaebacterial opsins. In general the mammalian GPCRs have been grouped into three classes, A, B and C (Kolakowski, 1994) excluding the subfamily IV in clan A comprising invertebrate opsin receptors.

1.1.2 Signal transduction mechanisms in GPCRs

Signal transduction at the cellular level refers to the transmission of signals from outside the cell to inside. In general this process can be simple but for GPCRs a more complex signal transduction pathway involves the coupling of ligand-receptor interactions to many intracellular events. Binding of an agonist induces or stabilizes an active receptor state, resulting in increased affinity for the G-protein located at the cytosolic side of the plasma membrane.

The G-proteins are composed of α, β and γ subunits, β and γ are tightly associated and can be considered as one functional unit. There are many classes of heterotrimeric G-proteins involved in signal transduction. At least 28 distinct G-protein α, 5 β and 12 γ subunits have been identified and subdivided into 4 families based on the degree of primary sequence similarities of the α subunit (Figure 1.1).

Mutagenesis and biochemical experiments suggest that receptor activation by an agonist affects the conformation of intacellular loops and thus uncovers previously masked binding sites for the G-protein. This leads to a rapid release of GDP from the α subunit (Figure 1.2) (Hamm, 1998; Sprang, 1997). Under physiological conditions GDP is immediately replaced by GTP. The nucleotide exchange reduces the affinity of the α subunit for the βγ complex and causes the dissociation of the heterotrimer into $G_{\alpha\text{-GTP}}$ and $G_{\beta\gamma}$. The $G_{\alpha\text{-GTP}}$ subunit activates ($G_{\alpha s}$, $G_{\alpha q}$, $G\alpha_{12}$) or inhibits ($G_{\alpha i}$) effector proteins such as adenylyl cyclases 1-9, phospholipases A2 and C β1-4, phosphodiesterase (PDE) and ion channels (for details, see Figure 1.2). This activation leads to the production of second messengers like cyclic 3',5'-adenosine monophosphate (cAMP), diacylglycerol (Adams et al.), or to the modulation of inositol-1,4,5-triphosphate (IP3).

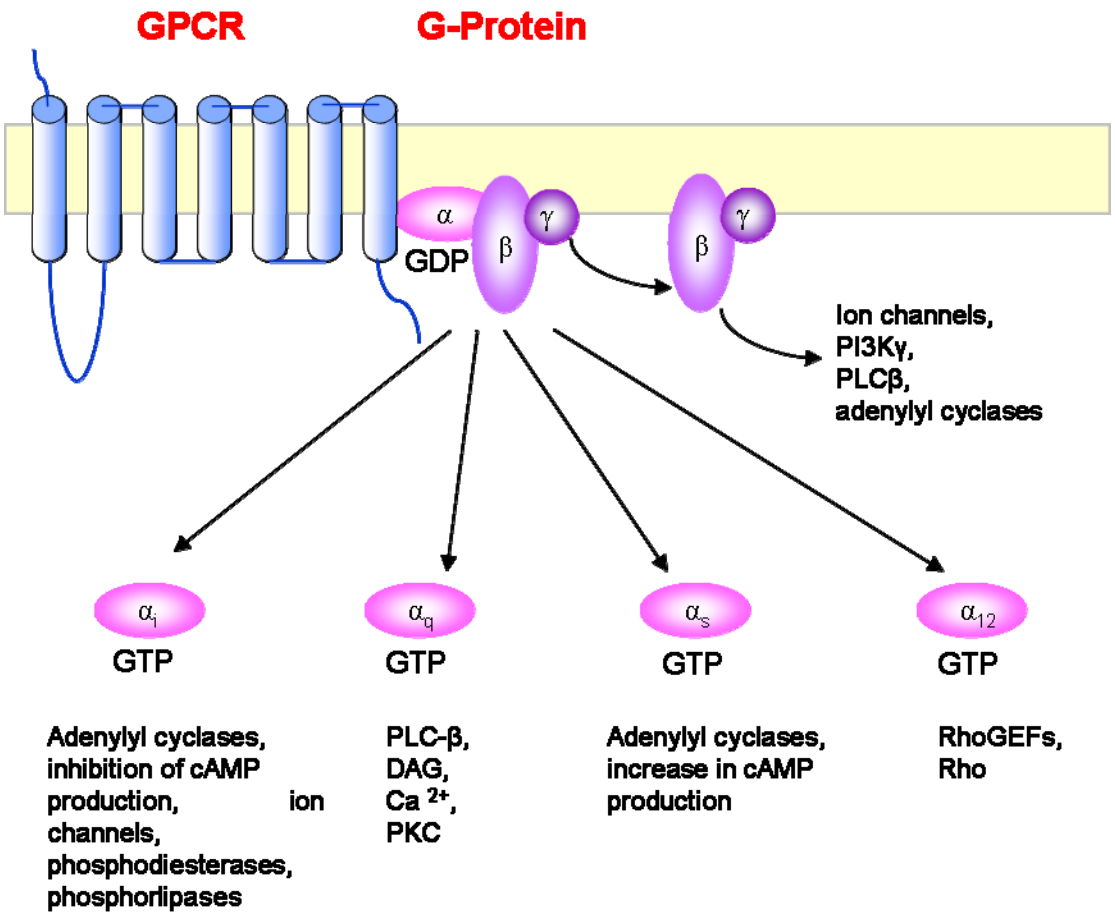

G-Protein	α-subunit subfamily	Effect of activation
G_s	**$G_{\alpha s}$ $G_{\alpha olf}$**	**Stimulation of adenilyl cyclases**
G_i	$G_{\alpha 1\text{-}3}$ $G_{\alpha 0}$ $G_{\alpha g}$ $G_{\alpha tr}$ $G_{\alpha tc}$	Inibition of adenylyl cyclases Activation of cGMP phosphodiesterases
G_q	**$G_{\alpha q}$ $G_{\alpha 11}$ $G_{\alpha 14}$ $G_{\alpha 16}$**	**Activation of phospholipases Cβ (PLCβ)**
G_{12}	$G_{\alpha 12}$ $G_{\alpha 13}$	Activation of RhoA signalling; activation of PLCβ

Figure 1.1: G-proteins: role in signal transduction and classification

These second messengers can induce changes in the intracellular ion concentration, regulate enzyme activity (especially protein kinases), modulate transcription factors, activate or inhibit gene expression and other fast cellular responses. All these effects described above are induced by de G_α subunit. It is however also known that the $G_{\beta\gamma}$ heterodimer can play an active role in the signal transduction in animal cells (Clapham and Neer, 1993; Sternweis, 1994), e.g. in the regulation of K^+ channels, of phospholipase Cβ and of certain isoforms of adenylyl cyclase. The activated state of the $G_{\alpha\text{-}GTP}$ subunit lasts until GTP is hydrolysed by the slow GTPase activity of G_α.

This hydrolysis induces the re-association between G_{α} and $G_{\beta\gamma}$ for the restart of a new cycle.

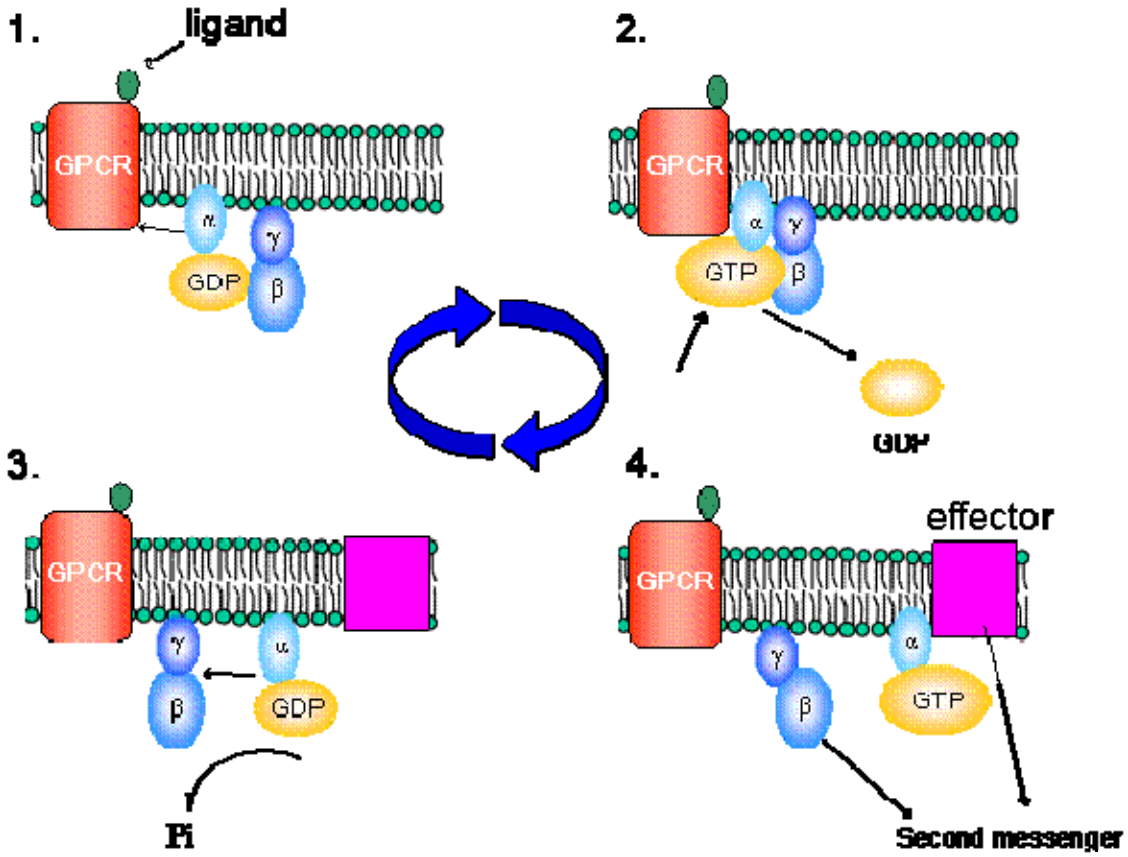

Figure 1.2: GPCR activation and deactivation cycle after stimulus by an agonist.

An omnipresent property of signalling through GPCRs is their desensitization when they are exposed to an agonist or partial agonist for a prolonged period of time. Typically, activation of a GPCR leads to a) activation and inhibition of specific signal pathways in the cell, b) short term desensitization mediated by phosphorylation of GPCRs by G protein-coupled receptor kinases (GRK) followed by β-arrestin binding to GPCRs that uncouple the receptor from the G-protein, and c) endocytosis of the receptor followed by postendocytotic sorting of the receptor, either back d) to the plasma membrane or e) to lysosomes for degradation. In general, for many GPCRs, prolonged exposure to agonists or partial agonists results in down-regulation, prolonged exposure to antagonists in receptor supersensivity (e.g., down-regulation of 5-HT_{2A} and 5-HT_{2C} receptors is produced by a chronic administration of 5-HT_2 agonists, however, in this case and uniquely among biogenic amine receptors, also by antagonists). The key reaction of this down-regulation is the phosphorylation of

the cytoplasmic receptor domain by protein kinases. There are two kinds of desensitization: 1) homologous desensitization, in which the activated GPCR is down-regulated; and 2) heterologous desensitization, where the activated GPCR causes down-regulation of a different GPCR. In the first case, agonist binding to the GPCR leads to GRK-mediated phosphorylation of the receptor. For the second mechanism, agonist occupancy of the target is not required; the second messenger, produced by activation of one GPCR, induces activation of protein kinases that could phosphorylate another GPCR target at the plasma membrane.

Another feature that characterizes GPCRs is constitutive activity which occurs from case to case. Until now, it has been observed in more than 60 wild-type GPCRs, and a large number of disease-causing GPCR mutants with increased constitutive activity has been identified. This property can be defined as the ability of a GPCR to adopt spontaneously (in absence agonists or antagonists) an active conformation that activates G-proteins (Lefkowitz et al., 1993; Samama et al., 1993; Seifert and Wenzel-Seifert, 2002).

1.2 Serotonin (5-hydroxytryptamine, 5-HT)

1.2.1 Historical overview

Serotonin is a monoamine neurotransmitter widely distributed in animals and plants, occurring in vertebrates, fruits, nuts and venoms. The synthesis in animals and human happens in serotonergic neurons in the central nervous system (CNS), blood platelets and enterochromaffine cells in the gastrointestinal tract. The discovery of serotonin can be attributed to an Italian pharmacologist, Dr. Vittorio Erspamer, who was looking for substances capable of causing smooth muscle contraction and who identified such a substance in an acetone extract of rabbit gastric mucosa in the 1930's (Erspamer and Asero, 1952, 1953). He named this substance enteramine. In the late 1940's the laboratory of Dr Irving Page isolated, partially purified and crystallised a vasoconstricting substance in serum and named it serotonin (Rapport et al., 1948). The structure was reported in 1949. Around 1952 it was realized that enteramine and serotonin were the same substance. It was initially recognised as powerful vasoconstrictor in blood serum, but after chemical identification other

physiological functions, especially in the CNS, were elucidated. In 1952 Dr. Betty Twarog joined the Page lab to test the idea that invertebrate neurotransmitters may similarly act in vertebrates. Her research resulted in the identification of serotonin in the brain (Twarog and Page, 1953). Afterwards the function as human neurotransmitter was suggested (Brodie and Shore, 1957).

Serotonin is associated with a broad range of actions in the human body, including the control of appetite, sleep, memory and learning, temperature regulation, effects on mood, behaviour, cardiovascular function, muscle contraction, endocrine regulation and depression. Subsequent to his discovery of serotonin, Page commented that no other physiological substance known performs such diverse actions in the body. A number of serotonin congeners are also present in nature and have been shown to possess a variety of peripheral and CNS activities.

Corresponding to these manifold actions of serotonin, but also to the large number and different localization of 5-HT receptor subtypes (see below), aberrations in the serotoninergic system including biosynthesis and metabolism of the neurotransmitter lead to malfunctions in the regulation of many psychophysiological processes. Accordingly, psychiatric disorders such as anxiety, depression, aggressiveness, panic, obsessive-compulsive disorders, schizophrenia, suicidal behaviour and autism, neurodegenerative disorders as Alzheimer's disease, Parkinsonism, and Huntington's chorea, migraine, emesis and alcoholism may result. Therefore, various drugs act on the 5-HT system, including some antidepressants, anxiolytics, antiemetics, antipsychotics and anti-migraine agents.

1.2.2 Biosynthesis and metabolism

Serotonin is ingested from various dietary sources but is also synthesized in a two-steps metabolic pathway from the essential amino acid tryptophan (Figure 1.3). Tryptophan hydroxylase, the rate-limiting enzyme, firstly converts tryptophan to 5-hydroxytryptophan, which is then decarboxylated by L-aromatic animo acid decarboxylase, a widely distributed enzyme with a broad substrate specificity. Prerequisite of the synthesis in the brain is the active transport of ingested tryptophan, performed by a carrier that also transports other bulky neutral amino acids. Therefore the tryptophan level in the brain is influenced not only by its own plasma concentration but also by the plasma levels of amino acids competing for the

brain uptake carrier. The principal route of serotonin inactivation involves monoamine oxydase forming 5-hydroxyindoleacetaldehyde which is then converted into 5-hydroxyindoleacetic acid by an ubiquitous enzyme, aldehyde dehydrogenase. The acid is transported out of the brain and eliminated through excretion in the urine. Other pathways of metabolism have been suggested. One of these, shown in Figure 1.3, involves the enzyme sulfatransferase causing, by sulfatation, the formation of tryptamine-O-sufate.

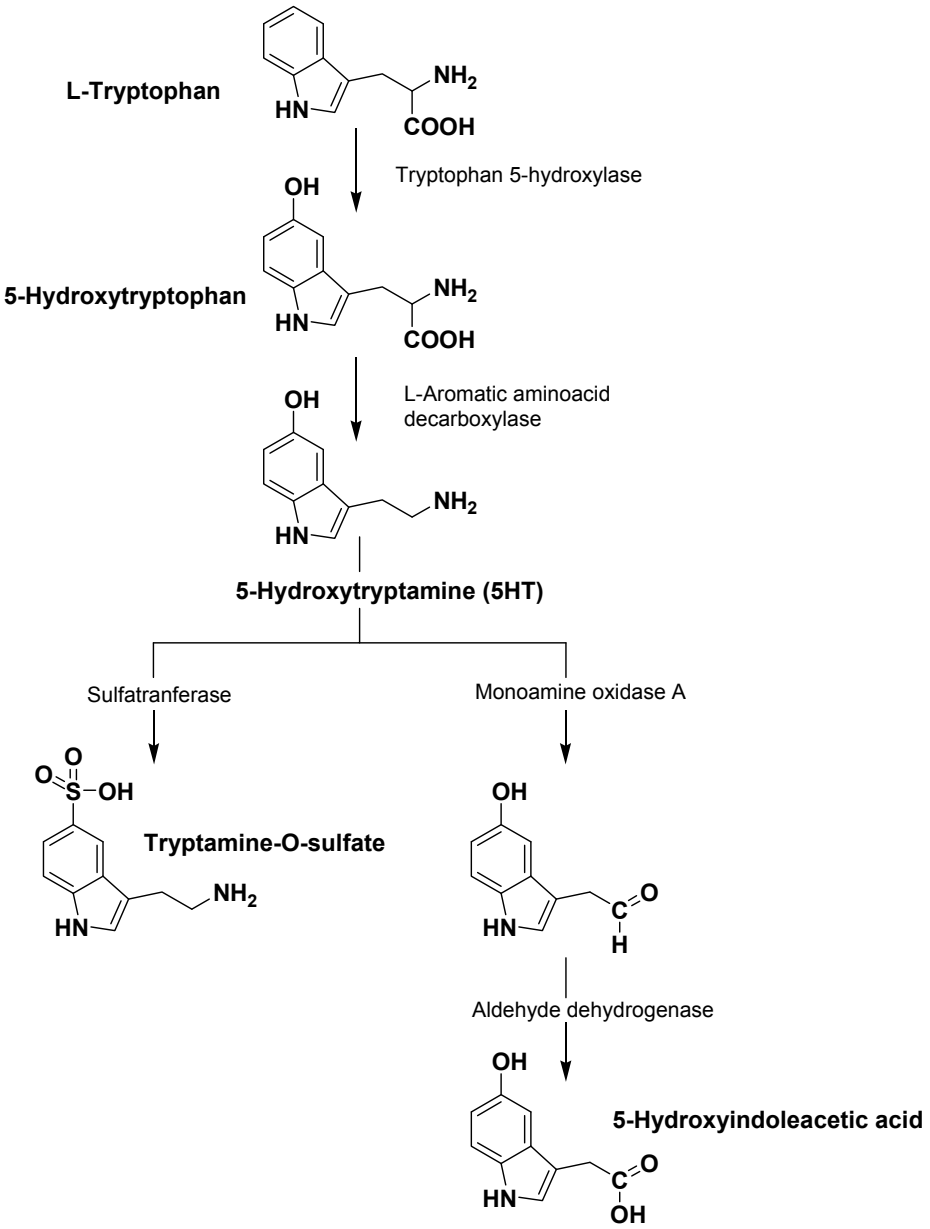

Figure 1.3: Catalytic mechanisms in serotonin metabolism.

1.3 Serotonin receptors (5-HTR)

5-HT receptors (5-HTR) are receptors for the neurotransmitter and peripheral signal mediator serotonin as endogenous agonist. They are located in the cell membrane of neurons and other cell types, including smooth muscle cells, in animals. In the intact brain the function of many 5-HTRs (see classification below) is associated with specific physiological responses, ranging from modulation of the neuronal activity and transmitter release to behavioural changes. Individual 5-HTR subtypes affect the release of other neurotransmitters such as glutamate, dopamine and GABA. At the molecular level, 5-HTRs are members of the 7TM type and, with exception of the 5-HT_3R subtype that is a ligand-gated ion channel, belong to the GPCR superfamily.

1.3.1 5-HTR classification

Evidence of the existence of 5-HT receptors was first presented in 1957 by Gaddum and Picarelli, who experimented with the isolated guinea pig ileum (Gaddum and Picarelli, 1957). They described two types of receptors affecting muscle contraction: D receptors blocked by dibenzyline and M receptors blocked by morphine. In 1970's, the ligand binding sites were tentatively explored using [^{3}H]5-HT, and it was shown that [^{3}H]LSD binding can be displaced by 5-HT (Farrow and Van Vunakis, 1972; Marchbanks, 1966, 1967). In the same decade also the earliest evidence for a selective high-affinity and saturable binding of [^{3}H]5-HT was published (Bennett and Snyder, 1975, 1976). The discrimination of two classes of 5-HT receptors, 5-HT_1R and 5-HT_2R, labeled with high affinity by [^{3}H]5-HT and [^{3}H]spiperone, respectively, was based on the discovery that [^{3}H]spiroperidol could also selectively label the suggested 5-HT_1R subtype (Leysen et al., 1978; Peroutka and Snyder, 1979). Additionally, 5-HT_1Rs appeared to be heterogeneous, because the inhibition of [^{3}H]5-HT binding by spiroperidol was biphasic. Pedigo indicated the existence of two subtypes labelled by [^{3}H]5-HT: 5-HT_{1A}R (high affinity for spiperidol) and 5-HT_{1B}R (low affinity for spiperidol). A third 5-HT_1R species, 5-HT_{1C}R, was then proposed on the basis of the high affinity displacement of [^{3}H]5-HT by mesulergide (Pazos et al., 1985b; Pedigo et al., 1981).

After functional studies, performed to attribute a physiological role to these binding sites, it became necessary to reclassify the 5-HT receptors. A group of scientists

proposed three major classes: 5-HT_1R-like (heterogeneous group of receptors with high affinity for 5-HT and methiothepin as selective antagonist), 5-HT_2R (D receptors described above, mediating a variety of peripheral actions of 5-HT) and 5-HT_3R (M receptors, present in peripheral neurons and mediating the depolarizing actions of 5-HT) (Bradley et al., 1986). This classification was later slightly modified (Peroutka, 1990) because of the detection of a new 5-HT_1R subtype, called 5-HT_{1D}R (Heuring and Peroutka, 1987), the pharmacological and molecular similarity of 5-HT_{1C}R and 5-HT_2R (Hartig, 1989a), and the verification of the functional role of 5-HT_1R-like receptors. In conclusion, three classes were proposed: 5-HT_1R (5-HT_{1A}R, 5-HT_{1B}R and 5-HT_{1D}R), 5-HT_2R (5-HT_{2A}R, 5-HT_{2B}R, 5-HT_{1C}R) and 5-HT_3R. However, this classification based on agonist and antagonist selectivities did not account for some specific sites characterized by binding, functional properties or individual pharmacological profiles (e.g., the 5-HT_4R). In 1989 a new and simplified classification was proposed (Hartig, 1989a) based on sequence homology, structural considerations from molecular biology and the signal transduction pathways. Moreover, the application of molecular biology techniques has led to the discovery of addtitonal 5-HTR subtypes (Boess and Martin, 1994; Peroutka, 1994). Now 5-HTR are assigned to one of seven families, 5-HT_{1-7}, comprising a total of 14 structurally and pharmacologically distinct subtypes (Hoyer et al., 1994) (Table 1.2).

Table 1.2: Classification of 5-HT receptors

Receptor subtype	Agonists	Antagonists	Expression	Transduction mechanism	Action
5-HT$_{1A}$	Buspirone, psilocin, LSD	spiperone, methiothepin, ergotamine, yohimbine	CNS, myenteric plexus	G_i/G_o	CNS: neuronal inhibition, behavioural effects (sleep, feeding, thermoregulation, aggression, anxiety)
5-HT$_{1B}$	Ergotamine, sumatriptan	Methiothepin, yohimbine, metergoline, Risperidone	CNS, vascular smooth muscle, automatic terminals	G_i/G_o	CNS: presynaptic inhibition, behavioural effects, vascular: pulmonary vasoconstriction
5-HT$_{1D}$	5-(Nonyloxy)tryptamine, sumatriptan	Methiothepin, yohimbine, metergoline, ergotamine	CNS, vascular smooth muscle; sympathoinhibition in automatic neurones	G_i/G_o	CNS: locomotion, anxiety; vascular: cerebral vasoconstriction
5-HT$_{1E}$			CNS	G_i/G_o	
5-HT$_{1F}$			CNS, uterus, mesentery	Gi/Go	
5-HT$_{2A}$	α-methyl-5-HT, LSD, psilocin, DOI	Nefazodone, trazodone, mirtazapine, ketanserin, cyproheptadine, pizotifen, atypical antipsychotics	CNS, gastrointestinal tract, vascular and bronchial smooth muscle, vascular endothelium, patelets	G_q/G_{11}	CNS: neuronal excitation, behavioural effects, learning, anxiety; smooth muscle: contraction, vasoconstriction / vasodilatation; platelets: aggregation
5-HT$_{2B}$	α-methyl-5-HT, LSD, DOI, Fenfluramine	yohimbine	Smooth muscle of ileum, stomac fundus, uterus vascular endothelium	G_q/G_{11}	stomach: contraction
5-HT$_{2C}$	α-methyl-5-HT, agomelatine, LSD, psilocin, DOI	mesulergine, agomelatine, fluoxetine, methysergide	CNS	G_q/G_{11}	CNS: anxiety, choroid plexus: cerebrospinal fluid (CSF) secretion
5-HT$_3$	2-methyl-5-HT	metoclopramide (high doses), renzapride, ondansetron, alosetron, mirtazapine, memantine	CNS, post-ganglionic sympathetic, sensory neurones	Intrinsic transmitter-gated ion channel	CNS, PNS: neuronal excitation, anxiety, emesis
5-HT$_4$	5-methoxytryptamine, metoclopramide, renzapride, tegaserod, RS 67333	GR113808 Piboserod	CNS, cardiac muscle, oesophageal and vascular smooth muscle, myenteric plexus	G_S	GIT: gastrointestinal motility; CNS: neuronal excitation, learning, memory
5-HT$_{5A}$	5-carboxytryptamine, LSD	Unknown	CNS	G_S	CNS (cortex, hippocampus, cerebellum): unknown
5-HT$_6$	LSD	SB271046 [b]	CNS	Not defined	CNS: unknown
5-HT$_7$	5-carboxytryptamine, LSD	Methiothepin, risperidone	CNS, superior cervical ganglion	G_S	CNS, GIT, blood vessels: unknown

1.4 5-HT_2 receptors (5-HT_2R)

5-HT_2 receptors belong to the GPCR class A or 1 (rhodopsin-like), subclass XV; currently three subtypes are identified, 5-HT_{2A}R (formerly 5-HT_2R), 5-HT_{2B}R (formerly 5-HT_{2F}R) and 5-HT_{2C}R (formerly 5-HT_{1C}R) which are similar in sequence, pharmacology and signal transduction pathways. The 5-HT_{2A}R is expressed in the brain and in the periphery, the 5-HT_{2B}R in the rat and mouse stomach fundus, in human in most peripheral organs and low-level in brain tissue and blood cells (Schmuck et al., 1994), and the 5-HT_{2C}R in the brain and the choroid plexus. The average amino acids identity between the three subtypes is 45-67% for the full-length receptor and 68-79% for the transmembrane segments (Nelson, 1993). 5-HT_2Rs are structurally quite distinct from other 5-HTR subtypes (Baxter et al., 1995). Phylogenetic analysis of class A aminergic GPCRs (Vassilatis et al., 2003) indicate that the whole serotonin group is considerably heterogeneous (Figure1.4). The 5-HT_4R is more related to the histamine H_2R than to the 5-HT_1R subtypes which, together with 5-HT_7R, are more closely connected with dopamine D_2, D_3 and D_4 receptors than with 5-HT_2R species and 5-HT_6Rs. Within the 5-HT_2R subfamily, 5-HT_{2A}Rs and 5-HT_{2C}Rs cluster together and differ from 5-HT_{2B}Rs.

The 5-HT_2R genes are characterized by the presence of two (5-HT_{2A}R and 5-HT_{2B}R) or three (5-HT_{2C}R) introns in the coding sequence (Chen et al., 1992; Stam et al., 1992b; Yu et al., 1991). 5-HT_2Rs are coupled to G_q, activate phospholipase C and mobilize intracellular calcium, mediating a large number of central and peripheral physiologic functions of serotonin. Cardiovascular effects include contraction of blood vessels and shape changes of platelets. In the CNS, e.g., neuronal sensitization after tactile stimuli and hallucinogenic effects arise. The development of selective antagonists for each receptor subtype is now at an advanced stage. They are used as drugs or are candidates for the treatment of various CNS disorders including schizophrenia, anxiety, sleep, feeding disorders and migraine.

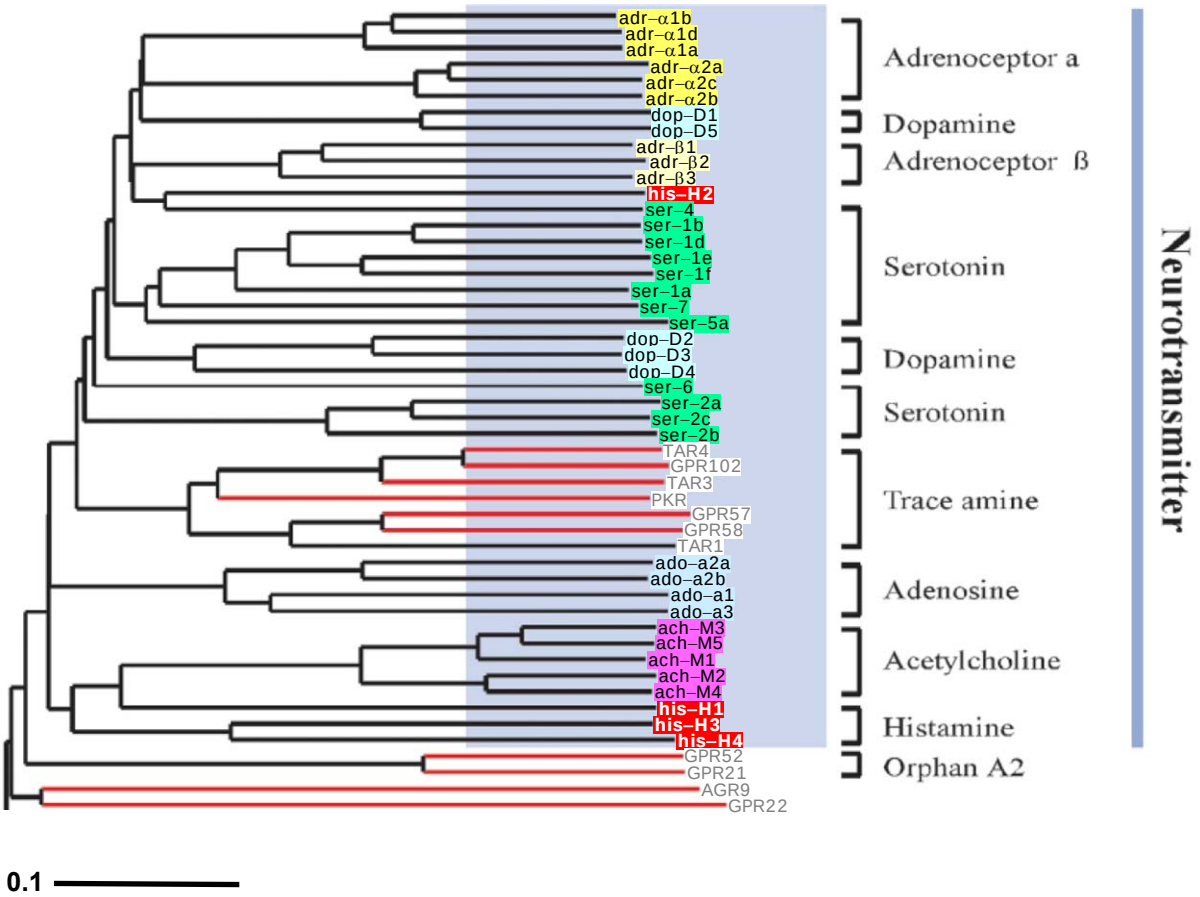

Figure 1.4 Phylogenetic tree of class A or 1 aminergic GPCRs. Red lines and black lines correspond to receptors with unknown ligands (orphan receptors) and known ligands, respectively. Adapted from Vassilatis et al., 2003. The line on the bottom indicates the horizontal distance equal to 10% sequence divergence.

1.4.1 5-HT$_{2A}$ receptor

The 5-HT$_{2A}$R was initially detected in rat cortical membranes as high affinity binding site for [^{3}H]spiperone with relatively low (micromolar) affinity for 5-HT, but a pharmacological profile of a 5-HT receptor (Leysen et al., 1978; Peroutka and Snyder, 1979). This receptor was originally defined as 5-HT$_{2}$R, but later reassigned to the 5-HT receptor classification as 5-HT$_{2A}$R. It is the main excitatory receptor subtype among the GPCRs for serotonin, although 5-HT$_{2A}$Rs may also have inhibitory effects on certain brain areas such as the visual and the orbitofrontal cortex. The 5-HT$_{2A}$R was first considered as target of psychedelic drugs like LSD, but later it was also found to mediate the action of antipsychotic drugs, especially the atypical ones.

1.4.1.1 5-HT$_{2A}$ receptor structure

Until now, the 5-HT$_{2A}$R of nine different species has been cloned: canine (Bonaventure et al., 2005; Masuda et al., 2004), guinea pig (Watts et al., 1994), Chinese hamster (Chambard et al., 1990), fruit fly (Adams et al., 2000), human (Saltzman et al., 1991; Stam et al., 1992a), Macaca mulatta (Johnson et al., 1995), mouse (Yang et al., 1992), pig (Johnson et al., 1995), rat (Julius et al., 1990). The nucleotide sequences of bovine and orangutan were submitted to the EMBL/GenBank/DDBJ database in 2003 by Tahara K. et al. and by Kitano T. et al. in 2000, respectively. The intronless gene encodes for 471 (Chinese hamster, macaca mulatta, mouse, orangutan, human and rat) or 470 (bovine, dog and pig) amino acids. The human 5-HT$_{2A}$R is located on chromosome 13q14-q21, consists of three exons separated by two introns, and spans over 20 Kb (Chen et al., 1992). It has a relatively high sequence identity with the human 5-HT$_{2C}$R (c.a. 80% in the 7TM regions). The human 5-HT$_{2A}$R is also 87% homologous with its rat counterpart with the highest amino acid identity (98%) within the 7TM domain. The regions of largest amino acid divergence between the rat and human receptors were at the N-terminal extracellular domain (75% homology) and the C-terminal intracellular domain (67% homology) (Figure 1.5).

5-HT receptors share a conserved topological structure within the lipid bilayer which is also present in all other GPCRs. Specific domains have been shown to be functional determinants. The structure of the 5-HT$_{2A}$R (Figure 1.6) can be divided into three domains:

1. the extracellular domain which includes the amino terminus (NT) and the extracellular loops E1, E2 and E3 between transmembrane helices TM 2 and 3, TM 4 and 5, and TM 6 and 7, respectively;
2. the membrane domain consisting of seven membrane spanning helical regions TM1 – TM7;
3. the intracellular domain which includes the carboxy terminus (Adams et al.) and the intracellular loops I1, I2 and I3 between TM 1 and 2, TM 3 and 4, and TM 5 and 6, respectively.

A disulfide bond that is highly conserved in all GPCRs connects the extracellular end of TM3 with E2.

```
                                        TM1
h5HT2A  MDILCEENTSLSSTTNSLMQLNDDTRLYSNDFNSGEANTSDAFNWTVDSENRTNLSCEGC 60
r5HT2A  MEILCEDNISLSSIPNSLMQLGDGPRLYHNDFNSRDANTSEASNWTIDAENRTNLSCEGY 60
                                                                TM1
h5HT2A  LSPSCLSLLHLQEKNWSALLTAVVIILTIAGNILVIMAVSLEKKLQNATNYFLMSLAIAD 120
r5HT2A  LPPTCLSILHLQEKNWSALLTTVVIILTIAGNILVIMAVSLEKKLQNATNYFLMSLAIAD 120
        TM2                                     TM3
h5HT2A  MLLGFLVMPVSMLTILYGYRWPLPSKLCAVWIYLDVLFSTASIMHLCAISLDRYVAIQNP 180
r5HT2A  MLLGFLVMPVSMLTILYGYRWPLPSKLCAIWIYLDVLFSTASIMHLCAISLDRYVAIQNP 180
                                TM4                             TM4
h5HT2A  IHHSRFNSRTKAFLKIIAVWTISVGISMPIPVFGLQDDSKVFKEGSCLLADDNFVLIGSF 240
r5HT2A  IHHSRFNSRTKAFLKIIAVWTISVGISMPIPVFGLQDDSKVFKEGSCLLADDNFVLIGSF 240
        TM5
h5HT2A  VSFFIPLTIMVITYFLTIKSLQKEATLCVSDLGTRAKLASFSFLPQSSLSSEKLFQRSIH 300
r5HT2A  VAFFIPLTIMVITYFLTIKSLQKEATLCVSDLSTRAKLASFSFLPQSSLSSEKLFQRSIH 300
                                        TM6
h5HT2A  REPGSYTGRRTMQSISNEQKACKVLGIVFFLFVVMWCPFFITNIMAVICKESCNEDVIGA 360
r5HT2A  REPGSYAGRRTMQSISNEQKACKVLGIVFFLFVVMWCPFFITNIMAVICKESCNENVIGA 360
                TM7
h5HT2A  LLNVFVWIGYLSSAVNPLVYTLFNKTYRSAFSRYIQCQYKENKKPLQLILVNTIPALAYK 420
r5HT2A  LLNVFVWIGYLSSAVNPLVYTLFNKTYRSAFSRYIQCQYKENRKPLQLILVNTIPALAYK 420

h5HT2A  SSQLQMGQKKNSKQDAKTTDNDCSMVALGKQHSEEASKDNSDGVNEKVSCV 471
r5HT2A  SSQLQVGQKKNSQEDAEQTVDDCSMVTLGKQQSEENCTDNIETVNEKVSCV 471
```

Figure 1.5: Alignment of the sequences of human ($h5HT_{2A}R$) and rat ($r5HT_{2A}R$) receptors. Identical amino acids are in bold, non-identical in italics, and the TM regions TM1-TM7 are indicated with bars.

As it is observed for all GPCRs, the 5-$HT_{2A}R$ is subject to post-translational modification and regulatory mechanisms. The N-terminal extracellular region contains glycosylation sites where complex sugar moieties bind to the receptor. The sugar groups play a role in processing the receptor to the cytoplasmic membrane, but apparently do not participate in ligand recognition or in functional mechanisms, for example, deletion of the N-terminus does not affect the receptor's biological response to the endogenous ligand (Buck et al., 1991; Rands et al., 1990). The C-terminal intracellular region is believed to play an important role in the desensitization of GPCRs via phosphorylation. The $5HT_{2A}R$ is known to be desensitized by various selective agonists, presumably through a common phosphorylation mechanism (Hausdorff et al., 1990). The C-terminal intracellular regions of the human and rat $5HT_{2A}R$ contain a total of 14 serine/threonine residues that represent possible phosphorylation sites, 11 of which are conserved. A C-terminal cysteine residue at position 397 of the rat 5-$HT_{2A}R$ has been found to be essential for receptor activity (Buck et al., 1991). This residue is conserved in a variety of GPCRs and is believed to play a role in G-protein coupling (O'Dowd et al., 1988).

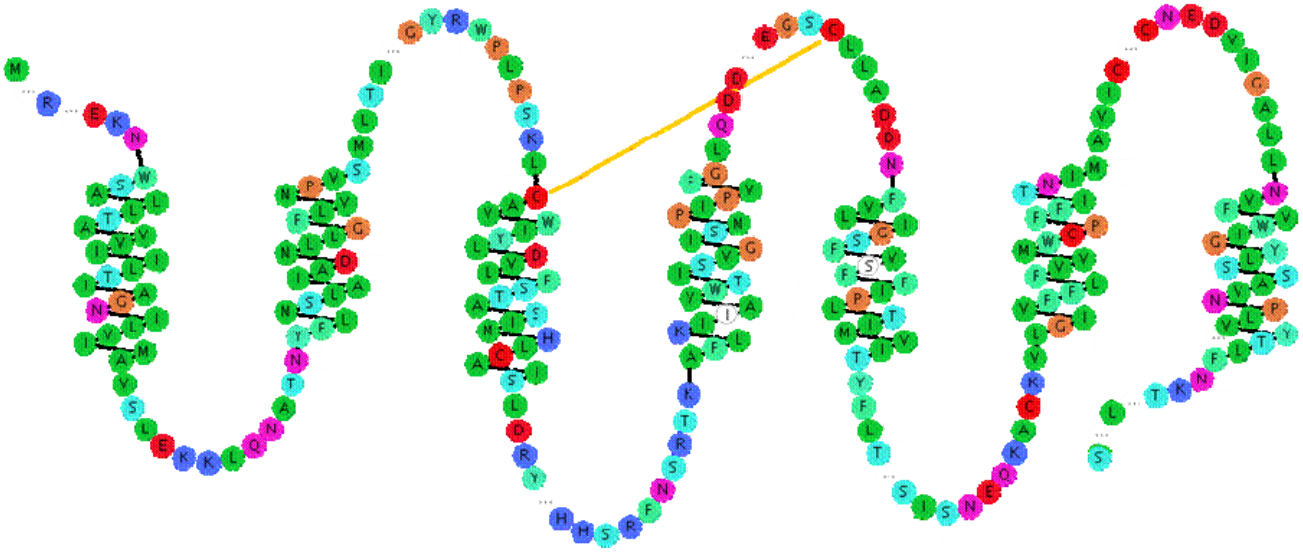

Figure 1.6: Snake plot of the human 5-HT_{2A}R adapted from the GPCR database (http://www.gpcr.org/). The disulfide bond between Cys-148 and Cys-227 is represented by a yellow line. The colours encode residue properties (polar, neutral or charged, hydrophobic, aromatic or aliphatic). Parts of the sequence were deleted to avoid long loops (represented by "...").

Analyses of aligned GPCRs identified residues highly conserved in subfamilies. These amino acids are probably involved in ligand binding or play a specific functional role as stabilization of receptor states by intramolecular contacts or interaction with G proteins.. This hypothesis has been confirmed by mutagenesis experiments. For 5-HT_{2A} receptors the residues involved in the binding of ligands are localized in the extracellular side of TM3, TM5, TM6 and TM7. As indicated by the properties of receptor mutants, the binding site of the human 5-HT_{2A}R is composed of Asp155$^{3.32}$, Ser159$^{3.36}$, Ser239$^{5.43}$, Ser242$^{5.46}$ that are possibly involved in polar interactions with ligands, Phe240$^{5.44}$, Phe243$^{5.47}$, Phe244$^{5.48}$, Phe339$^{6.51}$, Phe340$^{6.52}$, Trp336$^{6.68}$, Trp367$^{7.40}$ and Tyr370$^{7.43}$ that form two hydrophobic pockets surrounding the ligands.

Certain residues in the second extracellular loop (E2) may also be important for the binding of agonists and antagonists. A direct contact between ligands and E2 is possible, especially close to the disulfide bridge formed between a cysteine in E2 and another one near the N-terminus of TM3, which anchors the E2 loop in proximity to the ligand binding site

An important structural motif in all GPCRs is represented by the highly conserved triad DRY in the cytoplasmatic part of TM3 (Asp172$^{3.49}$, Arg173$^{3.50}$ and Tyr174$^{3.51}$ in

the 5-HT_{2A}R). Arg173 forms salt bridges with Asp172$^{3.49}$ and with Glu318$^{6.30}$, a highly conserved residue in the cytoplasmatic part of TM6. This so-called “ionic lock” is known to be responsible for the stabilization of the inactive receptor state. Conformational rearrangement of TM3 and TM6 after agonist binding involves cleavage of the ionic lock and activation of the receptor (Farrens et al., 1996; Gether et al., 1997; Rasmussen et al., 1999).

1.4.1.2 5-HT_{2A}R distribution, signal transduction and pharmacology

5-HT_{2A}Rs can be found in the CNS, gastrointestinal tract, vascular and bronchial smooth muscles, vascular endothelium and platelets. The CNS distribution has been extensively mapped by receptor autoradiography, *in situ* hybridization and immuno-cytochemistry. The autoradiography studies using [^{3}H]spiperone, [^{3}H]ketanserin, [^{125}I]DOI and [^{3}H]MDL 100907 as radioligands indicated high levels of 5-HT_{2A} binding sites in particular cortical areas (neocortex, entorhinal and pyriform cortex and claustrum), in the caudate nucleus, nucleus occumbens, olfactory tubercle and hippocampus (López-Giménez et al., 1997; Pazos et al., 1985) where they are postsynaptically located in the 5-HT neurons and regulate dopamine, adrenaline, GABA, and glutamate neurotransmission (Hoyer et al., 2002). The functions of 5-HT_{2A}Rs are based on the receptor localization and affect different tissues. The activation of the receptor by the endogenous neurotransmitter serotonin or with an agonist includes:

- neural excitation, behavioural effects, learning and anxiety in the CNS.
- contraction when the gastrointestinal tract and bronchial smooth muscles are considered
- vasoconstriction or vasodilatation in vascular smooth muscles
- platelet aggregation.

5-HT_{2A}Rs are coupled to the $G_{\alpha q}/G_{\alpha 11}$ signal transduction pathway. After receptor stimulation and activation with an agonist, $G_{\alpha q}/G_{\alpha 11}$ and βγ subunits dissociate to initiate downstream effector pathways (Figure 1.7). The α subunit activates phospholipase C (PLC), which subsequently promotes the release of diacylglycerol (DAG) (Adams et al.) and inositol triphosphate (IP3). IP_3 stimulates Ca^{2+} release from

the endoplasmatic reticulum, leading together with DAG to the activation of protein kinase C (PKC) (Urban et al., 2007).

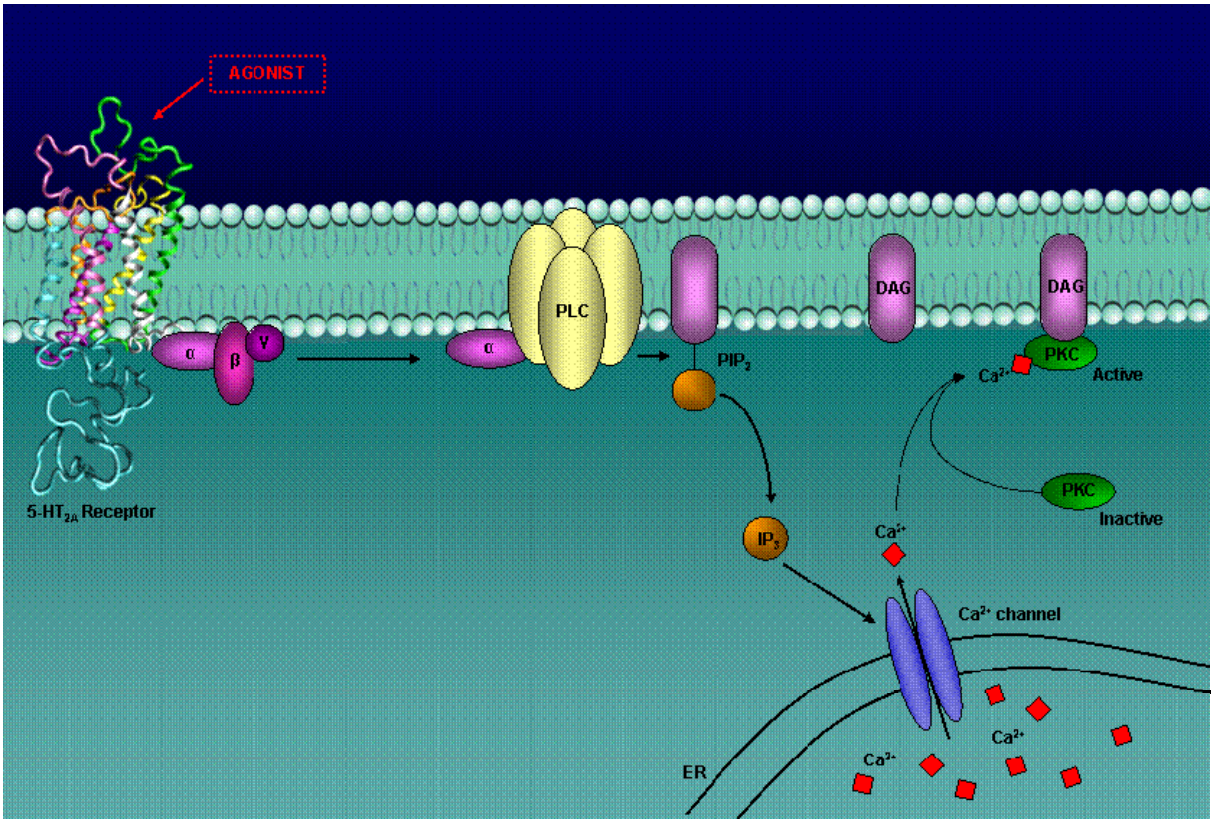

Figure 1.7: 5-HT_{2A}R signal transduction. Agonist binding activates the 5-HT_{2A}R, which in turn activates $G_{\alpha q}/G_{11}$. The α subunit activates PLC which cleaves PIP_2 into IP_3 and DAG. IP_3 interacts with a calcium channel in the endoplasmatic reticulum (ER), releasing Ca^{2+} into the cytoplasm. The increase in Ca^{2+} level activates PKC, which translocates to the membrane, anchoring DAG and phosphatidylserine.

The 5-HT_2 receptor subfamily is characterized by a low affinity for the endogenous ligand (5HT), a high affinity for the agonist DOI and its structural analogs DOB and DOM, and high affinity for various receptor antagonists such as metergoline, ritanserin and IC 170809. Until recently, it was difficult to discriminate between the 5-HT_2 subtypes, even though ketanserin and spiperone are about two orders of magnitude more affine for 5-HT_{2A}R than for 5-HT_{2B}R and 5-HT_{2C}R. However, these ligands do also bind to other monoamine receptors. With the development of selective antagonists it is now possible to discriminate the 5-HT_2R subtypes in more detail by pharmacological *in vitro* and *in vivo* models (Baxter et al., 1995). MDL 100907 is a potent and selective antagonist at 5-HT_{2A}R with low affinity for 5-HT_{2C}R

and other receptors. The discrimination of 5-HT_{2A}, 5-HT_{2C} and 5-HT_{2C} receptors was also advanced by the recent design of potent antagonists with selectivity for the 5-HT_{2B}R, SB 204741, and for the 5-HT_{2C}R, SB 242084 and RS-102221 (Baxter, 1996; Baxter et al., 1995; Bonhaus et al., 1997; Kennett et al., 1996a; Kennett et al., 1997a; Kennett et al., 1996b; Kennett et al., 1997b). The most selective 5-HT_{2A}R ligands are ketanserin and MDL 100907. Antagonists such as risperidone, ritanserin, olanzapine and MD 100907 show different selectivity and have been developed for the treatment of schizophrenia. It appears that the combination of dopamine D_2 and 5-HT_{2A} receptor antagonism may best explain the antipsychotic activity of drugs such as clozapine, olanzapine, seroquel and others. Moreover, it has been proposed that LSD exerts its hallucinogenic effect via interaction with the 5-HT_{2A}R.

At present, there are no selective agonists for 5-HT_{2A}Rs. The agonists for this receptor described until now like Me-5-HT, DOB and DOI also recognise other receptors of the 5-HT_2 receptor subfamily.

1.5 5-HT_{2A}R agonists and antagonists

1.5.1 5-HT_{2A}R agonists

Agonistic activity on 5-HT_{2A}R is essential for the psychopharmacology of serotonergic psychedelic or hallucinogenic drugs such as *d*-lysergic acid diethylamine (LSD), psylocibin, 5-MeO-DMT, mescaline and its derivatives (DOB, DOI, DOM). Molecules from different structural classes can act as agonists on this receptor, but no cases of sufficiently high subtype selectivity have been described up to now. In general, hallucinogens can be divided into two classes: 1) tryptamines and 2) phenylethylamines.

1.5.1.1 Tryptamines

This class includes two subclasses:

1. Indolylalkylamines

   5-hydroxytryptamine, the physiological ligand, is a non-selective agonist that

binds to all 5-HT receptors. In the 5-HT_2 receptor family the affinity for this molecule is in the order 5-HT_{2A}R › 5HT_{2B}R › 5HT_{2C}R (Baxter et al., 1995; Bonhaus et al., 1995). Structural modifications such as O-methylation or methylation in the alkyl chain (Figure 1.9) result in small effects on affinity and selectivity (Ismaiel et al., 1990; Nichols et al., 1988).

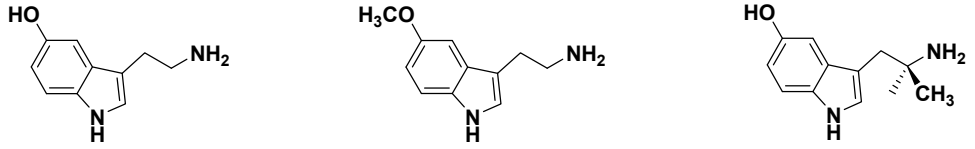

Figure 1.8: 5-HT_{2A}R (partial) agonists derived from tryptamine

Of particular relevance are 5-HT_{2A}R partial agonistic tryptamine derivatives with hallucinogenic activity (Nichols, 2004) such as DMT, 5-Me-O-DMT, bufotenin, a compound secreted from the skin of Common Toad (*Bufo Bufo*) and psylocibin, a prodrug of psilocin extracted from a mexican mushroom (*Psilocybe mexicana*) (Hasler et al., 1997; Horita, 1963; Horita and Weber, 1961) (Figure 1.10).

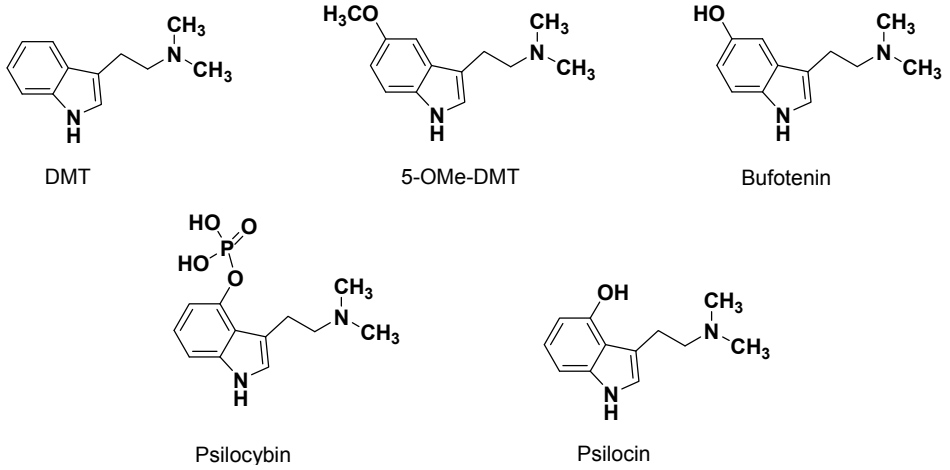

Figure 1.9: Representative 5-HT_{2A}R partial agonists with hallucinogenic effects

2. Ergolines

Ergolines, one of the pharmacologically most important groups of indole alkaloids isolated from the dried sclerotium of the fungus *Claviceps purpurea* (ergot), are relatively rigid analogs of tryptamine (e.g. lysergic acid diethylamide and some closely related compounds, see Figure 1.11). They are well known for their strong hallucinogenic effects. The scientific story of hallucinogens began in

1943, when Dr. Albert Hofmann, a natural products chemist from Sandoz experienced unusual mental effects following work with LSD. All compounds have two chiral centers in positions 5 and 8. Only the (5*R*,8*R*)-isomers display partial agonistic activity and hallucinogenic effects (Isbell et al., 1959; Rothlin, 1957). These molecules are without any selectivity for the 5-HT_{2A}R. Their affinities for 5-HT_{1A}, 5-HT_{1D}, 5-HT_{2A}, 5-HT_{2C}, 5-HT_5, 5-HT_6, 5-HT_7, D_2- and α_1 adrenergic receptors are very similar (Aghajanian and Marek, 1999; Glennon, 1990; Marek and Aghajanian, 1996).

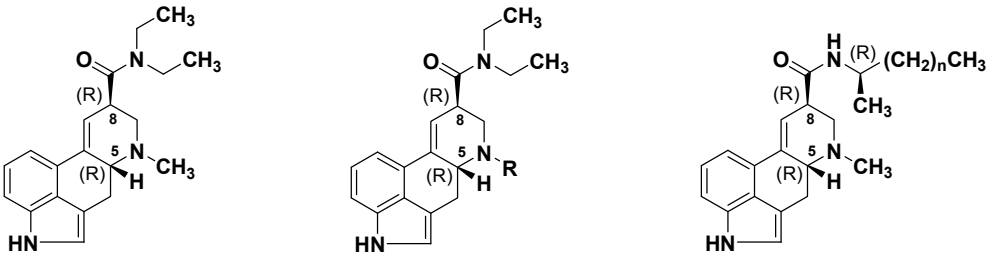

Figure 1.10: Nonselective 5-HT_{2A}R partial agonists: LSD and derivatives with hallucinogenic effect

1.5.1.2 Phenylalkylamines

Mescaline (3,4,5-trimethoxy-*β*-phenethylamine) is the main ingredient of peyote (*Lophophora williamsii*), a member of the *Cactaceae* family representing one of the earliest known hallucinogenic plants. This molecule was first identified by Heffter in 1896 and recognized as the active hallucinatory agent of this plant (Heffter, 1896). Following the first chemical synthesis of mescaline in 1919 (Späth, 1919), this molecule served as prototypical structure in more than 75 years of structure-activity relationships (SAR) studies linking molecular structure to hallucinogenic or psychedelic activity (Nichols, 1986). The SAR studies have led to agents with the common structure shown in Figure 1.11 and with low nanomolar affinity for 5-HT_{2A} and 5-HT_{2C} receptors (Glennon et al., 1992; Heller and Baraban, 1987; Lyon et al., 1988; Rasmussen et al., 1986; Sanders-Bush et al., 1988; Seggel et al., 1990). Some of which are among the most potent partial agonists with hallucinogenic effects known to data (Glennon et al., 1982; Glennon et al., 1980).

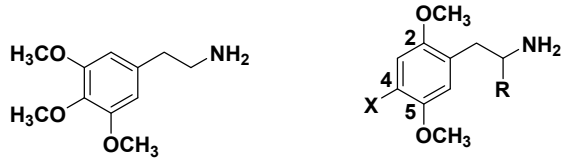

Mescaline General structure

Figure 1.11: Mescaline and the general structure of new potent 5-HT_{2A}R partial agonists obtained from SAR studies

The high affinity of these molecules is due to the two methoxy groups in position 2 and 5. Introduction of a substituent in position 4, such as a methyl (DOM), an ethyl (DOEt) or a halogen function like bromine (DOB) or iodine (DOI) further enhances 5-HT_{2A}R affinity and partial agonistic activity. Introduction of other lipophilic 4-substituents such as hexyl (DOHx) and benzyl (DOBz) also increases affinity, but leads to 5-HT_{2A}R antagonism (Seggel et al., 1990) (Figure 1.12).

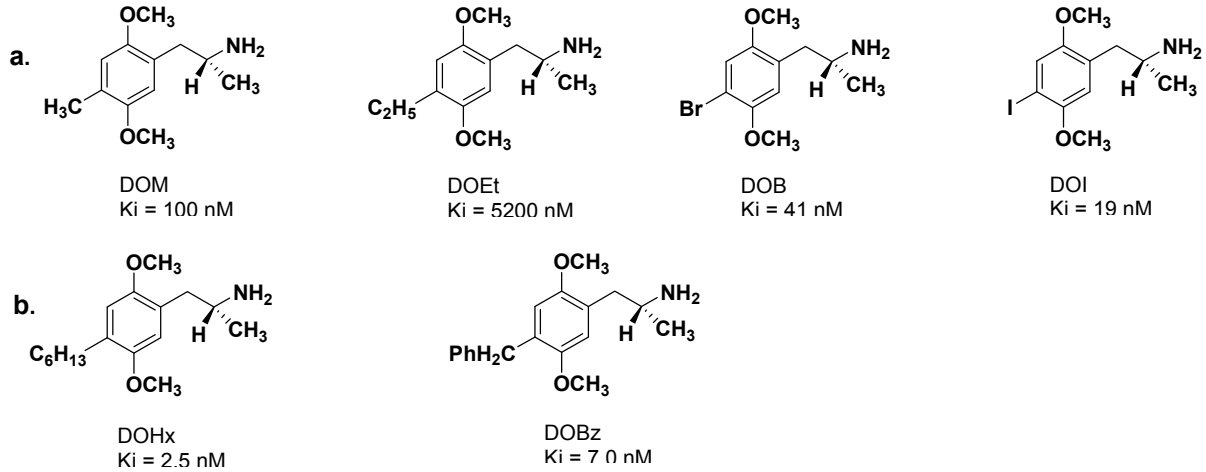

Figure 1.12: Dimethoxyphenylalkylamine derivatives with substituents in position 4: **a**. molecules with 5-HT_{2A}R partial agonistic activity, **b**. molecules with 5-HT_{2A}R antagonistic activity.

All these molecules contain a chiral centre in the alkyl chain. *In vitro* tests with DOB and DOI have clarified which enantiomer is the eutomer and which is the distomer (Johnson et al., 1987; Seggel et al., 1990). The HT_{2A}R affinity is two times higher for the *R* enantiomers than for the racemates. Therefore, the eutomers have an *R* configuration. A large number of compounds has been synthesised starting from DOB and DOI. This class of molecules and in particular DOB and DOI are also used as radioligands ([^{3}H]-DOB, [^{125}I]-DOI) for labelling 5-HT_2 receptors.

A very interesting class of tricyclic phenylalkylamines showing partial agonistic activity on 5-HT_{2A}R is represented by the general structure in Figure 1.13.

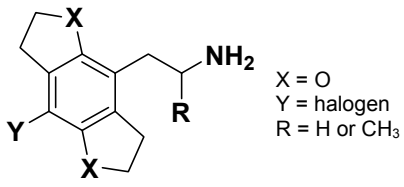

Figure 1.13: General structure of tricyclic phenylalkylamine 5-HT_{2A}R partial agonists.

In this structure a halogen substituent Y at the phenyl ring plays a key role for the affinity. The presence or absence of a alkyl substituent in α position (R) of the alkyl chain is of less influence. The tetrahydrobenzofuran ring representing a rigid analog of the dimethoxyphenyl moiety is in an optimal orientation for high 5-HT_{2A}R affinity (Oh et al., 2001). Figure 1.14 shows some tetrahydrobenzofuran derivatives.

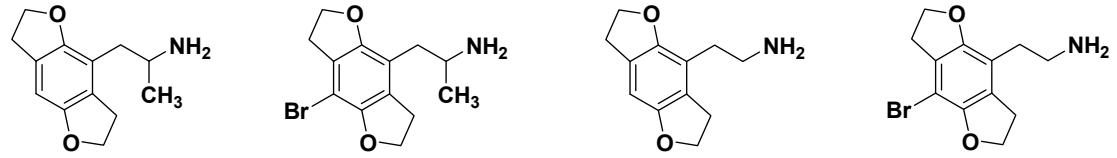

Figure 1.14: Selected tetrahydrobenzofuran derivatives with partial agonistic activity on the 5-HT_{2A}R and their K_i values.

1.5.1.3 Quinazolinediones – a new partial agonistic structure

A relatively new class of agonists identified in SAR studies focused on analogs of the 5-HT_{2A} receptor antagonist ketanserin is represented by quinazolinedione derivatives. EZS-8, quasi the quinazolinedioneethylamine moiety of ketanserin, unexpectedly displayed partial 5-HT_{2A}R agonistic activity. Further studies on this new chemical class led to the new potent partial agonist RH-34 (Figure 1.15).

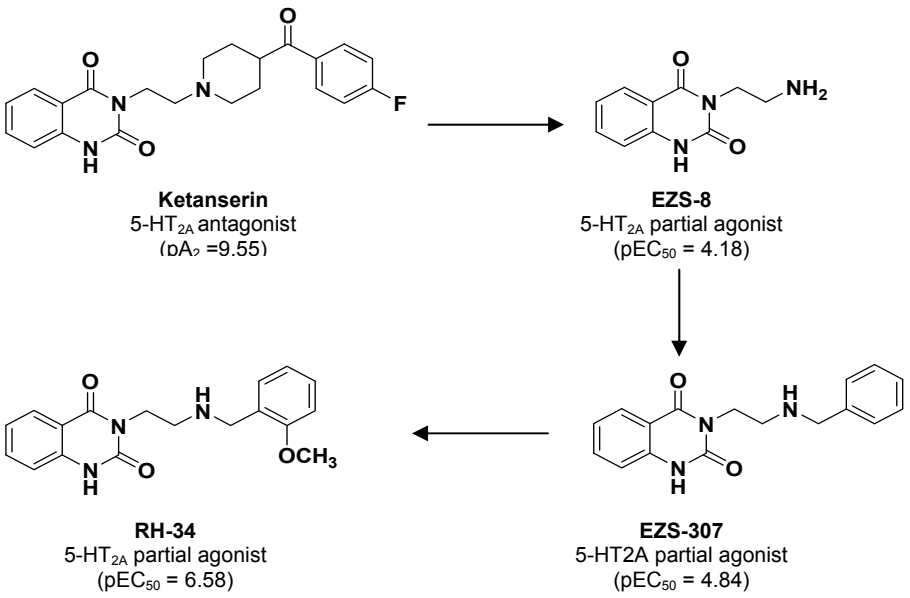

Figure 1.15: Lead discovery and optimization starting from the reference 5-HT_{2A} receptor antagonist ketanserin. Compound EZS-307 represents the new lead.

Surveying the different classes of arylalkylamines described above (including ergolines as cyclisized derivatives), it is possible to define three general requirements for optimal partial 5-HT_{2A}R agonistic activity:

1. An amino nitrogen (protonated at pH 7), separated from the aromatic ring by two carbon atoms.
2. Presence of two electron donors (or acceptors) in the aryl moiety.
3. A hydrophobic substituent at the aryl moiety increases affinity and activity.

1.5.2 5-HT_{2A}R antagonists

When serotonin interacts with the 5-HT_{2A}R, both peripheral and CNS processes are affected. Antagonists of this receptor (Figure 1.8) are potentially useful for the treatment of cardiovascular disorders (hypertension, ischemia, platelet aggregation and migraine), schizophrenia, anxiety, as well as sleep and nutritional disturbances.

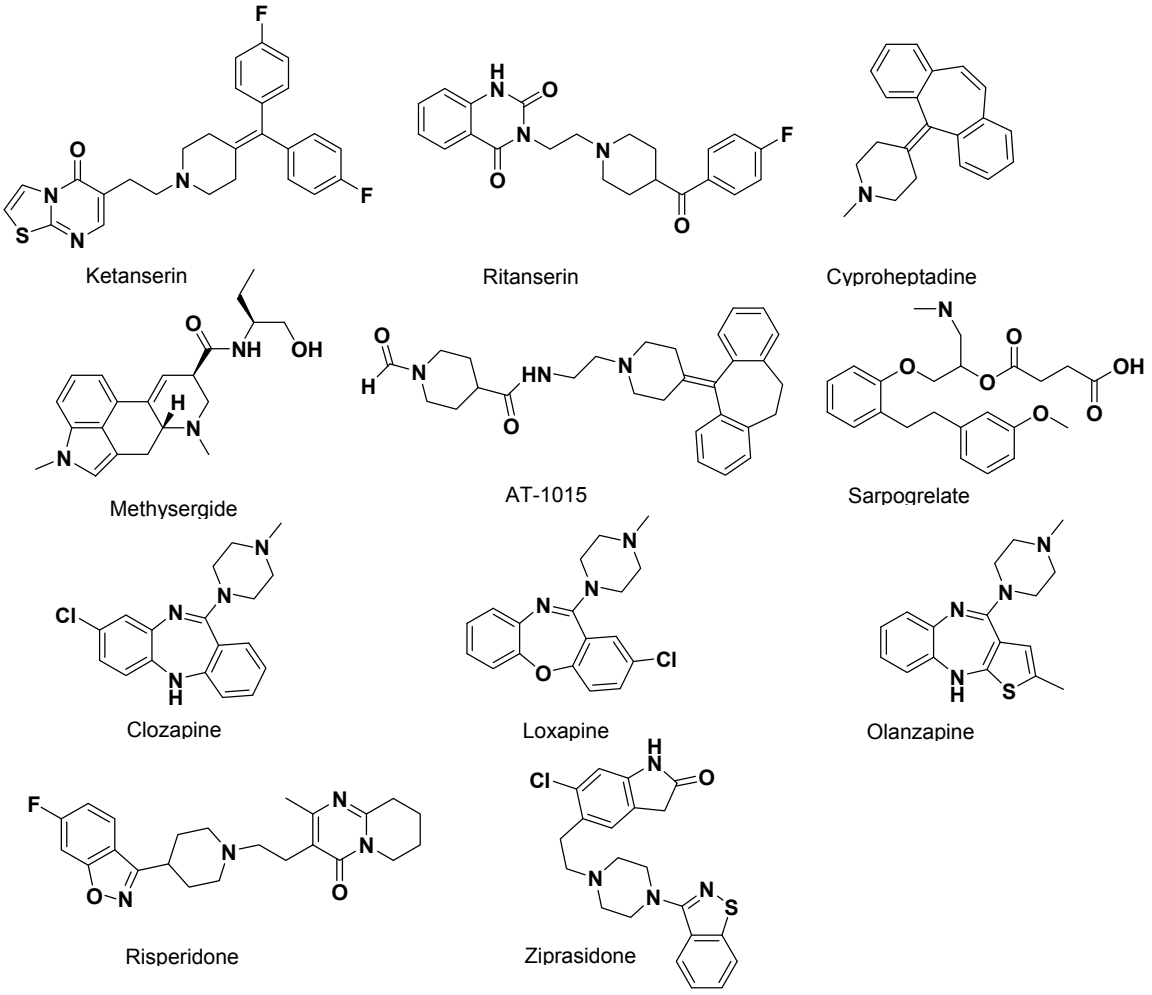

Figure 1.16: Structures of selected 5-HT_{2A}R antagonists active in the cardiovascular system and the CNS.

Many 5-HT_{2A}R antagonists contain an alkylpiperidine or alkylpiperazine partial structure. Ketanserin was discovered in 1981 (Leysen et al., 1981) and has been suggested to have therapeutic potential in hypertension as well as in peripheral vascular diseases (Brogden and Sorkin, 1990; Vanhoutte et al., 1988) and to protect the ischemic myocardium (Grover et al., 1993). Ketanserin is selective for 5-HT_{2A}R vs. 5-HT_{2C}R (15-80fold) and 5-HT_{2B}R (500-1000fold) (Jerman et al., 2001) and weakly active on 5-HT_3R, 5-HT_4R and members of the 5-HT_1R subfamily. It blocks 5-HT induced platelet adhesion. The antihypertensive effects of ketanserin are probably be due to its high affinity for α_1 adrenergic receptors. Ritanserin is a more specific 5-HT_{2A}R antagonist with low affinity for α_1-adrenergic receptors and, as it increases cerebral blood flow, can be used in the treatment of cerebral ischemia (Bach et al., 1998). Cyproheptadine, acting also as histamine H_1R and calcium

channel antagonist, blocks 5-HT activity on smooth muscles via the 5-HT_{2A}R but does not effectively lower blood pressure. (Xin et al., 1994). Another potent and selective 5-HT_{2A}R antagonist is AT-1015 inhibiting 5-HT_{2A}R-mediated platelet aggregation and 5-HT induced vasoconstriction (Kihara et al., 2000).

5-HT_{2A}R antagonists which cross the blood-brain barrier are antipsychotic and called atypical neuroleptics or atypical antipsychotics. In addition to their 5-HT_{2A}R antagonistic effect, they block different dopamine receptor subtypes. Most drugs of this kind of action belong to the class of tri- or tetracyclics. Clozapine was the first member, developed by Sandoz in 1961, and is the reference drug for atypical antipsychotics, used principally in treatment-resistant schizophrenia (Wahlbeck et al., 2000). The therapeutic effects are probably mediated by blocking both dopaminergic and serotonergic activity (Naheed and Green, 2001). Loxapine and olanzapine are molecules related to clozapine and are also used for the treatment of schizophrenia, but with less side effects. Other antipsychotic agents like risperidone and ziprasidone are not tricyclics but belong to the alkypiperidine class. They are 5-HT_{2A}R antagonists with more or less affinity on dopamine receptors and employed in the treatment of schizophrenia and bipolar disorders, respectively.

Also many ergolines show high affinity for 5-HT_{2A}R and 5-HT_{2C}R. An example is methysergide with additional partal agonistic activity on certain 5-HT_1 receptor subtypes. Methysergide is used for the prophylactic treatment of migraine. Another and quite new 5-HT_{2A}R antagonist acting on the cardiovascular system is sarpogrelate, not referable to the structural classes described above. This compound has been introduced as therapeutic agent for the treatment of ischemic diseases associated with thrombosis (Ito and Notsu, 1991).

1.6 References

Adams, M. D., S. E. Celniker, R. A. Holt, C. A. Evans, J. D. Gocayne, P. G. Amanatides, S. E. Scherer, P. W. Li, R. A. Hoskins, R. F. Galle, R. A. George, S. E. Lewis, S. Richards, M. Ashburner, S. N. Henderson, G. G. Sutton, J. R. Wortman, M. D. Yandell, Q. Zhang, L. X. Chen, R. C. Brandon, Y. H. Rogers, R. G. Blazej, M. Champe, B. D. Pfeiffer, K. H. Wan, C. Doyle, E. G. Baxter, G. Helt, C. R. Nelson, G. L. Gabor, J. F. Abril, A. Agbayani, H. J. An, C. Andrews-Pfannkoch, D. Baldwin, R. M. Ballew, A. Basu, J. Baxendale, L. Bayraktaroglu, E. M. Beasley, K. Y. Beeson, P. V. Benos, B. P. Berman, D. Bhandari, S. Bolshakov, D. Borkova, M. R. Botchan, J. Bouck, P. Brokstein, P. Brottier, K. C. Burtis, D. A. Busam, H. Butler, E. Cadieu, A. Center, I. Chandra, J. M. Cherry, S. Cawley, C. Dahlke, L. B. Davenport, P. Davies, B. de Pablos, A. Delcher, Z. Deng, A. D. Mays, I. Dew, S. M. Dietz, K. Dodson, L. E. Doup, M. Downes, S. Dugan-Rocha, B. C. Dunkov, P. Dunn, K. J. Durbin, C. C. Evangelista, C. Ferraz, S. Ferriera, W. Fleischmann, C. Fosler, A. E. Gabrielian, N. S. Garg, W. M. Gelbart, K. Glasser, A. Glodek, F. Gong, J. H. Gorrell, Z. Gu, P. Guan, M. Harris, N. L. Harris, D. Harvey, T. J. Heiman, J. R. Hernandez, J. Houck, D. Hostin, K. A. Houston, T. J. Howland, M. H. Wei, C. Ibegwam, et al., 2000, The genome sequence of Drosophila melanogaster: *Science*, v. **287**: p. 2185-95.

Aghajanian, G. K., and G. J. Marek, 1999, Serotonin and hallucinogens: *Neuropsychopharmacology*, v. **21**: p. 16S-23S.

Attwood, T. K., and J. B. Findlay, 1994, Fingerprinting G-protein-coupled receptors: *Protein Eng*, v. **7**: p. 195-203.

Bach, T., R. Prado, W. Zhao, B. D. Watson, and M. D. Ginsberg, 1998, Ritanserin, a 5-HT2 receptor antagonist, increase subcortical blood flow following photothombotic middle cerebral artery occlusion in rats: *Neurol Res*, v. **20**: p. 643-647.

Baxter, G., 1996, Novel discriminatory ligands for 5-HT_{2B} receptors: *Behav. Brain Res.*, v. **73**: p. 149-152.

Baxter, G., G. Kennett, F. Blaney, and T. Blackburn, 1995, 5-HT2 receptor subtypes: a family re-united? *Trends Pharmacol Sci*, v. **16**: p. 105-10.

Bennett, J. P., and S. H. Snyder, 1975, Stereospecific binding of *d*-lysergic acid diethylamide (LSD) to brain membrane: relationship to serotonin receptors: *Brain Res*, v. **94**: p. 523-544.

Bennett, J. P., and S. H. Snyder, 1976, Serotonin and lysergic acid diethylamide binding in rat brain membrane. Relationship to postsynaptic serotonin receptors: *Mol Pharmacol*, v. **12**: p. 373-389.

Boess, E. L., and I. L. Martin, 1994, Molecular biology of 5-HT receptors: *Neuropharmacology*, v. **33**: p. 275.

Bonaventure, P., D. Nepomuceno, K. Miller, J. Chen, C. Kuei, F. Kamme, D. T. Tran, T. W. Lovenberg, and C. Liu, 2005, Molecular and pharmacological characterization of serotonin 5-HT2A and 5-HT2B receptor subtypes in dog: *Eur J Pharmacol*, v. **513**: p. 181-92.

Bonhaus, D. W., C. Bach, A. DeSouza, F. H. Salazar, B. D. Matsuoka, P. Zuppan, H. W. Chan, and R. M. Eglen, 1995, The pharmacology and distribution of human 5-

hydroxytryptamine2B (5-HT2B) receptor gene products: comparison with 5-HT2A and 5-HT2C receptors: *Br J Pharmacol*, v. **115**: p. 622-8.

Bonhaus, D. W., K. K. Weinhardt, M. Taylor, A. DeSouza, P. M. McNeeley, K. Szczepanski, D. J. Fontana, J. Trinh, C. L. Rocha, M. W. Dawson, L. A. Flippin, and R. M. Eglen, 1997, RS-102221: a novel high affinity and selective, 5-HT2C receptor antagonist: *Neuropharmacology*, v. **36**: p. 621-9.

Bradley, P. B., G. Engel, W. Feniuk, J. R. Fozard, P. P. Humphrey, D. N. Middlemiss, E. J. Mylecharane, B. P. Richardson, and P. R. Saxena, 1986, Proposals for the classification and nomenclature of functional receptors for 5-hydroxytryptamine: *Neuropharmacology*, v. **25**: p. 563-76.

Brodie, B. B., and P. A. Shore, 1957, A concept for a role of serotonin and norepinephrine as chemical mediators in the brain: *Ann N Y Acad Sci*, v. **66**: p. 631-42.

Brogden, R. N., and E. M. Sorkin, 1990, Ketanserin. A review of its pharmacodynamic and pharmacokinetic properties, and therapeutic potential in hypertension and peripheral vascular disease: *Drugs*, v. **40**: p. 903-49.

Buck, F., W. Meyerhof, H. Werr, and D. Richter, 1991, Characterization of N- and C-terminal deletion mutants of the rat serotonin HT2 receptor in Xenopus laevis oocytes.: *Biochem Biophys Res Commun.*, v. **178**: p. 1421-1428.

Chambard, J.-C., E. van Obberghen-Schilling, R. J. Haslam, V. Vouret, and P. J., 1990, Chinese hamster serotonin (5-HT) type 2 receptor cDNA sequence.: *Nucleic Acids Res.*, v. **18**: p. 5282-5282.

Chen, K., W. Yang, and J. Grimsby, 1992, The human 5-HT_2 receptor is encoded by a multiple intron-exon gene: *Mol. Brain Res.*, v. **14**: p. 20-26.

Clapham, D. E., and E. J. Neer, 1993, New roles for G-protein (dimers in transmembrane signalling: *Nature*, v. **365**: p.,403 - 406.

Consortium, I. H. G. S., 2004, Finishing the euchromatic sequence of the human genome: *Nature*, v. **431**: p. 931-45.

Drews, J., 2000, Drug discovery: a historical perspective: *Science*, v. **287**: p. 1960-4.

Erspamer, V., and B. Asero, 1952, Identification of enteramine, the specific hormone of the enterochromaffin cell system, as 5-hydroxytryptamine: *Nature*, v. **169**: p. 800-1.

Erspamer, V., and B. Asero, 1953, Isolation of enteramine from extracts of posterior salivary glands of Octopus vulgaris and of Discoglossus pictus skin: *J Biol Chem*, v. **200**: p. 311-8.

Farrens, D. L., C. Altenbach, K. Yang, W. L. Hubbell, and H. G. Khorana, 1996, Requirement of rigid-body motion of transmembrane helices for light activation of rhodopsin: *Science*, v. **274**: p. 768-70.

Farrow, J. T., and H. Van Vunakis, 1972, Binding of d-lysergic acid diethylamide to subcellular fractions from rat brain: *Nature*, v. **237**: p. 164-6.

Foord, S., T. Bonner, R. Neubig, E. Rosser, J. Pin, A. Davenport, M. Spedding, and A. Harmar, 2005, International Union of Pharmacology. XLVI. G protein-coupled receptor lis: *Pharmacol Rev*, v. **57**: p. 279-88.

Fredriksson, R., and H. B. Schiöth, 2003, The G-Protein-Coupled-Receptor in the Human Genome Form Five Main Families. Phylogenetic Analysis, Paralogon Groups, and Fingerprint: *Mol Pharmacol*, v. **63**: p. 1256-1272.

Fredriksson, R., and H. B. Schiöth, 2005, The Repertoire of G-Protein-Coupled Receptor in Fully Sequence Genomes: *Mol Pharmacol*, v. **67**: p. 1414-1425.

Gaddum, J. H., and Z. P. Picarelli, 1957, Two kinds of tryptamine receptors: *Br. J. Pharmacol. Chemother*, v. **12**: p. 323-328.

Gether, U., S. Lin, P. Ghanouni, J. A. Ballesteros, H. Weinstein, and B. K. Kobilka, 1997, Agonists induce conformational changes in transmembrane domains III and VI of the beta2 adrenoceptor: *Embo J*, v. **16**: p. 6737-47.

Glennon, R. A., 1990, Do classical hallucinogens act as 5-HT2 agonists or antagonists? *Neuropsychopharmacology*, v. **3**: p. 509-17.

Glennon, R. A., R. Raghupathi, P. Bartyzel, M. Teitler, and S. Leonhardt, 1992, Binding of phenylalkylamine derivatives at 5-HT1C and 5-HT2 serotonin receptors: evidence for a lack of selectivity: *J Med Chem*, v. **35**: p. 734-40.

Glennon, R. A., R. Young, F. Benington, and R. D. Morin, 1982, Behavioral and serotonin receptor properties of 4-substituted derivatives of the hallucinogen 1-(2,5-dimethoxyphenyl)-2-aminopropane: *J Med Chem*, v. **25**: p. 1163-8.

Glennon, R. A., R. Young, J. A. Rosecrans, and M. J. Kallman, 1980, Hallucinogenic agents as discriminative stimuli: a correlation with serotonin receptor affinities: *Psychopharmacology (Berl)*, v. **68**: p. 155-8.

Grover, G. J., C. A. Sargent, S. Dzwonczyk, D. E. Normandin, and M. J. Antonaccio, 1993, Protective effect of serotonin (5-HT2) receptor antagonists in ischemic rat hearts: *J Cardiovasc Pharmacol*, v. **22**: p. 664-72.

Hamm, H. E., 1998, The many faces of G protein signaling: *J Biol Chem*, v. **273**: p. 669-672.

Hartig, P. R., 1989a, Molecular biology of 5-HT receptors: *Trends Pharmacol Sci*, v. **10**: p. 64-69.

Hasler, F., D. Bourquin, R. Brenneisen, T. Bar, and F. X. Vollenweider, 1997, Determination of psilocin and 4-hydroxyindole-3-acetic acid in plasma by HPLC-ECD and pharmacokinetic profiles of oral and intravenous psilocybin in man: *Pharm Acta Helv*, v. **72**: p. 175-84.

Hausdorff, W. P., M. G. Caron, and R. J. Lefkowitz, 1990, Turning off the signal: desensitization of beta-adrenergic receptor function.: *FASEB J.*, v. **4**: p. 3049.

Hebert, T. E., and M. Bouvier, 1998, Structural and functional aspects of G protein-coupled receptor oligomerization: *Biochem Cell Biol*, v. **76**: p. 1-11.

Heffter, A., 1896, Über Cacteenalkaloide: *Chem. Ber.*, v. **29**: p. 216-227.

Heller, W. A., and J. M. Baraban, 1987, Potent agonist activity of DOB at 5-HT2 receptors in guinea pig trachea: *Eur J Pharmacol*, v. **138**: p. 115-7.

Heuring, R. E., and S. J. Peroutka, 1987, Characterization of a novel 3H-5-hydroxytryptamine binding site subtype in bovine brain membranes: *J Neurosci*, v. **7**: p. 894-903.

Hofmann, A., 1979, How LSD originated: *J Psychedelic Drugs*, v. **11**: p. 53-60.

Hofmann, A., 1994, Notes and documents concerning the discovery of LSD. 1970: *Agents Actions*, v. **43**: p. 79-81.

Hopkins, A. L., and C. R. Groom, 2002, The druggable genome: *Nat Rev Drug Discov*, v. **1**: p. 727-30.

Horita, A., 1963, Some biochemical studies on psilocybin and psilogin: *J Neuropsychiatr*, v. **4**: p. 270-3.

Horita, A., and L. J. Weber, 1961, The enzymic dephosphorylation and oxidation of psilocybin and psilocin by mammalian tissue homogenates: *Biochem Pharmacol*, v. **7**: p. 47-54.

Hoyer, D., D. E. Clarke, J. R. Fozard, P. R. Hartig, G. R. Martin, E. J. Mylecharane, P. R. Saxena, and P. P. Humphrey, 1994, International Union of Pharmacology classification of receptors for 5-hydroxytryptamine (Serotonin): *Pharmacol Rev*, v. **46**: p. 157-203.

Hoyer, D., J. P. Hannon, and G. R. Martin, 2002, Molecular, pharmacological and functional diversity of 5-HT receptors: *Pharmacol Biochem Behav*, v. **71**: p. 533-54.

http://www.ebi.ac.uk/interpro/ISearch?query=gpcr.

http://www.gpcr.org/.

Iismaa, T. P., T. J. Biden, and J. Shine, 1995, G Protein-Coupled Receptors, 1-181 p.

Isbell, H., E. J. Miner, and C. R. Logan, 1959, Relationships of psychotomimetic to anti-serotonin potencies of congeners of lysergic acid diethylamide (LSD-25): *Psychopharmacologia*, v. **1**: p. 20-8.

Ismaiel, A. M., M. Titeler, K. J. Miller, T. S. Smith, and R. A. Glennon, 1990, 5-HT1 and 5-HT2 binding profiles of the serotonergic agents alpha-methylserotonin and 2-methylserotonin: *J Med Chem*, v. **33**: p. 755-8.

Ito, K., and T. Notsu, 1991, Effect of spargolete hydrochloride (MCI-9042) on peripheral circulation of chronic arterial occlusive diseases: *J Clin Ther Med*, v. **7**: p. 1243-1251.

Jacoby, E., R. Bouhelal, M. Gerspacher, and K. Seuwen, 2006, The 7 TM G-protein-coupled receptor target family: *ChemMedChem*, v. **1**: p. 761-82.

Jerman, J. C., S. J. Brough, T. Gager, M. Wood, M. C. Coldwell, D. Smart, and D. N. Middlemiss, 2001, Pharmacological characterisation of human 5-HT2 receptor subtypes: *Eur J Pharmacol*, v. **414**: p. 23-30.

Johnson, M. P., M. Baez, J. D. Kursar, and D. L. Nelson, 1995, Species differences in 5-HT2A receptors: cloned pig and rhesus monkey 5-HT2A receptors reveal conserved transmembrane homology to the human rather than rat sequence: *Biochim Biophys Acta*, v. **1236**: p. 201-6.

Johnson, M. P., A. J. Hoffman, D. E. Nichols, and C. A. Mathis, 1987, Binding to the serotonin 5-HT2 receptor by the enantiomers of 125I-DOI: *Neuropharmacology*, v. **26**: p. 1803-6.

Julius, D., K. N. Huang, T. J. Livelli, R. Axel, and T. M. Jessell, 1990, The 5HT2 receptor defines a family of structurally distinct but functionally conserved serotonin receptors: *Proc Natl Acad Sci U S A*, v. **87**: p. 928-32.

Kehene.

Kennett, G. A., F. Bright, B. Trail, G. S. Baxter, and T. P. Blackburn, 1996a, Effects of the 5-HT2B receptor agonist, BW 723C86, on three rat models of anxiety: *Br J Pharmacol*, v. **117**: p. 1443-8.

Kennett, G. A., F. Bright, B. Trail, T. P. Blackburn, and G. J. Sanger, 1997a, Anxiolytic-like actions of the selective 5-HT4 receptor antagonists SB 204070A and SB 207266A in rats: *Neuropharmacology*, v. **36**: p. 707-12.

Kennett, G. A., M. D. Wood, F. Bright, J. Cilia, D. C. Piper, T. Gager, D. Thomas, G. S. Baxter, I. T. Forbes, P. Ham, and T. P. Blackburn, 1996b, In vitro and in vivo profile of SB 206553, a potent 5-HT2C/5-HT2B receptor antagonist with anxiolytic-like properties: *Br J Pharmacol*, v. **117**: p. 427-434.

Kennett, G. A., M. D. Wood, F. Bright, B. Trail, G. Riley, V. Holland, K. Y. Avenell, T. Stean, N. Upton, S. Bromidge, I. T. Forbes, A. M. Brown, D. N. Middlemiss, and T. P. Blackburn, 1997b, SB 242084, a selective and brain penetrant 5-HT2C receptor antagonist: *Neuropharmacology*, v. **36**: p. 609-20.

Kihara, H., K. Hirose, H. Koganei, N. Sasaki, H. Yamamoto, A. Kimura, T. Nishimori, M. Shoji, and R. Yoshimoto, 2000, AT-1015, a novel serotonin (5-HT)2 receptor antagonist, blocks vascular and platelet 5-HT2A receptors and prevents the laurate-induced peripheral vascular lesion in rats: *J Cardiovasc Pharmacol*, v. **35**: p. 523-30.

King, N., C. T. Hittinger, and S. B. Carroll, 2003, Evolution of key cell signaling and adhesion protein families predates animal origins: *Science*, v. **301**: p. 361-3.

Kolakowski, L. J., 1994, GCRDb: a G-protein-coupled receptor database: *Receptors Channels*, v. **2**: p. 1-7.

Kuemmerle, J. F., and K. S. Murthy, 2001, Coupling of the insulin-like growth factor-I receptor tyrosine kinase to Gi2 in human intestinal smooth muscle: Gbetagamma - dependent mitogen-activated protein kinase activation and growth: *J Biol Chem*, v. **276**: p. 7187-94.

Lefkowitz, R. J., S. Cotecchia, P. Samama, and T. Costa, 1993, Constitutive activity of receptors coupled to guanine nucleotide regulatory proteins: *Trends Pharmacol Sci*, v. **14**: p. 303-7.

Leysen, J. E., F. Awouters, L. Kennis, P. M. Laduron, J. Vandenberk, and P. A. Janssen, 1981, Receptor binding profile of R 41 468, a novel antagonist at 5-HT2 receptors: *Life Sci*, v. **28**: p. 1015-22.

Leysen, J. E., C. J. Niemegeers, J. P. Tollenaere, and P. M. Laduron, 1978, Serotonergic component of neuroleptic receptors: *Nature*, v. **272**: p. 168-71.

López-Giménez, J. F., G. Mengod, J. M. Palacios, and e. al., 1997, Selective visualization of rat 5-HT_{2A} receptors by autoradiography with [^{3}H]MDL 100907: *Naunyn Schmiedebergs Arch Pharmacol*, v. **356**: p. 446-454.

Lyon, R. A., M. Titeler, M. R. Seggel, and R. A. Glennon, 1988, Indolealkylamine analogs share 5-HT2 binding characteristics with phenylalkylamine hallucinogens: *Eur J Pharmacol*, v. **145**: p. 291-7.

Marchbanks, R. M., 1966, Serotonin binding to nerve ending particles and other preparations from rat brain: *J Neurochem*, v. **13**: p. 1481-93.

Marchbanks, R. M., 1967, Inhibitory effect of lysergic acid derivate and reserpine on 5-HT binding to nerve endings particle: *Biochem Pharmacol*, v. **16**: p. 1971-1979.

Marek, G. J., and G. K. Aghajanian, 1996, LSD and the phenethylamine hallucinogen DOI are potent partial agonists at 5-HT2A receptors on interneurons in rat piriform cortex: *J Pharmacol Exp Ther*, v. **278**: p. 1373-82.

Masuda, K., C. Hashizume, N. Ogata, T. Kikusui, Y. Takeuchi, and M. Y., 2004, Sequencing of canine 5-hydroxytriptamine receptor (5-HTR) 1B, 2A, 2C genes and identification of polymorphisms in the 5-HTR1B gene

J. Vet. Med. Sci. 66:965-972(2004). *J. Vet. Med. Sci.*, v. **66**: p. 965-972.

Naheed, M., and B. Green, 2001, Focus on clozapine: *Curr Med Res Opin*, v. **17**: p. 223-9.

Nelson, D. L., 1993, The serotonin$_2$ (5-HT_2) subfamily of receptors: pharmacological challanges: *Med. Chem. Res.*, v. **3**: p. 306.

Nichols, D., 2004, Hallucinogens: *Pharmacology & Therapeutics*, v. **101**: p. 131-181.

Nichols, D. E., 1986, Studies of the relationship between molecular structure and hallucinogenic activity: *Pharmacol Biochem Behav*, v. **24**: p. 335-40.

Nichols, D. E., D. H. Lloyd, M. P. Johnson, and A. J. Hoffman, 1988, Synthesis and serotonin receptor affinities of a series of enantiomers of alpha-methyltryptamines: evidence for the binding conformation of tryptamines at serotonin 5-HT1B receptors: *J Med Chem*, v. **31**: p. 1406-12.

O'Dowd, B. F., M. Hnatowich, J. W. Regan, W. M. Leader, C. M.G., and R. J. Lefkowitz, 1988, Site-directed mutagenesis of the cytoplasmic domains of the human beta 2-adrenergic receptor. Localization of regions involved in G protein-receptor coupling: *J Biol Chem.*, v. **263**: p. 15985-15992.

Oh, S. J., H.-J. Ha, and H. K. Lee, 2001, Serotonin Receptor and Transporter Ligands-Current Status: *Current Medicinal Chemistry*, v. **8**: p. 999-1034.

Pazos, A., R. Cortes, and J. M. Palacios, 1985, Quantitative autoradiographic mapping of serotonin receptors in the rat brain. II. Serotonin-2 receptors: *Brain Res*, v. **346**: p. 231-49.

Pazos, A., D. Hoyer, and J. M. Palacios, 1985b, The binding of serotoninergic ligands to the porcine choroid pexus: characterization of a new type of serotonin recognition site: *Eur. J. Pharmacol.*, v. **106**: p. 539-546.

Pedigo, N. W., H. I. Yamamura, and D. L. Nelson, 1981, Discrimination of multiple [3H]5-hydroxytryptamine binding sites by the neuroleptic spiperone in rat brain: *J Neurochem*, v. **36**: p. 220-6.

Peroutka, S. J., 1990, 5-hydroxytriptamine receptor subtypes: *Pharmacol. Toxycol.*, v. **67**: p. 373-383.

Peroutka, S. J., 1994, Molecular biology of serotonin (5-HT) receptors: *Synapse*, v. **18**: p. 241-60.

Peroutka, S. J., and S. H. Snyder, 1979, Serotonin receptors binding site affected differentially by guanine nucleotides.: *Mol Pharmacol*, v. **16**: p. 700-706.

Rands, E., M. R. Candelore, A. H. Cheung, W. S. Hill, C. D. Strader, and R. A. Dixon, 1990, Mutational analysis of beta-adrenergic receptor glycosylation: *J Biol Chem*, v. **265**: p. 10759-64.

Rapport, M. M., A. A. Green, and I. H. Page, 1948, Serum vasoconstrictor, serotonin; isolation and characterization: *J Biol Chem*, v. **176**: p. 1243-51.

Rasmussen, K., R. A. Glennon, and G. K. Aghajanian, 1986, Phenethylamine hallucinogens in the locus coeruleus: potency of action correlates with rank order of 5-HT2 binding affinity: *Eur J Pharmacol*, v. **132**: p. 79-82.

Rasmussen, S. G., A. D. Jensen, G. Liapakis, P. Ghanouni, J. A. Javitch, and U. Gether, 1999, Mutation of a highly conserved aspartic acid in the beta2 adrenergic receptor: constitutive activation, structural instability, and conformational rearrangement of transmembrane segment 6: *Mol Pharmacol*, v. **56**: p. 175-84.

Rothlin, E., 1957, Pharmacology of lysergic acid diethylamide and some of its related compounds: *J Pharm Pharmacol*, v. **9**: p. 569-87.

Saltzman, A. G., B. Morse, M. M. Whitman, Y. Ivanshchenko, M. Jaye, and S. Felder, 1991, Cloning of the human serotonin 5-HT2 and 5-HT1C receptor subtypes.: *Biochem. Biophys. Res. Commun.*, v. **181**: p. 1469-1478.

Samama, P., S. Cotecchia, T. Costa, and R. J. Lefkowitz, 1993, A mutation-induced activated state of the β_2-adrenergic receptor. Extending the ternary complex model: *J Biol Chem*, v. **268**: p. 4625-4636.

Sanders-Bush, E., K. D. Burris, and K. Knoth, 1988, Lysergic acid diethylamide and 2,5-dimethoxy-4-methylamphetamine are partial agonists at serotonin receptors linked to phosphoinositide hydrolysis: *J Pharmacol Exp Ther*, v. **246**: p. 924-8.

Schmuck, K., C. Ullmer, P. Engels, and H. Lubbert, 1994, Cloning and functional characterization of the human 5-HT2B serotonin receptor: *FEBS Lett*, v. **342**: p. 85-90.

Seggel, M. R., M. Y. Yousif, R. A. Lyon, M. Titeler, B. L. Roth, E. A. Suba, and R. A. Glennon, 1990, A structure-affinity study of the binding of 4-substituted analogues of 1-(2,5-dimethoxyphenyl)-2-aminopropane at 5-HT2 serotonin receptors: *J Med Chem*, v. **33**: p. 1032-6.

Seifert, R., and K. Wenzel-Seifert, 2002, Constitutive activity of G-protein-coupled receptors: cause of disease and common property of wild-type receptors: *Naunyn Schmiedebergs Arch Pharmacol*, v. **366**: p. 381-416.

Sorensen, S. M., J. H. Kehne, G. M. Fadayel, T. M. Humphreys, H. J. Ketteler, C. K. Sullivan, V. L. Taylor, and C. J. Schmidt, 1993, Characterization of the 5-HT2 receptor antagonist MDL 100907 as a putative atypical antipsychotic: behavioral, electrophysiological and neurochemical studies: *J Pharmacol Exp Ther*, v. **266**: p. 684-91.

Späth, E., 1919, Übrer Die Anhalonium Alkaloidie. 1. Anhalin and Mezcalin.: *Monatsh. Chem.*, v. **40**: p. 129-154.

Sprang, S. R., 1997, G protein mechanisms: insights from structural analysis: *Annu Rev Biochem*, v. **66**: p. 639-78.

Stam, N. J., F. Van Huizen, C. Van Alebeek, J. Brands, R. Dijkema, J. A. Tonnaer, and W. Olijve, 1992a, Genomic organization, coding sequence and functional expression of human 5-HT2 and 5-HT1A receptor genes: *Eur J Pharmacol*, v. **227**: p. 153-62.

Stam, U., F. Vanhuize, and C. Vanalebeek, 1992b, Genomic organization, coding sequence and functional expression of human 5-HT_2 and 5-HT_{1A} receptor genes: *Eur. J. Pharmacol.*, v. **227**: p. 153-162.

Sternweis, P. C., 1994, The active role of beta gamma in signal transduction: *Curr Opin Cell Biol*, v. **6**: p. 198-203.

Twarog, B. M., and I. H. Page, 1953, Serotonin content of some mammalian tissues and urine and a method for its determination: *Am. J. Physiol. 175:157-161.*, v. **175**: p. 157-161.

Urban, J., W. Clarke, M. von Zastrow, D. Nichols, B. Kobilka, H. Weinstein, J. Javitch, B. Roth, A. Christopoulos, P. Sexton, K. Miller, M. Spedding, and R. F. s. a. c. c. o. q. p. J. o. P. A. E. T. Mailman, 2007, Functional selectivity and classical concepts of quantitative pharmacology: *Journal of Pharmacology And Experimental Therapeutics*, v. **320**: p. 1–13.

Vanhoutte, P., A. Amery, W. Birkenhager, A. Breckenridge, F. Buhler, A. Distler, J. Dormandy, A. Doyle, E. Frohlich, L. Hansson, and et al., 1988, Serotoninergic mechanisms in hypertension. Focus on the effects of ketanserin: *Hypertension*, v. **11**: p. 111-33.

Vassilatis, D. K., J. G. Hohmann, H. Zeng, F. Li, J. E. Ranchalis, M. T. Mortrud, A. Brown, S. S. Rodriguez, J. R. Weller, A. C. Wright, J. E. Bergmann, and G. A. Gaitanaris, 2003, The G protein-coupled receptor repertoires of human and mouse: *Proc Natl Acad Sci U S A*, v. **100**: p. 4903-8.

Wahlbeck, K., M. Cheine, and M. A. Essali, 2000, Clozapine versus typical neuroleptic medication for schizophrenia: *Cochrane Database Syst Rev*: p. CD000059.

Watts, S. W., M. L. Cohen, P. Q. Mooney, B. G. Johnson, D. D. Schoepp, and B. M., 1994, Disruption of potential alpha-helix in the G loop of the guinea pig 5-hydroxytryptamine2 receptor does not prevent receptor coupling to phosphoinositide hydrolysis: *J. Neurochem.*, v. **62**: p. 934-943.

Xin, H. B., B. H. Zhang, and H. J. Shen, 1994, [Protective effects of cyproheptadine on myocardial reperfusion injury in isolated rat hearts]: *Zhongguo Yao Li Xue Bao*, v. **15**: p. 253-7.

Yang, W., K. Chen, N. C. Lan, T. K. Gallaher, and S. J.C., 1992, Gene structure and expression of the mouse 5-HT2 receptor: *J. Neurosci. Res.*, v. **33**: p. 196-204.

Yu, L., H. Nguyen, H. Le, L. J. Bloem, C. A. Kozak, B. J. Hoffman, T. P. Snutch, H. A. Lester, N. Davidson, and H. Lubbert, 1991, The mouse 5-HT1C receptor contains eight hydrophobic domains and is X-linked: *Brain Res Mol Brain Res*, v. **11**: p. 143-9.

Chapter 2
Scope and Objective

Serotonin (5-hydroxytryptamine, 5-HT) receptors belong, with one exception, to the class of G-protein coupled neurotransmitter receptors (GPCR). Minor structural modifications of their ligands often result in major changes of the qualitative activity profile (Heim et al., 1998; Pertz et al., 2000). E.g., structurally closely related molecules may behave as full agonists, partial agonists or pure, "silent" antagonists in functional *in-vitro* assays on isolated organs. The rational base of such phenomena is not known up to date. Their investigation can considerably contribute to our knowledge about how signal molecules activate receptors at the molecular level.

In the context of SAR studies on chiral und achiral ligands of 5-HT_{2A} receptors (Elz et al., 2002; Heim et al., 2002), a structural concept has been derived by which the partial agonistic activity of mostly less potent 5-HT_{2A} agonistic primary amines as serotonin (5-HT), 3-(2-aminoethyl)quinazoline-2,4-dione, mescaline, and 1-(4-bromo-2,5-dimethoxyphenyl)-isopropylamine (DOB) was increased by a factor of 50 to 2000 (Elz et al., 2002; Heim et al., 1998; Pertz et al., 2000). The most interesting derivatives are partial agonists (E_{max} 30-60% in vascular *in-vitro* assays on rats) and up to 400-1400 times more potent than 5-HT. This was obtained by introduction of an *ortho*-methoxybenzyl or -hydroxybenzyl substituent at the amine nitrogen and has been successfully confirmed, e. g., in a series of phenethylamines related to mescaline.

The present study was based on a series of 51 arylethylamines from the group of S. Elz. All the compounds are 5-HT_{2A}R partial agonists and belong to three different structural classes, (1) indoles, (2) methoxybenzenes (including benzodifurans as cyclic analogs) and (3) quinazolinediones. The aim of the project was to analyze the

quantitative structure-activity relationships (QSAR) and to suggest 5-HT_{2A}R binding modes. Following a hierarchical strategy, different methods should be applied which all contribute to the investigation of ligand-receptor interactions: fragment regression analysis (FRA), receptor modeling, docking studies and 3D QSAR approaches (comparative molecular field analysis, CoMFA, and comparative molecular similarity index analysis, CoMSIA).

Initially homology models of the human and rat 5-HT_{2A}R had to be derived from the bovine rhodopsin crystal structure (Palczewski et al., 2000). During the last phase of the project and after completion of the QSAR study, the crystal structure of the human β_2-adrenoceptor was released (Cherezov et al., 2007; Rasmussen et al., 2007; Rosenbaum et al., 2007). With this template, more reliable homology 5-HT_{2A}R models have been possible. Therefore all the structure-based methods and analyses applied before were to be repeated, also offering the opportunity to compare the models and docking results from both approaches.

Due to the similarity of GPCRs and also of both templates in the structurally conserved regions of the seven transmembrane domains, homology modeling was expected to yield reliable structural models of human and rat 5-HT_{2A} receptors. Conserved intramolecular interactions predicted to be involved in receptor stabilization and to play a functional role as well as putative ligand binding sites had to be explored considering *in-vitro* mutagenesis data and SAR of agonists and partial agonists. The docking of representative compounds of each structural class was to suggest common and/or individual ligand-receptor interactions which must not disagree with the fragment regression analysis and with the ligand-binding properties of receptor mutants. The docking poses should serve as templates for a common, binding-site based alignment of the whole series. Based on this alignment, the CoMFA and CoMSIA approaches were to analyze the QSAR in detail, leading to interaction fields which may be projected onto the binding site models and, by this, may refine the exploration of the SAR and the ligand-receptor interactions.

Since the series to be analyzed consists of partial agonists assumed to stabilize either a specific, partially active state of the receptor or a fully active state to a lesser extent than agonists, and since the existing crystal structures represent inactive states, more informations about active receptor conformations are needed. Based on models of different rhodopsin states (*refs. Ishiguro*), a homology modeling study on corresponding 5-HT_{2A}R states suggested to be specific to agonist and partial agonist

binding, respectively, was to be performed. Two photointermediates in the rhodopsin photocascade, metarhodopsin I_{380}, and metarhodopsin II, should serve as templates for the partially active and the fully active h5-HT_{2A}R state, respectively. The homology models to be derived and docking studies with representative partial agonists and agonists should provide informations on specific interhelical and ligand-receptor interactions accounting for differences between active and inactive states, for the stabilization of the individual conformations and for possible reasons that the compounds of the arylethylamine series act as partial agonists.

In summary, this thesis was aimed to investigate the QSAR of 5-HT_{2A}R partial agonists at a structure-based level and to provide reasonable suggestions how the compounds interact with the receptor.

2.1 References

Cherezov, V., D. M. Rosenbaum, M. A. Hanson, S. G. Rasmussen, F. S. Thian, T. S. Kobilka, H. J. Choi, P. Kuhn, W. I. Weis, B. K. Kobilka, and R. C. Stevens, 2007, High-resolution crystal structure of an engineered human beta2-adrenergic G protein-coupled receptor: *Science*, v. **318**: p. 1258-65.

Elz, S., T. Kläß, U. Warnke, and H. H. Pertz, 2002, Developpement of highly potent partial agonists and chiral antagonists as tool for the stsudy of 5-HT2A-receptor mediated function: *Naunyn-Schmiedeberg's Arch. Pharmacol*, v. **365**: p. R29.

Heim, R., H. H. Pertz, I. Walther, and S. Elz, 1998, Congeners of 3-(2-Benzylaminoethyl)-2,4-quinazolindione: partial agonists for rat vascular 5-HT2A receptors: *Naunyn-Schmiedeberg's Arch. Pharmacol*, v. **358**: p. R105.

Heim, R., H. H. Pertz, M. Zabel, and S. Elz, 2002, Stereoselective synthesis, absolute configuration and 5-HT_{2A} agonism of chiral 2-methoxybenzylamines: *Arch. Pharm. Pharm. Med. Chem.*, v. **335**: p. 82.

Palczewski, K., T. Kumasaka, T. Hori, C. A. Behnke, H. Motoshima, B. A. Fox, I. Le Trong, D. C. Teller, T. Okada, R. E. Stenkamp, M. Yamamoto, and M. Miyano, 2000, Crystal structure of rhodopsin: A G protein-coupled receptor: *Science*, v. **289**: p. 739-45.

Pertz, H. H., R. Heim, and S. Elz, 2000, *N*-Benzylated Phenylethanamines are Highly Potent Partial Agonists at 5-HT_{2A} Receptors: *Arch. Pharm. Pharm. Med. Chem.*, v. **333**: p. 30.

Rasmussen, S. G., H. J. Choi, D. M. Rosenbaum, T. S. Kobilka, F. S. Thian, P. C. Edwards, M. Burghammer, V. R. Ratnala, R. Sanishvili, R. F. Fischetti, G. F. Schertler, W. I. Weis, and B. K. Kobilka, 2007, Crystal structure of the human beta2 adrenergic G-protein-coupled receptor: *Nature*, v. **450**: p. 383-7.

Rosenbaum, D. M., V. Cherezov, M. A. Hanson, S. G. Rasmussen, F. S. Thian, T. S. Kobilka, H. J. Choi, X. J. Yao, W. I. Weis, R. C. Stevens, and B. K. Kobilka, 2007, GPCR engineering yields high-resolution structural insights into beta2-adrenergic receptor function: *Science*, v. **318**: p. 1266-73.

Chapter 3
Computational Methods

3.1 GPCR homology models in medicinal chemistry

Direct and detailed insights into GPCR structures were limited for a long time. Today, however, the crystal structures of two GPCRs are available:

1. The 2.8 Å resolution structure of bovine rhodopsin published in 2000 (Palczewski et al., 2000), and four additional structures which can be retrieved from the Brookhaven Protein Data Bank (PDB) (Bernstein et al., 1977) by the identity codes 1F88 (Palczewski et al., 2000), 1HZX (Teller et al., 2001), 1L9H (Okada et al., 2002), 1GZM (Li et al., 2004), and 1U19 (Okada et al., 2004).
2. Crystal structures of the first GPCR, the human β_2 adrenoceptor, resolved in 2007 with different resolution (3.7 Å, 3.4 Å and the best 2.4 Å) The PDB identity codes are 2R4R, 2R4S (Rasmussen et al., 2007) and 2RH1 (Cherezov et al., 2007; Rasmussen et al., 2007; Rosenbaum et al., 2007).

The crystal structure of bovine rhodopsin has been used for 7 years as template for modeling of GPCRs. With the acquisition of the β_2 adrenoceptor the world of GPCR modeling is going to change in particular with respect to more reliable approximations of the ligand binding sites of biogenic amine receptors.

In general the modeling of a GPCR based on a homologous template is named homology modeling. The lack of detailed information about GPCR structures led to the quest for three dimensional (3D) structural models. Knowledge-based approaches were developed to predict the 3D structure of proteins based on experimental data of the 3D structure of homologous reference proteins. Using these approaches it

is possible to provide insight into molecular mechanisms of GPCR function and activity (Kristiansen, 2004). The steps used to predict the specific role of amino acids for the binding of ligands and the regulation of GPCR activity are shown in Figure 3.1. The prediction can subsequently be used as guideline for the construction and characterization of point mutations, studies of ligand-receptor interaction, and the design of new leads by application of flexible docking and virtual screening methods (Bissantz et al., 2003).

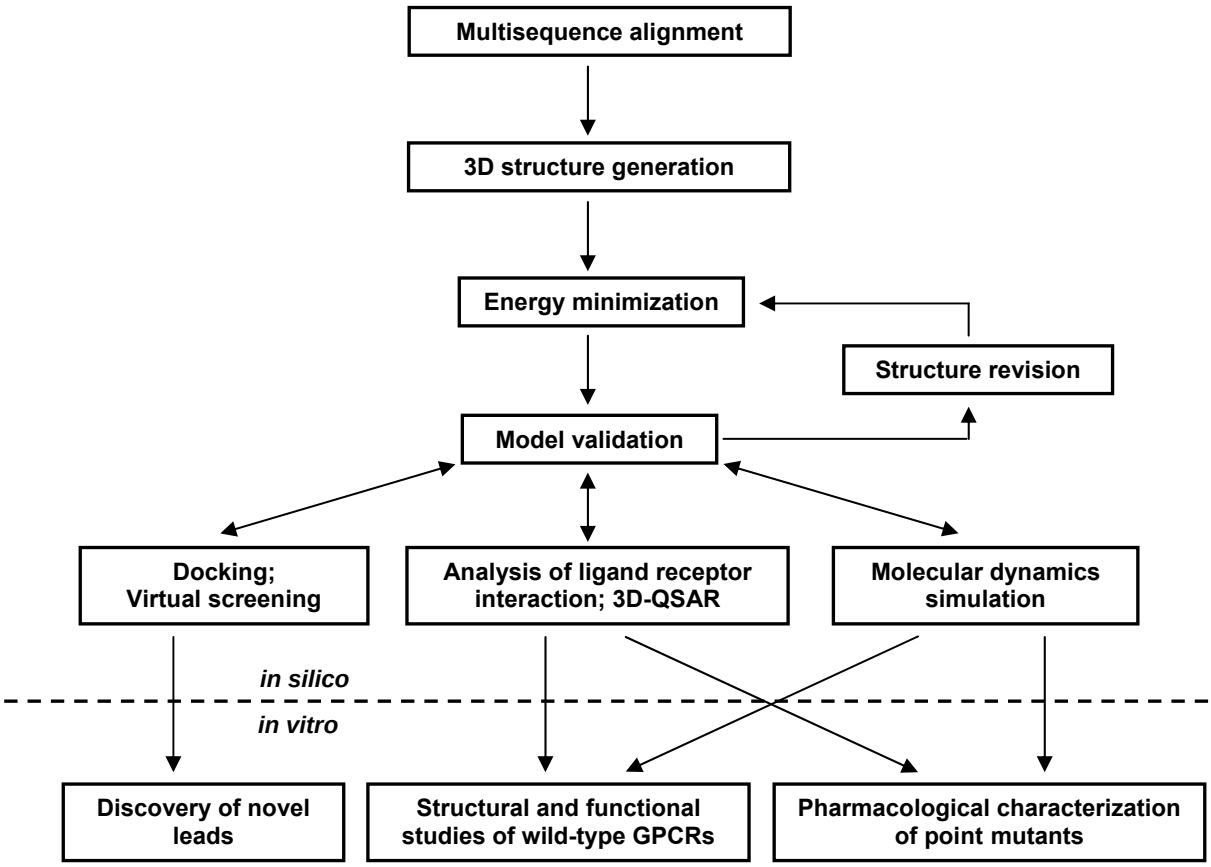

Figure 3.1: Flowchart of steps in homology modeling and possible application of homology models in computational (**in silico**) medicinal chemistry and **in vitro** pharmacology.

3.2 Protein Database

The first step in homology modeling is to obtain the amino acids sequence of the protein from a protein database. These and additional informations from the database website are used with different aims such as the prediction of the secondary and tertiary structure of the protein and the identification of functional properties (Figure 3.2).

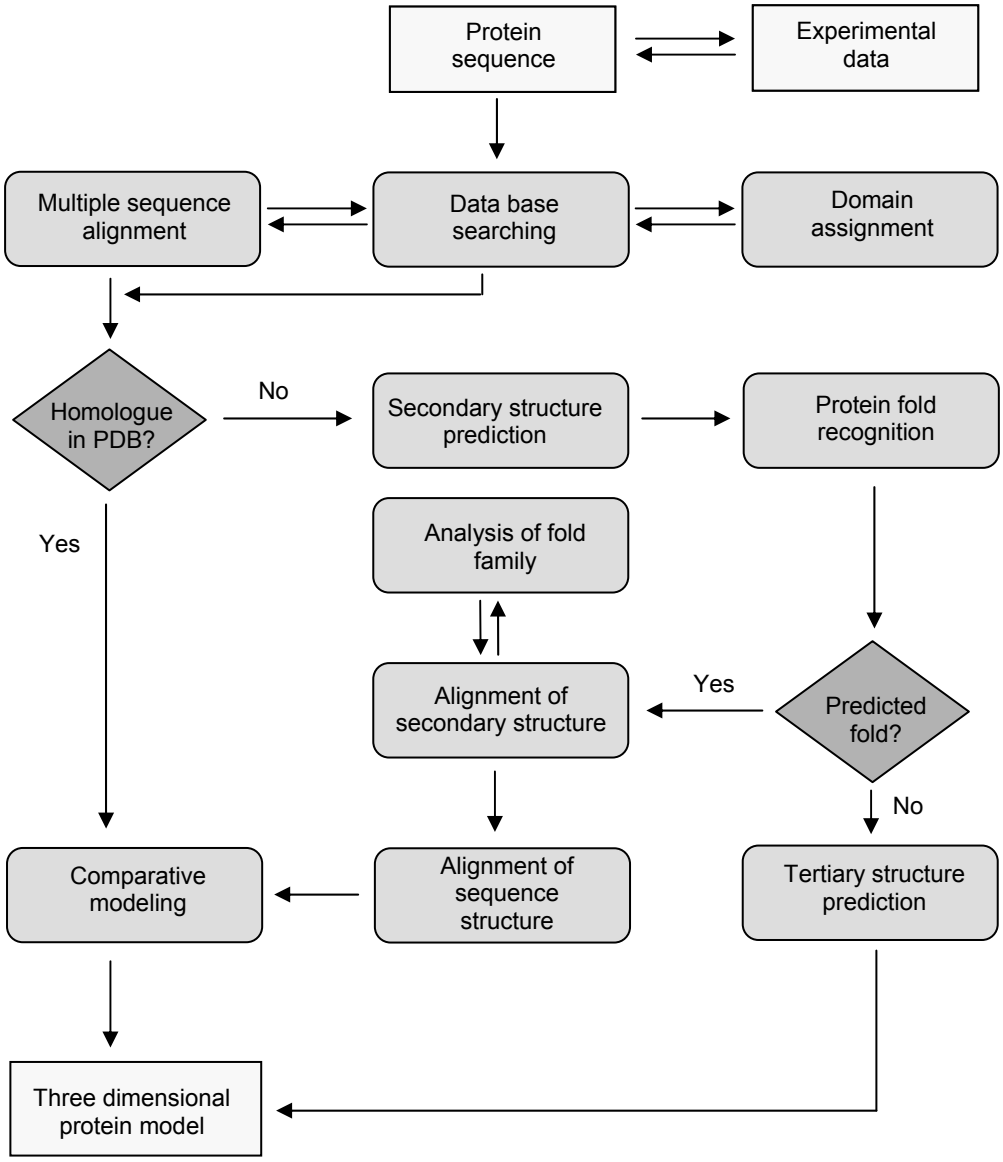

Figure 3.2: Flowchart for the prediction of a protein tertiary structure

Of particular relevance are the databases of three dimensional structures such as the Cambridge Structure Database, CSD (Allen, 2002) and the Protein Data Bank, PDB

(Berman et al., 2000). The first is an archive of structures, fragments and molecules with low molecular weight used for virtual screening or de novo design with the aim to identify new molecules with pharmacological activity. The second, the PDB database contains structures of macromolecules (proteins and nucleic acids) obtained experimentally (NMR or X-ray) or by homology modeling.

3.3 Sequence alignment

An important step in homology modeling is to align the amino acid sequence of the target protein with the sequence(s) of the template protein(s). Correspondences (identities and conserving mutations) of amino acids are the basis for transferring the coordinates from the template(s) to the target.
Usually automatic sequence alignment tools are used to search for optimal similarity of the sequences. Sequence comparisons are carried out either pairwisely (e.g. ALIGN (Devereux et al., 1984)) or as multisequence alignment (e.g. CLUSTAL W (Thompson et al., 1994)). Most sequence alignment algorithms try to retrace the evolutionary conversion of one sequence into another. For this operation homology matrices are used that specify the weight for aligning a particular type of amino acid substitution according to physical and chemical properties and/or statistical and evolutionary probabilities. In cases of different sequence lengths and variations in the locations of conserved regions, gaps are introduced into the alignment. To minimize the number of gaps, a gap penalty function is used.

3.4 3D structure generation

The 3D structure of the target protein is generated in a stepwise approach. The first step is the construction of structurally conserved regions (SCRs). This can be obtained by two different methods. The first approach is often sufficient if only one template is available. It starts from a good sequence alignment and proceeds with manual mutation of the template protein into the target sequence in conserved streches (stretches without gaps and deletions). For GPCR modeling, the SCRs are

the TMs and short loop regions. Nearly the same results can be obtained using a second class of multiple-template methods, namely Composer (originally derived by the group of Tom Blundell before 1990, (Sali et al., 1990)) or Fugue/Orchestrar (Shi et al., 2001) which is available online, too. Fugue permits to recognize distant homologs by sequence-structure comparison and is based on three key features: (1) Improved environment-specific substitution tables. Substitutions of an amino acid are constrained by its local structural environment, which can be defined in terms of secondary structure, solvent accessibility, and hydrogen bonding state. (2) Automatic selection of an alignment algorithm with detailed structure-dependent gap penalties (global-local algorithm when sequence-structure pairs greatly differ in lengths and global algorithm in other cases). The gap penalty at each position of the structure is determined according to its solvent accessibility, its position relative to the secondary structure elements (SSEs) and the conservation of the SSEs. (3) Combined information from both multiple sequences and multiple structures. Fugue is designed to align multiple sequences against multiple structures to enrich the conservation/variation information. Based on such optimal sequence alignments, Composer or Orchestrar determine the SCRs and an average SCR-Cα framework structure of the templates by an iterative approach, improving both the multiple alignment and the subsequent SCR framework by pair-wise Needleman and Wunsch dynamic programming procedures with a similarity matrix constructed from inter-Cα distances. The backbone of each SCR of the target is then built by fitting the corresponding SCR from one of the known homologs (namely that with the highest block sequence identity) to the appropriate region of the framework. The least-squares fits are inversely weighted by the variation of the residue positions across the known structures. This approach provides a sufficient degree of diversity on constructing the SCRs of the target and avoids an arbitrary focus on one of the templates.

The second step in homology modeling is the construction of structurally variable regions (SVRs) including regions in the amino acid sequence that contain gaps and deletions. In GPCRs these regions usually comprise the extracellular and intracellular loops (except I1, E1 and I2), the N-terminus and the C-terminus that show a low sequence homology and different lengths. A convenient method to build such regions is to perform loop searches for appropriate peptide segments in a 3D structure

database (usually a binary version of the PDB). The selected segments are chosen on the basis of their superposition with the anchor regions (the terminal amino acids of the loop to be constructed) and their fit into the spatial environment of the target model. Another possibility is to generate loops using a *de novo* strategy.

After the generation of the complete receptor backbone the next step is the addition of the side chains. Normally this step starts from the assumption that identical and conserved residues in homologous proteins adopt similar side chain conformations. In case of non conserved amino acids rotamer libraries can help in the selection of reasonable geometries. Rotamer libraries such as the Lovell library (Lovell et al., 2000) implemented in Sybyl 7.3 (Tripos, St. Luis, MO) contain a collection of statistically favoured side chain conformations from which the most frequent one without clashes with other residues can be selected.

Modeling software suites like Sybyl contain structure preparation tools to complete the models. Such tools are to add hydrogens, to provide the atoms with net charges, and to remove bad contacts from individual side chains. The last step in the 3D model generation is the energy minimization. For biopolymers, Kollman et al. (Weiner et al., 1984) originally derived a force field with energy terms, parameters and functions especially suited for proteins and nucleic acids. The most recent versions of this force field are now available as Amber_FF99 and Amber_FF02 (Cieplak et al., 2001; Wang et al., 2000) in all advanced modeling packages.

3.5 Model validation

After GPCR homology models have been generated and structurally optimized, validation of the resulting models is an essential task to guarantee applicability of the models for the particular purposes of the project. The most important parameters evaluated are described in Figure 3.3.

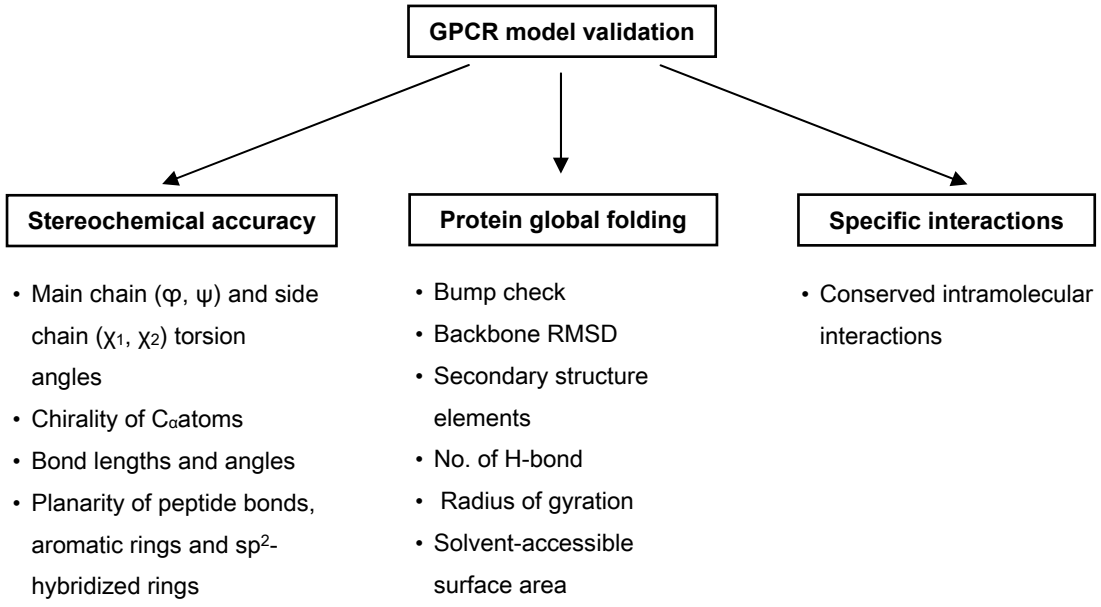

Figure 3.3: Overview of parameters for the validation of GPCR homology models

For an evaluation of the stereochemical quality of a structure model, programs such as PROCHECK (Laskowski et al., 1993) and WHATCHECK (Hooft et al., 1996) have been developed. An overall estimation of structural differences between the backbone structures of the target and the template can be obtained by calculating the root mean square deviation (RMSD) of all backbone or Cα atoms. Additionally, the total number of intramolecular H-bonds, the radius of gyration, and the solvent-accessible surface area give valuable measures of the protein global folding. Finally, distinct interactions between adjacent residues that may play a functional role in GPCR function and/or structural arrangement of the TM domains have to be checked.

3.6 3D Quantitative Structure-Activity Relationships (3D QSAR)

A major goal in chemical research is to predict the potency or receptor affinity of new molecules, using relationships derived from analysis of the properties of previously tested molecules. Quantitative Structure-Activity Relationships (QSAR) (Kubinyi, 1993, 1995) correlate measurable or calculable physical, chemical or topological

descriptors with biological activity by (mostly linear) mathematical models. A QSAR study can help to decide which features of a molecule give rise to its potency and help to predict compounds with desired properties. A large number of descriptors have been used in QSAR equations, designed to represent hydrophobic, electronic or steric properties of the molecule. An important point for their choice is that they should be uncorrelated with each other to obtain a reliable QSAR equation.

3D-QSAR methods are to correlate biological activities with molecular field variables, representing the geometry of the molecules and their spatial interaction potential. Several 3D-QSAR approaches have been described: methods based on molecular shapes, the “distance geometry” method, DYLLOMMS, a prototype version of CoMFA, as well as CoMFA and CoMSiA.

Comparative Molecular Field Analysis (CoMFA) (Cramer et al., 1988) is an approach to structure-activity correlation based on two observations: (1) at the molecular level, the interactions which produce a biological effect are usually noncovalent; and (2) molecular mechanics force fields, most of which treat noncovalent interactions only as steric and electrostatic forces, can sufficiently account for a great variety of observed molecular properties. Thus it seems reasonable that a suitable sampling of steric and electrostatic fields surrounding a set of ligand (drug) molecules might provide all the information necessary for understanding their biological actions. In general the CoMFA approach correlates the interaction potential of ligands, calculated from the interaction energy with probe atoms at regular spaced grid points surrounding the aligned structures, with the biological activity.

Comparative Molecular Similarity Index Analysis (CoMSIA) (Klebe et al., 1994) is based on the same assumption as CoMFA: changes in biological activities or binding affinities of ligands are related to changes in molecular properties, represented by fields. CoMSIA is an extension of the CoMFA approach. In addition to the electrostatic and steric fields, hydrophobic, H-bond donor and H-bond acceptor fields are considered. Moreover, the CoMSIA field variables are based on "soft" Gaussian functions showing a more continuous distribution of the interaction potentials around the molecules, compared to the mostly large gradients of the CoMFA potentials in regions close to or within the van der Waals surfaces.

The 3D-QSAR models are solved by the partial least squares (PLS) approach (Wold et al., 1984) which, in general, decomposites the huge number of more or less intercorrelated field variables into only a few orthogonal principal components (PCs) being in turn maximally correlated with the biological activity. The justification of the models and the number of PCs describing activity without noise are evaluated by the error of predictions from leave-n out runs (activity of omitted compounds predicted by the model of all other compounds). Finally, a model including all molecules is calculated, and the components are transformed into regression coefficients describing the direction and the strength of the influence of each field variable on activity.

3.7 References

Allen, F. H., 2002, The Cambridge Structural Database: a quarter of a million crystal structures and rising: *Acta Crystallogr B*, v. **58**: p. 380-8.

Berman, H. M., J. Westbrook, Z. Feng, G. Gilliland, T. N. Bhat, H. Weissig, I. N. Shindyalov, and P. E. Bourne, 2000, The Protein Data Bank: *Nucleic Acids Res*, v. **28**: p. 235-42.

Bernstein, F. C., T. F. Koetzle, G. J. Williams, E. F. Meyer, Jr., M. D. Brice, J. R. Rodgers, O. Kennard, T. Shimanouchi, and M. Tasumi, 1977, The Protein Data Bank: a computer-based archival file for macromolecular structures: *J Mol Biol*, v. **112**: p. 535-42.

Bissantz, C., P. Bernard, M. Hibert, and D. Rognan, 2003, Protein-based virtual screening of chemical databases. II. Are homology models of G-Protein Coupled Receptors suitable targets? *Proteins*, v. **50**: p. 5-25.

Cherezov, V., D. M. Rosenbaum, M. A. Hanson, S. G. Rasmussen, F. S. Thian, T. S. Kobilka, H. J. Choi, P. Kuhn, W. I. Weis, B. K. Kobilka, and R. C. Stevens, 2007, High-resolution crystal structure of an engineered human beta2-adrenergic G protein-coupled receptor: *Science*, v. **318**: p. 1258-65.

Cieplak, P., J. Caldwell, and P. Kollman, 2001, Molecular mechanical models for organic and biological systems going beyond the atom centered two body additive approximation: aqueous solution free energies of methanol and N-methyl acetamide, nucleic acid base, and amide hydrogen bonding and chloroform/water partition coefficients of the nucleic acid bases: *J Comput Chem*, v. **22**: p. 1048-1057.

Cramer, I., R.D., D. E. Patterson, and J. D. Buce, 1988, Comparative Molecular Field Analysis (CoMFA): Effect of Shape on Binding of Steroids to Carrier Protein: *J. Am. Chem. Soc.*, v. **110**: p. 5959-5967.

Devereux, J., P. Haeberli, and O. Smithies, 1984, A comprehensive set of sequence analysis programs for the VAX: *Nucleic Acids Res*, v. **12**: p. 387-95.

Hooft, R. W., G. Vriend, C. Sander, and E. E. Abola, 1996, Errors in protein structures: *Nature*, v. **381**: p. 272.

Klebe, G., U. Abraham, and T. Mietzner, 1994, Molecular similarity indices in a comparative analysis (CoMSIA) of drug molecules to correlate and predict their biological activity: *J Med Chem*, v. **37**: p. 4130-46.

Kristiansen, K., 2004, Molecular mechanisms of ligand binding, signaling, and regulation within the superfamily of G-protein-coupled receptors: molecular modeling and mutagenesis approaches to receptor structure and function: *Pharmacol Ther*, v. **103**: p. 21-80.

Kubinyi, H., 1993, 3D QSAR in Drug Desig, Theory, Methods and Appication.: Leiden, ESCOM.

Kubinyi, H., 1995, The Quantitative Analysis of Structure-Activity Relationship: Burger's Medicinal Chemistry and Drug discovery, v. 1: New York, John Wiley &Sons, 497-571 p.

Laskowski, R. A., M. W. MacArthur, D. S. Moss, and J. M. Thorton, 1993, PROCHECK: a program to check the stereochemical quality of protein structure: *J Appl Cryst*, v. **26**: p. 283-291.

Li, J., P. C. Edwards, M. Burghammer, C. Villa, and G. F. Schertler, 2004, Structure of bovine rhodopsin in a trigonal crystal form: *J Mol Biol*, v. **343**: p. 1409-38.

Lovell, S. C., J. M. Word, J. S. Richardson, and D. C. Richardson, 2000, The penultimate rotamer library: *Proteins*, v. **40**: p. 389-408.

Okada, T., Y. Fujiyoshi, M. Silow, J. Navarro, E. M. Landau, and Y. Shichida, 2002, Functional role of internal water molecules in rhodopsin revealed by X-ray crystallography: *Proc Natl Acad Sci U S A*, v. **99**: p. 5982-7.

Okada, T., M. Sugihara, A. N. Bondar, M. Elstner, P. Entel, and V. Buss, 2004, The retinal conformation and its environment in rhodopsin in light of a new 2.2 A crystal structure: *J Mol Biol*, v. **342**: p. 571-83.

Palczewski, K., T. Kumasaka, T. Hori, C. A. Behnke, H. Motoshima, B. A. Fox, I. Le Trong, D. C. Teller, T. Okada, R. E. Stenkamp, M. Yamamoto, and M. Miyano, 2000, Crystal structure of rhodopsin: A G protein-coupled receptor: *Science*, v. **289**: p. 739-45.

Rasmussen, S. G., H. J. Choi, D. M. Rosenbaum, T. S. Kobilka, F. S. Thian, P. C. Edwards, M. Burghammer, V. R. Ratnala, R. Sanishvili, R. F. Fischetti, G. F. Schertler, W. I. Weis, and B. K. Kobilka, 2007, Crystal structure of the human beta2 adrenergic G-protein-coupled receptor: *Nature*, v. **450**: p. 383-7.

Rosenbaum, D. M., V. Cherezov, M. A. Hanson, S. G. Rasmussen, F. S. Thian, T. S. Kobilka, H. J. Choi, X. J. Yao, W. I. Weis, R. C. Stevens, and B. K. Kobilka, 2007, GPCR engineering yields high-resolution structural insights into beta2-adrenergic receptor function: *Science*, v. **318**: p. 1266-73.

Sali, A., J. P. Overington, M. S. Johnson, and T. L. Blundell, 1990, From comparisons of protein sequences and structures to protein modelling and design: *Trends Biochem Sci*, v. **15**: p. 235-40.

Shi, J., T. L. Blundell, and K. Mizuguchi, 2001, FUGUE: sequence-structure homology recognition using environment-specific substitution tables and structure-dependent gap penalties: *J Mol Biol*, v. **310**: p. 243-57.

Teller, D. C., T. Okada, C. A. Behnke, K. Palczewski, and R. E. Stenkamp, 2001, Advances in determination of a high-resolution three-dimensional structure of rhodopsin, a model of G-protein-coupled receptors (GPCRs): *Biochemistry*, v. **40**: p. 7761-72.

Thompson, J. D., D. G. Higgins, and T. J. Gibson, 1994, CLUSTAL W: improving the sensitivity of progressive multiple sequence alignment through sequence weighting, position-specific gap penalties and weight matrix choice: *Nucleic Acids Res*, v. **22**: p. 4673-80.

Wang, J., P. Cieplak, and P. A. Kollman, 2000, How well does a restrained electrostatic potential (RESP) model perform in calculating conformational energies of organic and biological molecules? v. **21**: p. 1049-1074.

Weiner, S. J., P. A. Kollman, D. A. Case, U. C. Singh, C. Ghio, G. Alagona, S. Profeta, and P. Weiner, 1984, A new force field for molecular mechanical simulation of nucleic acids and proteins: *J. Am. Chem. Soc*, v. **106**: p. 765 - 784.

Wold, S., A. Ruhe, H. Wold, and W. J. Dunn, 1984, The covariance problem in linear regression. The Partial Least Square (PLS) approach to generalized inverses: *SIAM J. Sci. Stat.*, v. **Comp. 5**: p. 735-743.

Chapter 4
Docking of representative partial agonists at 5-HT_{2A} receptor models based on rhodopsin

4.1 Introduction

5-HT_{2A} receptors (5-HT_{2A}R) (Peroutka, 1990) belong to the G-protein coupled receptor superfamily (GPCR) and mediate the effects of the endogenous neurotransmitter serotonin (5-hydroxytryptamine, 5-HT) As described in Chapter 1, 5-HT_{2A}R mediated signal transduction affects a large number of key physiological processes including vascular and nonvascular smooth muscle contraction, platelet aggregation, perception and affective behaviour (Roth et al., 1998; Zifa and Fillion, 1992). Additionally, 5-HT_{2A} receptors represent a major site of action of hallucinogens like ergolines (e.g., lysergic acid diethylamine), phenylalkylamines (e.g., 1-(4-iodo-2,5-dimethoxyphenyl)-isopropyl amine, DOI) and substituted tryptamines (e.g., N,N-dimethyltryptamine, DMT). In most assays, these compounds act as partial 5-HT_{2A}R agonists. The affinity of the endogenous agonist 5-HT is relatively low (pK_D ca. 6). Dimethoxyphenylalkylamines like mescaline and 1-(4-bromo-2,5-dimethoxyphenyl)-isopropylamine (DOB) are more affine and potent. By introduction of larger substituents at the amine nitrogen it is possible to gain partial agonists that are up to

400-1400 times more active than 5-HT due to higher affinity. This "affinity-conferring" principle may be applied to other structural classes as indoles and quinazolinediones. To obtain still more potent 5-HT_{2A}R agonists and to investigate structure-activity relationships (SAR), a series of more than 60 compounds was synthesized and tested for 5-HT_{2A}R agonistic potency (pEC_{50}) and intrinsic activity (E_{max}) on rat arteries (Elz et al., 2002; Heim et al., 1998; Heim et al., 2002; Pertz et al., 2000; Ratzeburg et al., 2003). The series comprises diverse primary and secondary arylethylamines belonging to different structural classes (mainly indoles, methoxybenzenes and quinazolinediones), and shows a high variability of pEC_{50} from 4 to 10 and of E_{max} (intrinsic activity compared to 5-HT) from 15 to 70%. The QSAR of the compounds were analyzed following a hierarchical strategy with successive application of different methods: fragment regression analysis (FRA), receptor modeling, docking studies, and 3D-QSAR approaches. Generally, all these methods contribute to the investigation of ligand-receptor interactions.

During the first 2 ½ years of the present PhD project, homology modeling had to be based on bovine rhodopsin, the only available GPCR structure at that time (Okada et al., 2002; Okada et al., 2004; Palczewski et al., 2000; Teller et al., 2001).This chapter is to analyze the docking of key compounds at 5-HT_{2A}R models derived from this template. In the meantime, crystal structures of the human β_2-adrenoceptor have been released (Cherezov et al., 2007; Rasmussen et al., 2007) that are better suited for the generation of homology models of GPCRs. Therefore, it was necessary to repeat all the steps except FRA which does not depend on the template. To avoid battologies, the QSAR analysis of the series, derived from using the recent 5-HT_{2A}R models, will be presented and discussed as a whole (see Chapter 5).

In principle it should be possible to explore the putative 5-HT_{2A}R binding modes of the ligands in considering one ligand of each class. Homology models of the rat (r5-HT_{2A}R) and the human (h5-HT_{2A}R) 5-HT_{2A} receptor based on the crystal structure of bovine rhodopsin (Filipek et al., 2003a; Filipek et al., 2003b) together with results from in-vitro mutagenesis studies predict the location, topology and the amino acids of the agonist binding site. The docking of a representative compound of each structural class into this site suggests common and/or individual ligand-receptor interactions, which must not disagree with the ligand binding properties of the receptor mutants.

4.2 Material and Methods

4.2.1 Model construction

Three-dimensional models of the human (h5-HT_{2A}R) and the rat $5HT_{2A}$ receptor (r5-HT_{2A}R) were generated by homology modeling. The amino acid sequences were retrieved from the Swissprot database. The homology between both receptor species is very high. The most different regions are the N- and C-terminal segments. The identity of the transmembrane domains amounts to 97%, only three amino acids in TM1, TM3 and TM5 are different. The crystal structure of bovine rhodopsin at 2.8 Å resolution (Palczewski et al., 2000) strongly supports the homology modeling of GPCRs (Filipek et al., 2003a; Filipek et al., 2003b) and permits to construct a backbone model of the almost full length of the studied protein by a Fugue/Orchestrar approach (Shi et al., 2001). The full sequence of the h5-HT_{2A}R was submitted using bovine rhodopsin as template. The starting structure was chosen from several models on the basis of:

a) the sequence alignment with bovine rhodopsin considering the TM domains (with the dopamine D_2 receptor – rhodopsin alignment as reference (Ballesteros et al.)) and the intra- and extracellular loops with corresponding lengths;
b) the known packing of the seven transmembrane helices;
c) the disulfide bridge between Cys (148) and Cys (272);
d) the length of gaps.

Orchestrar was not able to predict the 3D structure of some domains of the receptor (E2 loop, I3 loop and C-terminus). The gaps in E2 and I3 were filled by the Biopolymer loop search facility (Sybyl 7.3 (Luthy et al., 1992b)) with appropriate peptide chains from a binary protein database based on PDB structures (Palczewski et al., 2000). The final insertions resulted from:

a) the source of the fragment;
b) the sequence homology score;
c) the fit of the chain into the model.

The C-terminus was truncated after the H8 helix. Side chains and hydrogens were added using the Biopolymer package of Sybyl 7.3. The model was initially relaxed with steepest descent minimization using the Amber FF99 force field, Amber FF99 charges and a distant dependent dielectric constant of 4, until the RMS gradient approaches 0.5 kcal $mole^{-1}$ $Å^{-1}$. During the first 100 cycles, the backbone was fixed. This initial optimization was followed by a Powell minimization (end RMS gradient 0.01 kcal $mole^{-1}$ $Å^{-1}$). To verify the integrity of the structure, as last step the optimized receptor model was submitted to 3D-Verify and Procheck (Luthy et al., 1992a). Starting from the initial h5-HT_{2A}R model some amino acids were mutated to obtain the corresponding model of the rat receptor which was energy optimized and verified as described for the h5-HT_{2A}R model.

4.2.2 Ligand selection, structure generation and docking

The selection of one representative compound from each structural class – (1) indoles, (2) methoxybenzenes, (3) quinazolinediones – of the arylethylamine series of 5-HT_{2A}R partial agonists was based on high potency and reproduction of all favourable ligand-receptor interactions. Among the substituents at the amino nitrogen which were similarly varied in each subseries (see Table 5.1) a 2-methoxybenzyl group is optimal. Therefore each class was represented by a derivative containing this substituent. Figure 4.1 depicts the selected compounds, namely, **201** (indole), **231** (methoxybenzene) and **169** (quinazolinedione class) (numbering according to Table 5.1).

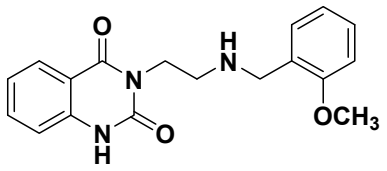

Cpd. 169

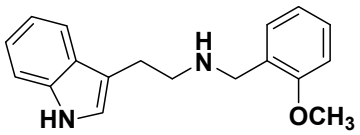

Cpd. 201

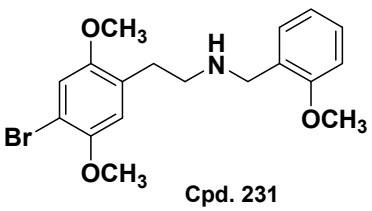

Cpd. 231

Figure 4.1: Representative structure used in the docking studies

The structures were constructed using Sybyl 7.3. All molecules were assumed to be protonated under physiological conditions. AmberFF99 atom types and Gasteiger-Hückel charges were assigned to the ligands. Based on the assumption that the ligands share a common binding site at the receptor, a structure-based alignment was to be achieved. I.e., the docking modes (bioactive conformations) must rely on informations about the location of putative binding site residues. Site-directed mutagenesis studies have indicated that the highly conserved $Asp155^{3.32}$ (Sealfon et al., 1995; Wang et al., 1993), the serines $Ser159^{3.36}$, $Ser239^{5.43}$, $Ser242^{5.46}$ (Ala242 in r5-HT_{2A}R), (Johnson et al., 1994) and the phenylalanines $Phe243^{5.47}$, $Phe244^{5.48}$, $Phe340^{6.52}$ (Choudhary et al., 1993; Choudhary et al., 1995) are important for binding and efficacy of agonists and partial agonists at 5-HT_{2A} receptors. These results restrict the agonist binding site to a well defined region between TMs 3 to 6 and suggest $Asp155^{3.32}$ as counterpart of the protonated amine, $Ser159^{3.36}$, $Ser239^{5.43}$ and $Ser242^{5.46}$ as hydrogen donors or acceptors, and the phenylalanines in TM 5 and 6 as hydrophobic pocket and anchor for the aryl moiety of the ligands.

The ligands were manually docked into the putative binding site, also considering the QSAR obtained from fragment regression analysis (see Chapter 5). During docking, the conformations of the ligands were varied in order to get maximal overlap of the scaffolds and shared interactions with the essential amino acids described above. The fit of the "affinity conferring" N-benzyl groups was based on the examination of proximate amino acids and on low-energy conformations. The complexes were optimized by a stepwise approach: (1) 50 cycles AmberFF99 force field with fixed ligands (distant dependent dielectric constant 4, steepest descent method), (2) subset minimization of the ligand and a receptor region 6 Å around using the combined protein-ligand force field MMFF64 (distant dependent dielectric constant 1, Powell method) up to an RMS gradient of 0.05 kcal $mole^{-1}$ $Å^{-1}$), (3) AmberFF99 force field with fixed ligands (distant dependent dielectric constant 4, Powell method, final RMS gradient 0.01 kcal $mole^{-1}$ $Å^{-1}$). Range constraints were occasionally applied between $Asp155^{3.32}$ and the protonated nitrogen of the ligands, additionally for cpd. **231** between $Ser159^{3.36}$ and the 2-OCH_3 group and between $Ser239^{5.43}$ and the 5-OCH_3 substituent.

4.3 Results and Discussion

4.3.1 5-HT_{2A} receptor models

In the h5-HT_{2A}R and the r5-HT_{2A}R models, the packing of the seven transmembrane regions and the typical interactions stabilizing the inactive state (dark state) of bovine rhodopsin are conserved (Figure 4.2).

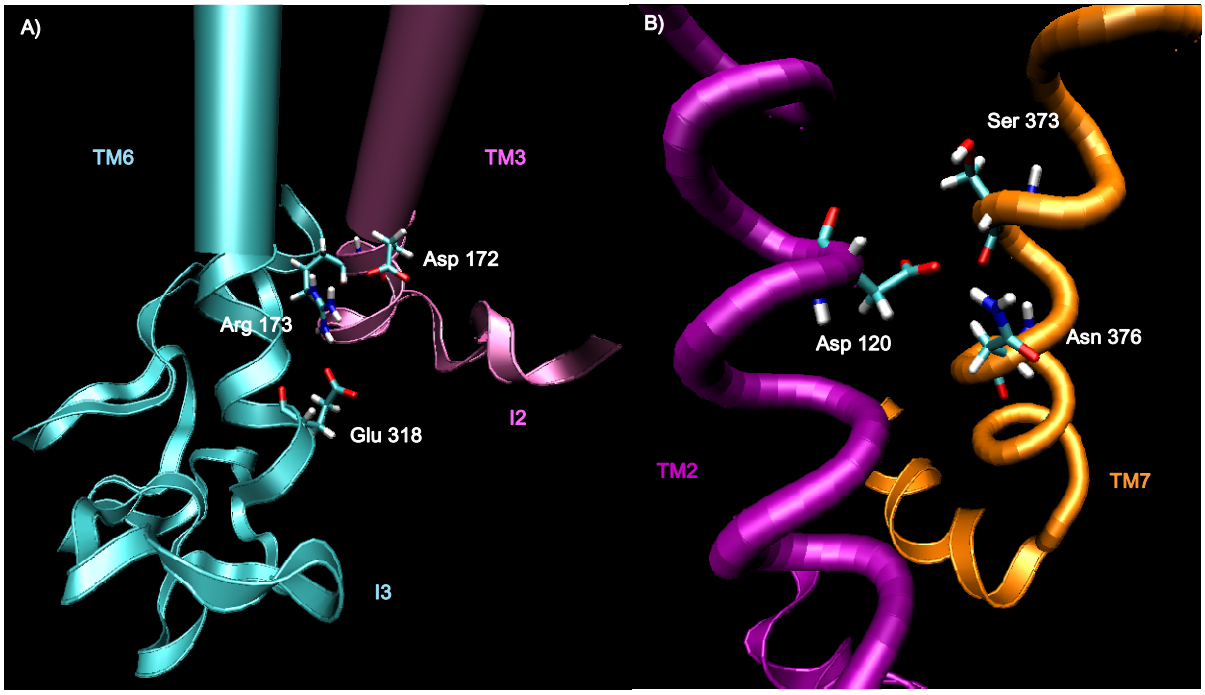

Figure 4.2: Selected interactions responsible for the inactive state of 5-HT_{2A} receptors. **A)** Ionic interactions between two amino acids belonging to the DRY motif (Asp $172^{3.49}$ and Arg $173^{3.50}$) and Glu $318^{6.30}$. **B)** Polar interactions between TM2 ($Asp120^{2.50}$) and TM7 ($Asn376^{4.49}$ and $Ser373^{7.46}$).

The homology model suggests that the inactive state is stabilized by two salt bridges of $Arg173^{3.50}$ with the neighbouring $Asp172^{3.49}$ and with $Glu318^{6.30}$, respectively. The three amino acids are highly conserved in the GPCR superfamily, $Arg173^{3.50}$ and $Asp172^{3.49}$ belong to the DRY consensus motif. Other polar interactions suggested to stabilize the inactive state involve the transmembrane domains TM1 ($Asn72^{1.50}$), TM2 ($Asp120^{2.50}$) and TM7 ($Ser373^{7.46}$, $Asn376^{7.49}$). All these interactions break during receptor activation. The second extracellular loop (E2) is only constrained by the

disulfide bridge between $Cys148^{3.25}$ and $Cys227^{E2.15}$. This implies that E2 is partially inserted into the transmembrane part of the receptor. However, the cap derived from rhodopsin is rather typical for this template due to the covalently bound retinal and is therefore not reliable in the case of biogenic amine GPCRs. In the model, the course of E2 is stabilized by a network of intraloop hydrogen bonds. E.g., the backbone of $Gln216^{E2.4}$ is linked with the side chain of $Asp231^{5.35}$ and with the backbone of $Asp218^{E2.6}$ and $Leu229^{E2.17}$, and the side chain of $Glu224^{E2.12}$ with the backbone of $Lys223^{E2.11}$ (Table 4.1).

Table 4.1: Conserved intramolecular interaction responsible for the inactive state

Domain	Residues	Min. distance (Å)*	
		h5HT2A	r5HT2A
TM3	$Arg173^{3.50}$ - $Asp172^{3.49}$	2.11	2.63
TM3-TM6	$Arg173^{3.50}$ - $Glu318^{6.30}$	1.95	2.01
TM7-TM2	$Asn376^{7.49}$ - $Asp120^{2.50}$	2.04	2.38
TM7	$Asn376^{7.49}$ - $Ser373^{7.46}$	3.65	4.86
E2-TM5	$Glu216^{E2.4}$ - $Asp231^{5.35}$	2.05	2.17
E2	$Glu216^{E2.4}$ - $Asp218^{E2.6}$	2.26	2.75
E2	$Glu216^{E2.4}$ - $Leu229^{E2.17}$	1.98	2.04
E2	$Glu224^{E2.12}$ - $Lys223^{E2.11}$	2.03	2.01

* Distance between the nearest heavy atoms of interacting residues

4.3.2 Docking of representative partial agonists

As representative 5-HT_{2A}R partial agonists of the arylethylamine series (Elz et al., 2002; Heim et al., 1998; Heim et al., 2002; Pertz et al., 2000; Ratzeburg et al., 2003), the compounds **201** (indole), **231** (methoxybenzene) and **169** (quinazolinedione class) were selected (see Figure 4.1). The contributions of these aryl fragments to the pEC_{50} values differ by only ca. 0.8 orders of magnitude (ranging from 0.95 for quinazolinedione to 1.75 for 2,5-dimethoxyphenyl, see results of FRA, Chapter 5). Furthermore, the effects of a 5-methoxy group at the aryl moiety and of a benzyl group as R^N are similar in each structural class. Therefore an overlapping binding mode of the different partial agonists is likely which can be derived from the docking of the three ligands into the r5-HT_{2A}R model.

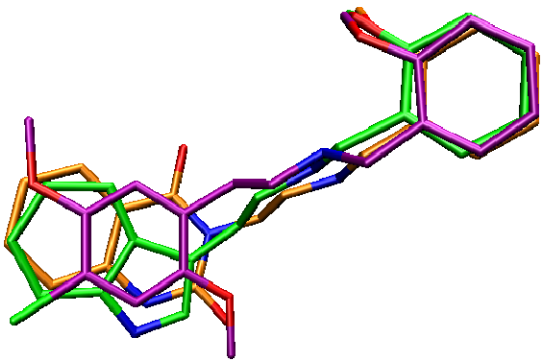

Figure 4.3: Binding conformation and alignment of compounds **169** (orange), **201** (green), and **231** (purple).

Figure 4.4 shows the complexes of r5-HT_{2A}R with the representative compounds **169**, **201**, and **231**, respectively, after energy optimization. The alignment of the resulting binding conformations is demonstrated in Figure 4.3.

The binding of the arylethylamine moieties depends on three sites, (1) $Asp155^{3.32}$ forming a salt bridge with the protonated amine, (2) a hydrophobic pocket consisting of $Phe243^{5.47}$, $Phe244^{5.48}$ and $Phe340^{6.52}$, and (3) serine and threonine residues ($Ser159^{3.36}$, $Thr160^{3.37}$, $Ser239^{5.43}$) as possible hydrogen bond acceptors or donors.

The close and rather flat alignment of the aryl moieties covering TMs 5 and 6 is enforced by the "phenylalanine pocket". The binding of many agonists, including 5-HT, 5-methoxytryptamine, DOB and DOI, is strongly reduced on a Phe340Leu mutant (Choudhary et al., 1993; Roth et al., 1997). Phe243Ala mutation increases, Phe244Ala mutation decreases DOI affinity (Shapiro et al., 2000). In Figure 4.4, this finding is reflected by a projection of the 4-Br substituent of the dimethoxyphenyl compound **231** onto $Phe243^{5.47}$ and $Phe244^{5.48}$. The resulting hydrophobic interactions may be conserved in the case of an Ala243 mutation. Interestingly, both alanine mutants reduce the affinity of the quinazolinedione ketanserin (5-HT_{2A}R antagonist) (Shapiro et al., 2000), indicating that the phenyl moiety of cpd. **169** also approaches the phenylalanines 243 and 244. Both seem to be important also in the active state of the 5-HT_{2A}R, since the alanine mutations strongly reduce the intrinsic activity of indole and quinazolinedione agonists.

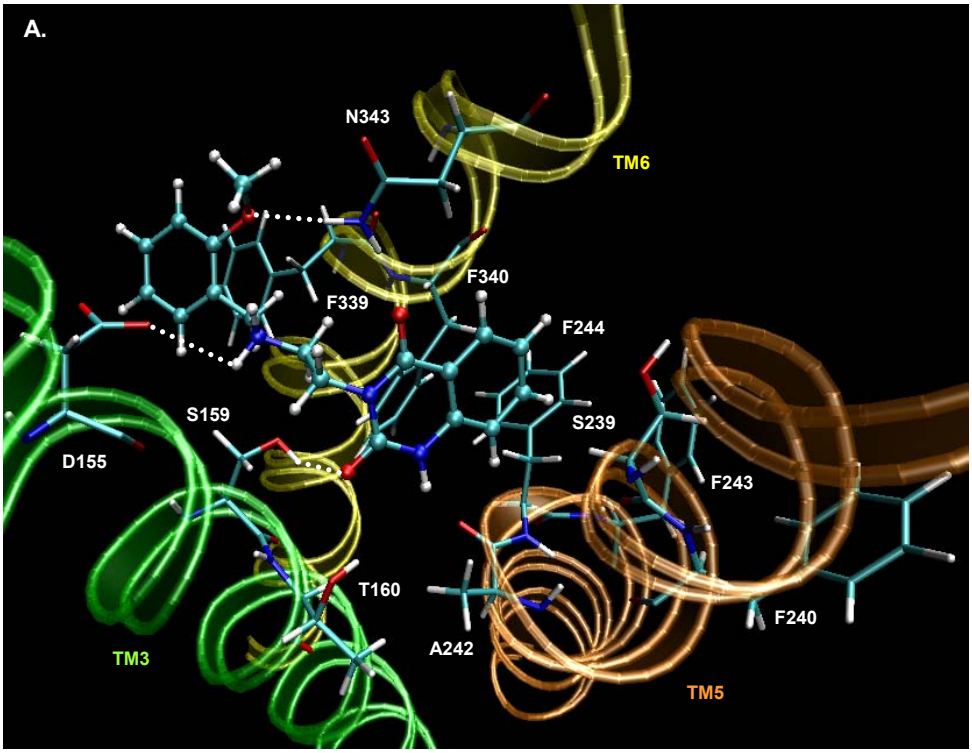
A.
N343
TM6
F340
F339
F244
S159
S239
D155
F243
T160
F240
A242
TM3
TM5

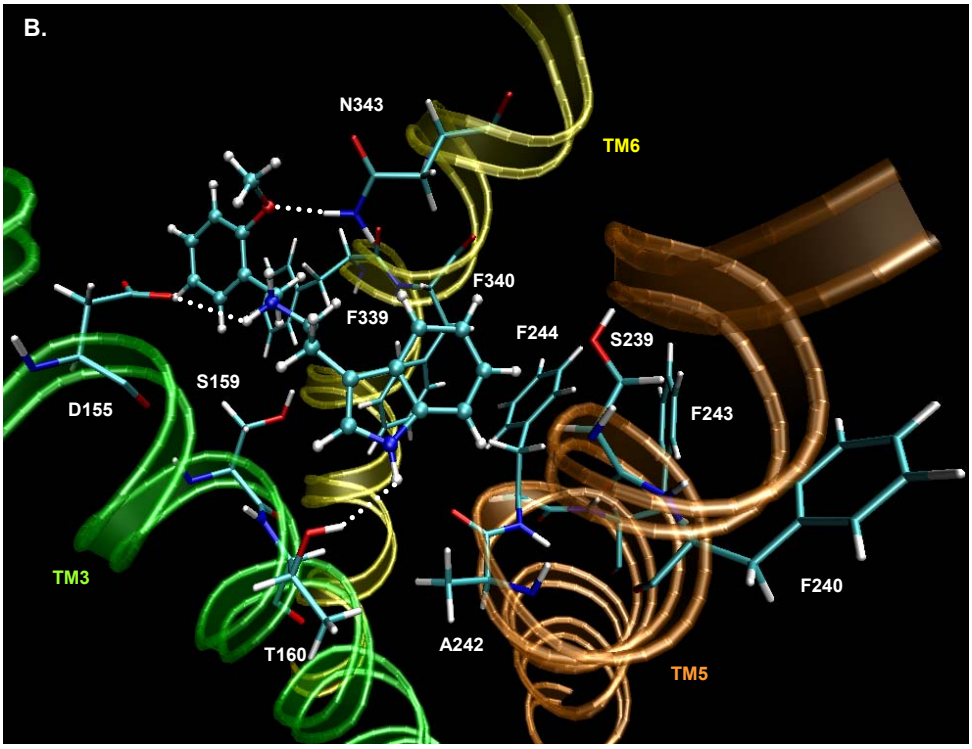
B.
N343
TM6
F340
F339
F244
S239
S159
D155
F243
TM3
F240
T160
A242
TM5

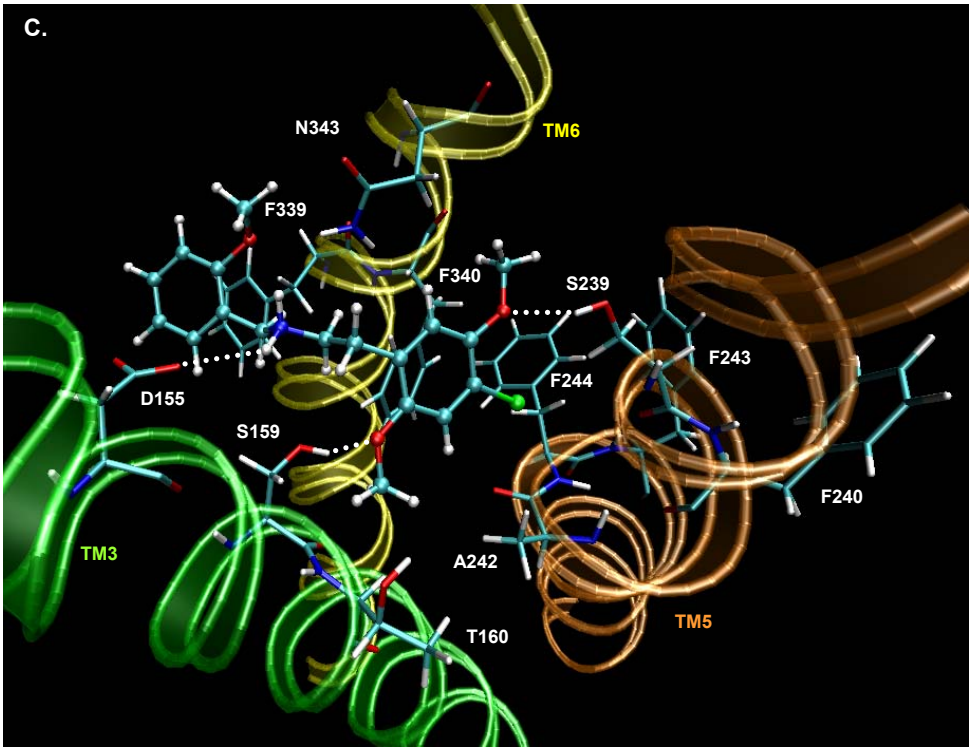

Figure 4.4: View of the r5-HT$_{2A}$ receptor model in complex with cpd. **169** (A.), cpd. **201** (B.) and cpd. **231** (C.). The putative agonist binding site (C atoms of amino acids in cyan) and the three α helices (TM3 in green, TM5 in orange and TM6 in yellow) are shown. The dotted lines in white represent the interaction between the ligand and the residues.

For 5-HT, two alternative binding modes have been published. Whereas Shapiro et al. (Shapiro et al., 2000) suggested a H bond of the indole NH with Ser239$^{5.43}$, Johnson et al. (Johnson et al., 1994) postulated an interaction of this serine with the 5-OH group. The latter mode is more probable since a Ser239Ala mutant reduces the affinity of 5-HT 10-fold whereas the binding of tryptamine, 5-methoxytryptamine, ketanserin and DOI is less affected. Possibly an H bond of the 5-OMe groups in 5-methoxytryptamine and DOI is replaced by a hydrophobic or dispersion interaction with the alanine residue in the mutant. The FRA results (see Chapter 5) indicate an alignment of the 5-OMe substituents of the indole and dimethoxyphenyl derivatives which is optimally achieved in close proximity to Ser239$^{5.43}$.

An interaction of the indole NH with Ser242$^{5.46}$ was inferred by Johnson et al. (Johnson et al., 1994) from the finding that 5-HT *and* tryptamine are more affine at the human than at the rat 5-HT$_{2A}$R (Ala242$^{5.46}$). The question is whether Ser159$^{3.36}$ and/or Thr160$^{3.37}$ may compensate for this interaction in the case of the rat receptor,

possibly also as H donor(s) for the indole nitrogen. From results on Ser159Ala mutants, Almaula et al. (Almaula et al., 1996) suggested a charge-assisted H bond of the hydroxy oxygen with the protonated amino group of 5-HT. As shown in Fig. 4.4, on the other hand, Ser159$^{3.36}$ may be in a position to act as donor in additional H bonds with a quinazolinedione oxygen and with the 2-OMe group of the dimethoxyphenyl compounds, respectively. In the r5-HT_{2A}R model, the indole NH function should rather interact with the side chain of Thr160$^{3.37}$.

In conclusion, the models predict bidentate polar interactions of the aryl moieties in the case of 5-OH and 5-MeO substituted indoles and 2,5-dimethoxyphenethyl compounds, whereas quinazolinediones can form only one H bond in the case of the r5-HT_{2A} receptor due to the Ser242Ala mutation. This may contribute to the lower activity of the latter.

The docking pose of the benzyl group at the amino nitrogen was derived from the finding that a Phe339Leu mutation does not affect the binding of primary amines like 5-HT and DOI, whereas secondary amines like ketanserin show reduced affinity (Choudhary et al., 1993). In Fig. 4.4, the phenyl moiety of R^N aligns with Phe339$^{6.51}$. Since an oxygen in *ortho* position of the phenyl group (2-OH, 2-OMe) further enhances activity, an additional interaction with a hydrogen donor may be suggested. In the rhodopsin-based models, the most probable candidate for this interaction is the amide group of Asn343$^{6.55}$.

4.4 Conclusion

In this study, the bioactive conformations and the binding modes of three different structural classes of 5-HT_{2A}R partial agonistic arylethylamines – (1) indoles, (2) methoxybenzenes, (3) quinazolinediones – were derived. Rat and human 5-HT_{2A}R models were generated using the X-ray structure of bovine rhodopsin as template. Results from in vitro mutagenesis experiments contributed to the identification of important binding site amino acids. Three compounds representing the structural classes could be docked at this site in a consistent mode, resulting in a structure-based alignment which may serve as starting point for 3D QSAR analysis. The

question is whether new 5-HT_{2A}R models based on the recent crystal structures of the human β_2 adrenoceptor will confirm the binding models derived so far.

4.1 References

Almaula, N., B. J. Ebersole, D. Zhang, H. Weinstein, and S. C. Sealfon, 1996, Mapping the binding site pocket of the serotonin 5-Hydroxytryptamine2A receptor. Ser3.36(159) provides a second interaction site for the protonated amine of serotonin but not of lysergic acid diethylamide or bufotenin: *J Biol Chem*, v. **271**: p. 14672-5.

Cherezov, V., D. M. Rosenbaum, M. A. Hanson, S. G. Rasmussen, F. S. Thian, T. S. Kobilka, H. J. Choi, P. Kuhn, W. I. Weis, B. K. Kobilka, and R. C. Stevens, 2007, High-resolution crystal structure of an engineered human beta2-adrenergic G protein-coupled receptor: *Science*, v. **318**: p. 1258-65.

Choudhary, M. S., S. Craigo, and B. L. Roth, 1993, A single point mutation (Phe340-->Leu340) of a conserved phenylalanine abolishes 4-[125I]iodo-(2,5-dimethoxy)phenylisopropylamine and [3H]mesulergine but not [3H]ketanserin binding to 5-hydroxytryptamine2 receptors: *Mol Pharmacol*, v. **43**: p. 755-61.

Choudhary, M. S., N. Sachs, A. Uluer, R. A. Glennon, R. B. Westkaemper, and B. L. Roth, 1995, Differential ergoline and ergopeptine binding to 5-hydroxytryptamine2A receptors: ergolines require an aromatic residue at position 340 for high affinity binding: *Mol Pharmacol*, v. **47**: p. 450-7.

Elz, S., T. Kläß, U. Warnke, and H. H. Pertz, 2002, Developpement of highly potent partial agonists and chiral antagonists as tool for the stsudy of 5-HT2A-receptor mediated function: *Naunyn-Schmiedeberg's Arch. Pharmacol*, v. **365**: p. R29.

Filipek, S., R. E. Stenkamp, D. C. Teller, and K. Palczewski, 2003a, G protein-coupled receptor rhodopsin: a prospectus: *Annu Rev Physiol*, v. **65**: p. 851-79.

Filipek, S., D. C. Teller, K. Palczewski, and R. Stenkamp, 2003b, The crystallographic model of rhodopsin and its use in studies of other G protein-coupled receptors: *Annu Rev Biophys Biomol Struct*, v. **32**: p. 375-97.

Heim, R., H. H. Pertz, I. Walther, and S. Elz, 1998, Congeners of 3-(2-Benzylaminoethyl)-2,4-quinazolindione: partial agonists for rat vascular 5-HT2A receptors: *Naunyn-Schmiedeberg's Arch. Pharmacol*, v. **358**: p. R105.

Heim, R., H. H. Pertz, M. Zabel, and S. Elz, 2002, Stereoselective synthesis, absolute configuration and 5-HT_{2A} agonism of chiral 2-methoxybenzylamines: *Arch. Pharm. Pharm. Med. Chem.*, v. **335**: p. 82.

Johnson, M. P., R. J. Loncharich, M. Baez, and D. L. Nelson, 1994, Species variations in transmembrane region V of the 5-hydroxytryptamine type 2A receptor alter the structure-activity relationship of certain ergolines and tryptamines: *Mol Pharmacol*, v. **45**: p. 277-86.

Luthy, R., J. U. Bowei, and D. Eisenberg, 1992a, Assessment of protein modes with three-dimentional profile: *Nature*, v. **356**: p. 493-500.

Luthy, R., J. U. Bowie, and D. Eisenberg, 1992b, Assessment of protein models with three-dimensional profiles: *Nature*, v. **356**: p. 83-5.

Okada, T., Y. Fujiyoshi, M. Silow, J. Navarro, E. M. Landau, and Y. Shichida, 2002, Functional role of internal water molecules in rhodopsin revealed by X-ray crystallography: *Proc Natl Acad Sci U S A*, v. **99**: p. 5982-7.

Okada, T., M. Sugihara, A. N. Bondar, M. Elstner, P. Entel, and V. Buss, 2004, The retinal conformation and its environment in rhodopsin in light of a new 2.2 A crystal structure: *J Mol Biol*, v. **342**: p. 571-83.

Palczewski, K., T. Kumasaka, T. Hori, C. A. Behnke, H. Motoshima, B. A. Fox, I. Le Trong, D. C. Teller, T. Okada, R. E. Stenkamp, M. Yamamoto, and M. Miyano, 2000, Crystal structure of rhodopsin: A G protein-coupled receptor: *Science*, v. **289**: p. 739-45.

Peroutka, S. J., 1990, 5-Hydroxytryptamine receptor subtypes: *Pharmacol Toxicol*, v. **67**: p. 373-83.

Pertz, H. H., R. Heim, and S. Elz, 2000, *N*-Benzylated Phenylethanamines are Highly Potent Partial Agonists at 5-HT_{2A} Receptors: *Arch. Pharm. Pharm. Med. Chem.*, v. **333**: p. 30.

Rasmussen, S. G., H. J. Choi, D. M. Rosenbaum, T. S. Kobilka, F. S. Thian, P. C. Edwards, M. Burghammer, V. R. Ratnala, R. Sanishvili, R. F. Fischetti, G. F. Schertler, W. I. Weis, and B. K. Kobilka, 2007, Crystal structure of the human beta2 adrenergic G-protein-coupled receptor: *Nature*, v. **450**: p. 383-7.

Ratzeburg, K., R. Heim, S. Mahboobi, J. Henatsch, H. H. Pertz, and S. Elz, 2003, Potent partial 5-HT_{2A}-receptor agonism of phenylethamines related to mescaline in the rat tail artery model: *Naunyn-Schmiedeberg's Arch. Pharmacol*, v. **367**: p. R31.

Roth, B. L., M. Shoham, M. S. Choudhary, and N. Khan, 1997, Identification of conserved aromatic residues essential for agonist binding and second messenger production at 5-hydroxytryptamine2A receptors: *Mol Pharmacol*, v. **52**: p. 259-66.

Roth, B. L., D. L. Willins, K. Kristiansen, and W. K. Kroeze, 1998, 5-Hydroxytryptamine2-family receptors (5-hydroxytryptamine2A, 5-hydroxytryptamine2B, 5-hydroxytryptamine2C): where structure meets function: *Pharmacol Ther*, v. **79**: p. 231-57.

Sealfon, S. C., L. Chi, B. J. Ebersole, V. Rodic, D. Zhang, J. Ballesteros, and H. Weinstein, 1995, Related Contribution of Specific Helix 2 and 7 Residues to Conformational Activation of the Serotonin 5-HT_{2A} Receptor: *The Journal of Biological Chemistry*, v. **28**: p. 16683-16688.

Shapiro, D. A., K. Kristiansen, W. K. Kroeze, and B. L. Roth, 2000, Differential modes of agonist binding to 5-hydroxytryptamine(2A) serotonin receptors revealed by mutation and molecular modeling of conserved residues in transmembrane region 5: *Mol Pharmacol*, v. **58**: p. 877-86.

Shi, J., T. L. Blundell, and K. Mizuguchi, 2001, FUGUE: sequence-structure homology recognition using environment-specific substitution tables and structure-dependent gap penalties: *J Mol Biol*, v. **310**: p. 243-57.

Teller, D. C., T. Okada, C. A. Behnke, K. Palczewski, and R. E. Stenkamp, 2001, Advances in determination of a high-resolution three-dimensional structure of rhodopsin, a model of G-protein-coupled receptors (GPCRs): *Biochemistry*, v. **40**: p. 7761-72.

Wang, C. D., T. K. Gallaher, and J. C. Shih, 1993, Site-directed mutagenesis of the serotonin 5-hydroxytrypamine2 receptor: identification of amino acids necessary for ligand binding and receptor activation: *Mol Pharmacol*, v. **43**: p. 931-40.

Zifa, E., and G. Fillion, 1992, 5-Hydroxytryptamine Receptors: *Pharmacol. Rev.*, v. **44**: p. 401-457.

Chapter 5
5-HT_{2A} receptor partial agonists: QSAR and interactions with the binding site

5.1 Introduction

5-HT_{2A} receptors represent a major site of action of hallucinogens like ergolines (e.g., lysergic acid diethylamine), phenylisopropylamines (e.g., 1-(4-iodo-2,5-dimethoxy-phenyl)-isopropylamine, DOI) and substituted tryptamines (e.g., *N,N*-dimethyltrypt-amine, DMT). In most assays, these compounds act as partial 5-HT_{2A}R agonists. The affinity of the endogenous agonist, 5-HT, is relatively low (pK_i ca. 6). Dimethoxy-phenylalkylamines like mescaline and 1-(4-bromo-2,5-dimethoxyphenyl)-isopropyl-amine (DOB) are more affine and potent 5HT_{2A}R agonists. By introduction of larger substituents at the amine nitrogen it is possible to gain partial agonists that are up to 400-1400 times more active than 5-HT due to higher affinity. This "affinity-conferring" principle may be applied to other structural classes as indoles and quinazolinediones. Following this strategy and with the intention to obtain still more potent 5-HT_{2A}R agonists and to investigate structure-activity relationships (SAR), a series of more than 60 compounds was synthesized and tested for 5-HT_{2A}R agonistic potency (pEC_{50}) and intrinsic activity (E_{max}) on rat arteries (Elz et al., 2002; Heim et al., 1998; Heim et al., 2002; Pertz et al., 2000; Ratzeburg et al., 2003). The series comprises diverse primary and secondary arylethylamines belonging to different structural classes (mainly indoles, methoxybenzenes and quinazolinediones), and shows high variability of pEC_{50} from 4 to 10 and of E_{max} from 15 to 70%. To analyse the

quantitative structure-activity relationship (QSAR) and to explore the putative 5-HT_{2A}R binding modes, a hierarchical approach combining different methods was applied: (1) fragment regression analysis (FRA), (2) receptor modeling, (3) docking studies based on mutagenesis data and FRA results, and (4) 3D QSAR methods – comparative molecular field analysis, CoMFA (Cramer et al., 1988b) and comparative molecular similarity index analysis, CoMSIA (Klebe et al., 1994).

Generally, all these methods contribute to the investigation of ligand-receptor interactions. FRA provides information about the substructures and substituents which strongly affect affinity and potency and, by this, about the nature of effects which may play a role in a certain position. Homology models of the rat (r5-HT_{2A}R) and the human (h5-HT_{2A}R) 5-HT_{2A}R based on the crystal structure of the β_2 adrenoceptor together with results from in-vitro mutagenesis studies predict the location, topology and the amino acids of the agonist binding site. The docking of representative compounds of each structural class (indoles, methoxybenzenes and quinazolinediones) into this site generates common and/or individual ligand-receptor interactions, which must not disagree with the SAR from FRA and with the ligand-binding properties of the receptor mutants, and provides the templates for a common, binding-site based alignment of the whole series. Finally, CoMFA and CoMSIA approaches are to analyze the QSAR in detail, leading to interaction fields which may be projected onto the binding site model and, by this, refine the exploration of the SAR and the ligand-receptor interactions.

5.2 The β_2 adrenoceptor, a new template for GPCR homology modeling

5.2.1 Crystal structures of the β_2 adrenoceptor

For many years, rhodopsin has been the only GPCR with crystallographic information available (Okada et al., 2002; Okada et al., 2004; Palczewski et al., 2000; Schertler et al., 1993; Teller et al., 2001), providing essential and reliable suggestions about the structure and the mechanism of activation of other GPCRs (Hubbell et al., 2003; Sakmar et al., 2002). Conclusions relied on mutagenesis experiments combined with

sequence comparison and homology modeling. The approach is based on the general assumption that evolutionary related proteins, i.e. homologous proteins, conserve their 3D structure rather than their amino acid sequence, enabling to derive protein models even from significantly distant templates (Costanzi et al., 2006). However, the use of rhodopsin as template for GPCR modeling is limited due to covalent ligand binding and light-mediated activation, both in contrast to other GPCRs (non-covalent binding, ligand-mediated activation). Thus, structurally and functionally more similar templates are needed to obtain authentic GPCR models which provide further insight into ligand binding and activation mechanisms.

The recently published crystal structures of the human β_2 adrenoceptor (hβ_2AR) (Cherezov et al., 2007; Rasmussen et al., 2007; Rosenbaum et al., 2007) and of the turkey β_1 adrenoceptor (tβ_1AR, released 1 month before finishing this thesis) (Warne et al., 2008) now affords to analyze in particular biogenic amine GPCRs by homology modeling without the above limitations.

A major problem for the crystallization of GPCRs is their low concentration in membranes. Other problems arise from the solubilisation by detergents prior to the purification of membrane proteins, leading to desintegration of the stabilizing membrane lipids. Moreover, the structural flexibility required for the signaling function of GPCRs produces conformational heterogeneity that hinders formation of well-ordered crystals.

To overcome these problems, the β_2AR was modified by:

- truncation of the C-terminal tail
- mutation of a site for N-linked glycosylation
- either replacing residues 231 to 262 of the third intracellular loop (I3) by T4 lysozyme (T4L), a soluble, easily crystallisable globular protein (Cherezov et al., 2007; Rosenbaum et al., 2007) or forming a complex with a Fab5 antibody fragment which interacts with an epitope in I3 (Rasmussen et al., 2007) (Figure 5.1).
- binding of a high-affinity inverse agonist, carazolol, to stabilize the structure

The modification of I3 was a key step for the crystallization, and only the first approach (lysozyme insertion) yielded a high resolution structure (2.4Å vs. 3.4-3.7Å using Fab5),

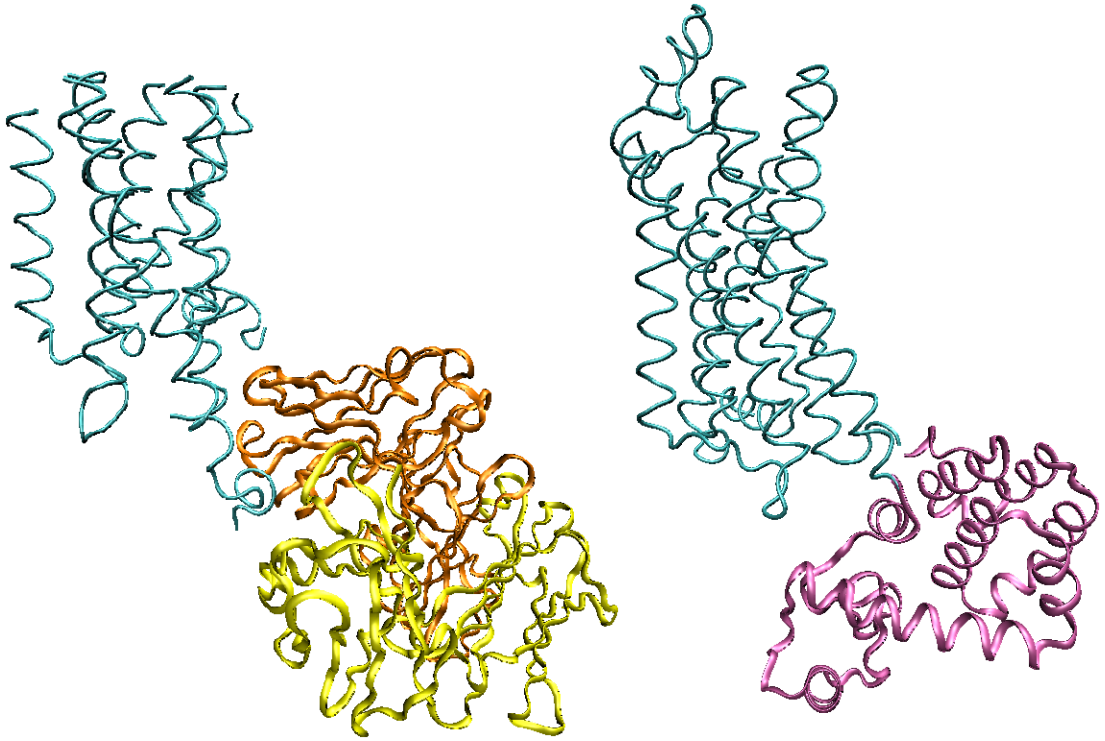

Figure 5.1: Modifications of the β_2 adrenoceptor. The left structure is in complex with a Fab5 fragment (two subunits represented in yellow and orange, respectively), and the right structure is an engineered β_2-AR-T4L fusion protein (T4L violet). The resolution of the two structures is 3.4Å and 2.4Å respectively.

5.2.2 Comparison of β_2AR and rhodopsin crystal structures

The β_2AR consists of seven TM helices connected by intra- and extracellular loops (see Figure 5.1). The receptor fold is very similar to that of rhodopsin in its inactive state. The overall root-mean-square deviation (rmsd) between the Cα atoms of the two structures is 2.3Å. For the TM helices, the rmsd amounts to only 1.6Å. The sequence identities are 21% (overall) and 23% (TM domain), respectively. Thus, there is a very high level of 3D structure conservation in spite of low sequence homology.

Similar to the suggested activation mechanism of rhodopsin, the conserved $Trp^{6.48}$ in TM6 of the β_2AR may serve as “toggle switch" that is involved in the transition between the inactive and the active state. A series of water molecules is also observed in both structures, extending from the binding site via the space between the helical bundle formed by TM2, 3, 6 and 7 to the cytoplasmic surface.

The location and the topology of the ligand binding sites as well as their hydrophobic nature are similar in the two structures, but the accessibility of the binding pocket from the extracellular side is significantly different. In rhodopsin, the covalently bound retinal is covered by a buried β-sheet in E2 ("cap" function) that effectively shields the ligand site from the extracellular compartment. In contrast, the E2 loop in the β_2AR contains a short helix and is in a conformation that permits extracellular ligands to easily intrude into the binding site (Figure 5.2).

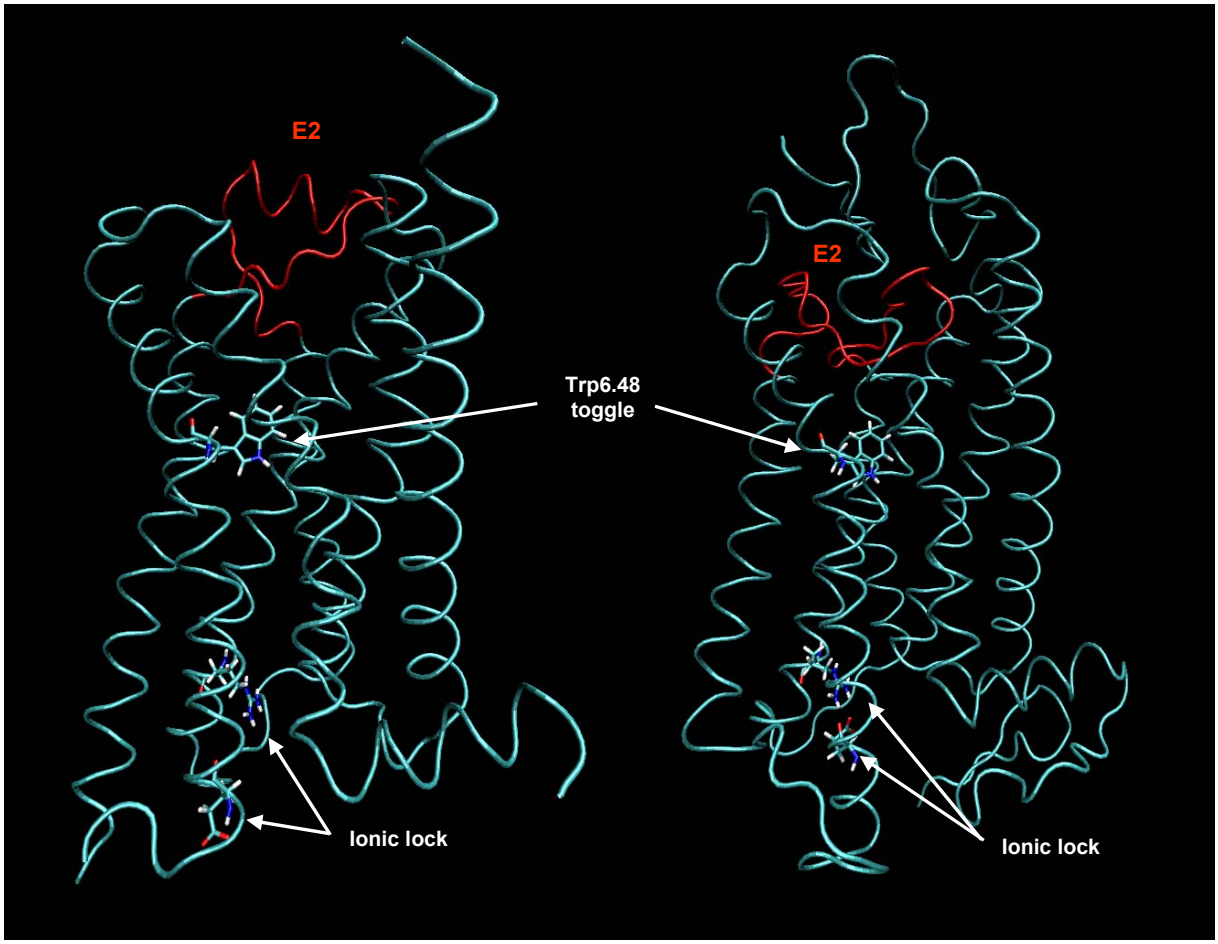

Figure 5.2: Structure of the hβ_2AR (left structure, T4L omitted) and rhodopsin (right structure). The structures are shown as cyan tubes, the E2 loops as red tubes. The ionic lock is represented by the two residues involved in the ionic interaction, and the "toggle switch" by $Trp^{6.48}$.

Compared to rhodopsin, the extracellular ends of TM3 and, in particular, TM1 are laterally more distant from the ligand binding site, while TM5 is slightly moved inwards. Another important difference is that the β_2AR crystal structure does not contain the "ionic lock" formed by electrostatic interactions and hydrogen bonds

between the cytoplasmic ends of TM3 and TM6 (Ballesteros et al., 2001). The ionic lock is known to be important for the stabilization of the inactive state of the receptor since point mutations of the interacting residues lead to constitutively active mutants (Kjelsberg et al., 1992; Lefkowitz et al., 1993). In the inactive conformation of rhodopsin the lock is closed with a distance of 2.9Å between $Glu^{6.30}$ and $Arg^{3.50}$. In the active state the ionic lock opens up (distance 4.1Å) (Salom et al., 2006). Surprisingly, this is also the case in both β_2AR structures.although carazolol, an inverse agonist, is co-crystallized. The distance between the two conserved amino acids, $Glu^{6.30}$ and $Arg^{3.50}$, amounts to 6.2Å in the β_2AR-T4L construct. However, differences between the intracellular ends of TM5 and TM6 as well as between the equivalent parts of I3 of the two β_2AR structures indicate that these regions are probably artificial due to the adducts (T4L and Fab5, respectively) which specifically alter the topology of the cytoplasmic domain. Thus, no reliable conclusions about the native structure of this region can be drawn.

5.3 Material and Methods

5.3.1 Data set

The 5-HT_{2A} partial agonists considered and their biological data (Table 5.1) were obtained from Elz et al. (Elz et al., 2002; Heim et al., 1998; Heim et al., 2002; Pertz et al., 2000; Ratzeburg et al., 2003). The design of the series was based on a structural concept derived from SAR studies on diverse 5-HT_{2A}R ligands (Elz et al., 2002; Heim et al., 2002). The 5-HT_{2A}R agonistic activity of mostly less potent primary amines as 5-HT, 3-(2-aminoethyl)quinazoline-2,4-dione, mescaline, and 1-(4-bromo-2,5-dimeth-oxyphenyl)-isopropylamine (DOB) (Figure 5.1) was increased by a factor of 50 to 2000 (Elz et al., 2002; Heim et al., 1998; Pertz et al., 2000). The most interesting derivatives showing partial agonistic activity were obtained by introduction of an *ortho*-methoxybenzyl substituent at the amine nitrogen and are up to 400-1400 times more potent than 5-HT.

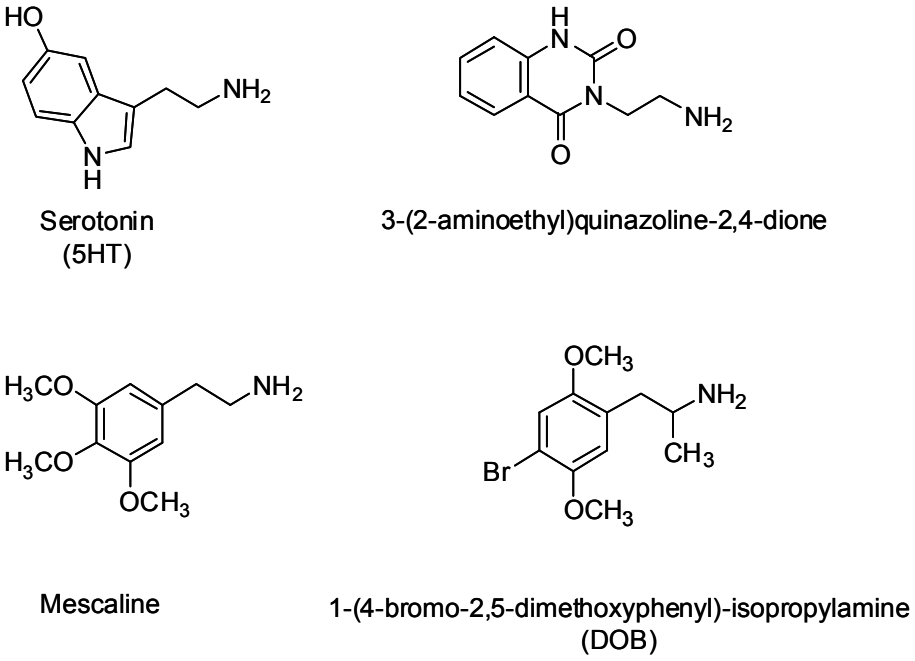

Figure 5.3: Primary amines with less potent 5-HT_{2A}R agonistic activity

5-HT_{2A}R agonistic potency (pEC_{50}) and intrinsic activity (efficacy, E_{max}) were measured by a functional in-vitro assay using cylindrical segments from rat tail arteries. The nature of the assay suggests that pEC_{50} values largely represent binding affinities since additional effects as transport and distribution do not play a major role.

5.3.2 Fragment Regression Analysis (FRA)

Fragment regression analysis was performed using the in-house program FRAREG. As an extension of the Fujita-Ban variant of simple Free-Wilson analysis, FRAREG permits more arbitrary fragmentations of the molecules and the multiple presence of a substituent in a given position. The definition of "pseudo fragments" reflecting interactions like intramolecular H bonds or steric hindrance is possible. The descriptors in the regression analysis are discrete 0-n variables. As result, the biological activity is decomposed into additive contributions of fragments and pseudo fragments. The FRAREG approach was applied to pEC_{50} (representing the 5-HT_{2A}R agonistic potency) and log K* (representing the receptor activation). The derivation of K* values was based on a simple induced fit model:

$$A+R \underset{}{\overset{K_D}{\rightleftharpoons}} AR \overset{K^*}{\rightleftharpoons} AR^* \qquad K^* = \frac{[AR^*]}{[AR]} = \frac{E_{max}}{100 - E_{max}}$$

with the aim to transform intrinsic activities into a logarithmic scale linearly related to the free energy of receptor activation.

Table 5.1: Agonistic potency (pEC_{50}) and intrinsic activity (E_{max}) of 5-HT_{2A}R partial agonistic arylethylamines (indole, methoxybenzene and quinazolinedione derivatives) used in the study.

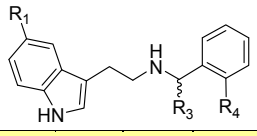

Nr	R_1	R_3	R_4	pEC_{50}	E_{max}
5-HT	OH	H	-	7.00	100
199	H	H	H	6.39	26
200	H	H	OH	6.87	47
201	H	H	OMe	6.81	44
202	H	H	OEt	6.06	19
203	H	Me	OMe	6.20	27
204	OMe	H	H	7.00	30
205	OMe	H	OH	7.50	38
206	OMe	H	OMe	7.08	54

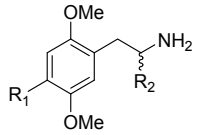

Nr	R_1	R_2	pEC_{50}	E_{max}
211	H	H	4.41	47
41	Br	H	7.20	58
35	Br	Me	7.99	71
36	I	Me	8.13	68

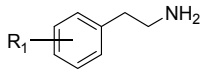

Nr	R_1	pEC_{50}	E_{max}
CH**37**	2,3,4-$(OMe)_3$	5.88	59
CH**52**	2,4,5-$(OMe)_3$	5.86	60

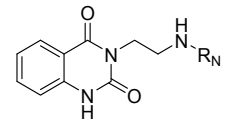

Nr	R_N	pEC_{50}	E_{max}
93	H	4.18	46
94	Bz	4.84	33
181	CH_2-2Thioph	5.47	22

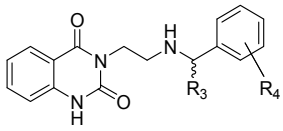

Nr	R_3	R_4	pEC_{50}	E_{max}
157	H	2-Cl	5.08	15
160	H	2-Br	5.05	16
166	H	2-Me	5.52	22
169	H	2-OMe	6.58	49
298S	*S*-Me	2-OMe	6.26	41
298R	*R*-Me	2-OMe	4.93	11
172	H	2-OEt	6.05	34
173	H	2-NH_2	5.05	54
177	H	2-OH	6.38	51

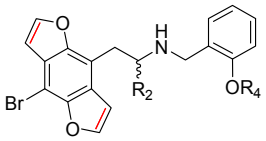

Nr	R_2	R_4	pEC_{50}	E_{max}
270	H	H	9.87	34
271	H	Me	10.15	27
273	Me	Me	8.33	17
283	H	H	9.94	24

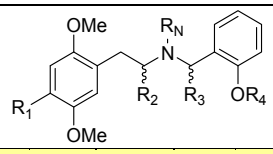

Nr	R_1	R_2	R_N/R_3	R_4	pEC_{50}	E_{max}
229	H	H	H	Me	7.73	40
230	Br	H	H	H	9.66	35
231	Br	H	H	Me	9.58	38
304S	Br	H	*S*-Me	Me	9.32	26
304R	Br	H	*R*-Me	Me	8.24	29
307	Br	H	N-Me	Me	7.41	27
234	Br	Me	H	Me	8.10	20
235	I	H	H	H	10.13	29
236	I	H	H	Me	10.09	30
305S	I	H	*S*-Me	Me	9.21	29
305R	I	H	*R*-Me	Me	8.41	28
239	CF_3	H	H	H	9.13	28
240	CF_3	H	H	Me	9.02	36

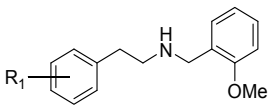

Nr	R_1	pEC_{50}	E_{max}
CH**13**	3-Br	6.90	38
CH**17**	2-Br	6.62	26
CH**45**	2,3,4-$(OMe)_3$	7.66	50
CH**54**	2,4,5-$(OMe)_3$	8.14	57
CH**55**	2,4,6-$(OMe)_3$	8.78	49
KR**5**	3,4-$(OMe)_2$	6.47	44
KR**12**	3,5-$(OMe)_2$	7.02	40
KR**22**	2,6-$(OMe)_2$	7.81	31

5.3.3 Generation of 3D structure models of 5-HT_{2A} receptors

For the construction of h5-HT_{2A}R and r5-HT_{2A}R homology models, the most complete crystal structure of the β_2AR (β_2AR-T4L, pdb ID 2rh1 (Cherezov et al., 2007)) was used as template after excision of the lysozyme adduct. The sequence of the β_2AR was mutated into that of the h5-HT_{2A}R at positions without gaps and deletions, i.e. TM1 to TM7, intracellular loops I1 and I2, and the C-terminus (C-Ter) up to Cys397, using the alignment shown in Figure 5.4. Since the 5-HT_{2A}R N- and C-termini are longer than the N- and C-termini of the β_2AR, and since the homology of the terminal sequences is low, the prediction of the chains preceding TM1 and following H8 would be highly speculative. Therefore, the first 69 N-terminal and the last 76 C-terminal residues were not considered in the construction of the models.

The remaining intracellular and extracellular loops (E1, E2, E3 and I3) were filled by the Biopolymer loop search facility in Sybyl 7.3 (Tripos, St. Luis, MO) with appropriate segments from a binary protein database based on PDB structures as described in chapter 4. Side chains and hydrogens were added using the Biopolymer module of Sybyl 7.3. The model was initially relaxed with steepest descent minimization using the Amber FF99 force field, Amber FF99 charges and a distant dependent dielectric constant of 4, until the RMS gradient approaches 0.5 kcal $mole^{-1}$ $Å^{-1}$. During the first 100 cycles, the backbone was fixed. This initial optimization was followed by a Powell minimization (end RMS gradient 0.01 kcal $mole^{-1}$ $Å^{-1}$). To verify the integrity of the structure, as last step the optimized receptor model was submitted to 3D-Verify and Procheck (Luthy et al., 1992)

```
                                        N-Ter
B2AR      ---------------------------------MGQPGNGSAF---LLAPNRSHAPDHDVTQQR-
h5HT2A    MDILCEENTSLSSTTNSLMQLNDDTRLYSNDFNS.EANTSD..NWTVDSE..TNLSCEGCLSPSC
r5HT2A    MEILCEDNISLSSIPNSLMQLGDGPRLYHNDFNSRDANTSE.SNWTIDAE..TNLSCEGCLPPTC

                    TM1                    I1              TM2
B2AR      ----DEVWVVGMGIVMSLIVLAIVFGNVLVITAIAKFERLQTVTNYFITSLACADLVMGLAVVPF
h5HT2A    LSLLHLQEKNWSALLTAVVIILTIA..I...M.VSLEKKL.NA....LM...I..MLL.FLVM.V
r5HT2A    LSILHLQEKNWSALLTTVVIILTIA..I...M.VSLEKKL.NA....LM...I..MLL.FLVM.V

          E1              TM3                        I2
B2AR      GAAHILMK-MWTFGNFWCEFWTSIDVLCVTASIETLCVIAVDRYFAITSPFKYQSLLTKNKARVI
h5HT2A    SMLT..YGYR.PLPSKL.AV.IYL...FS....MH..A.SL...V..QN.IHHSRFNSRT..FLK
r5HT2A    SMLT..YGYR.PLPSKL.AI.IYL...FS....MH..A.SL...V..QN.IHHSRFNSRT..FLK

          TM4                    E2                    TM5
B2AR      ILMVWIVSGLTSFLPIQMHWYRATHQEAINCYANETCCDFFTNQAYAIASSIVSFYVPLVIMVFV
h5HT2A    .IA..TI.VGISMPIPVFGLQDDS---KVF-KEGS—-.LLA-DDNFVLIG.F...FI..T...IT
r5HT2A    .IA..TI.VGISMPIPVFGLQDDS---KVF-KEGS—-.LLA-DDNFVLIG.F.A.FI..T...IT

                                        I3
B2AR      YSRVFQEAKRQLQKIDKSEG-RFHVQNLSQVEQDGRTG--------------HGLRRSSKFCLKE
h5HT2A    .FLTIKSLQKEATLCVSDL.T.AKLASF.FLP.SSLSSEKLFQRSIHREPGSYTG..TMQSISN.
r5HT2A    .FLTIKSLQKEATLCVSDLST.AKLASF.FLP.SSLSSEKLFQRSIHREPGSYTG..TMQSISN.

                    TM6                    E3              TM7
B2AR      HKALKTLGIIMGTFTLCWLPFFIVNIVHVIQD—-NLIR—-KEVYILLNWIGYVNSGFNPLIYCRS
h5HT2A    Q..C.V...VFFL.VVM.C....T..MA..CKESCNEDVIGALLNVFV....LS.AV...V.TLF
r5HT2A    Q..C.V...VFFL.VVM.C....T..MA..CKESCNENVIGALLNVFV....LS.AV...V.TLF

          H8                                   C-Ter
B2AR      P-DFRIAFQELLCLRRSSLKAYGNGYSSNGN---TGEQSGYHVEQEKENKLLCEDLPGTEDFVGH
h5HT2A    NKTY.S..SRYIQCQYKEN.KPLQLILV.TIPALAYKS.QLQMG.K.NS.QDAKTTDNDCSMVAL
r5HT2A    NKTY.S..SRYIQCQYKENRKPLQLILV.TIPALAYKS.QLQVG.K.NSQEDAEQTVDDCSMVTL


B2AR      QGTVPSDNIDSQGRNCSTNDSLL
h5HT2A    GKQHSEEASKDNSDGVNEKV.CV
r5HT2A    GKQQSEENCTDNIETVNEKV.CV
```

Figure 5.4: Sequence alignment of the β_2AR with 5-HT$_{2A}$Rs. Dots in the sequence indicate identity with the β_2AR. Amino acids shown with grey shading represent the most conserved position in each TM. For the r5-HT$_{2A}$R, the positions which differ from the h5-HT$_{2A}$R are indicated in bold.

5.3.4 Ligand selection, structure generation and docking

The selection of one representative compound from each structural class – (1) indoles, (2) methoxybenzenes, (3) quinazolinediones – of 5-HT$_{2A}$R partial agonistic arylethylamines was based on high potency and reproduction of all favourable ligand-receptor interactions, also taking into account results from FRA. Among the

substituents at the amino moiety which were similarly varied in each subseries (see Table 5.1), a 2-methoxybenzyl group is optimal. Therefore each class was represented by a derivative containing this substituent. The selected compounds, 5OH-**201** (indole, additionally representing interaction of a 5-OH substituent like in 5-HT), **231** (methoxybenzene) and **169** (quinazolinedione), are represented in Figure 5.5.

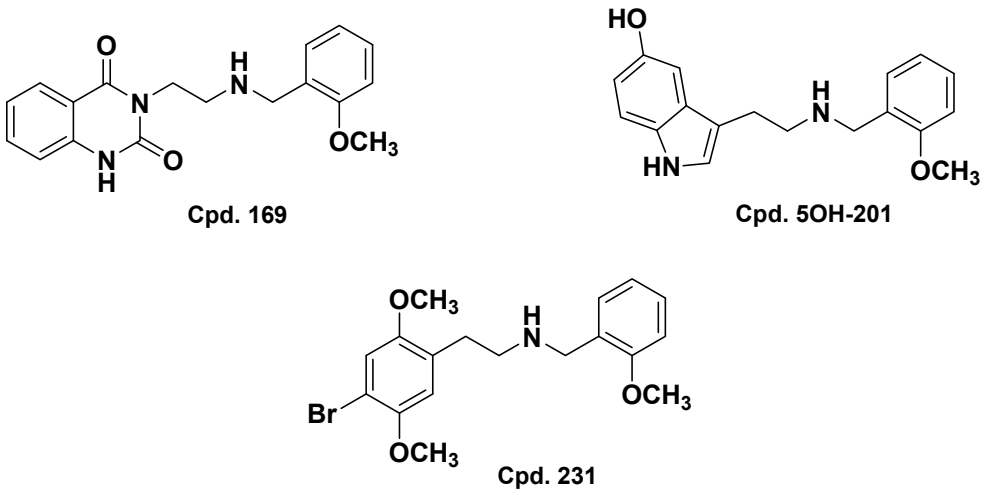

Figure 5.5: Representative structures used for the docking studies

The structures were constructed using Sybyl 7.3. All molecules were assumed to be protonated under physiological conditions. AmberFF99 atom types and Gasteiger-Hückel charges were assigned to the ligands. Assuming that the ligands share a common binding site at the receptor, a structure-based alignment was to be achieved. I.e., the docking modes (bioactive conformations) must rely on informations about the location of putative binding site residues. Site-directed mutagenesis studies, as already described in Chapter 4, indicate that the highly conserved Asp155$^{3.32}$ (Sealfon et al., 1995; Wang et al., 1993), the serines Ser159$^{3.36}$, Ser239$^{5.43}$, Ser242$^{5.46}$ (Ala242 in r5-HT_{2A}R) (Johnson et al., 1994) and the phenylalanines Phe243$^{5.47}$, Phe244$^{5.48}$, Phe340$^{6.52}$ (Choudhary et al., 1993; Choudhary et al., 1995) are important for binding and efficacy of agonists and partial agonists at the 5HT_{2A}R. The three ligands were manually docked into the binding site considering the mutagenesis data and the QSAR obtained from fragment regression analysis. During docking, the conformation of the ligands was varied in order to get maximal overlap of the scaffolds and shared interactions with the essential amino acids described above. The complexes were optimized by a stepwise approach: (1) 50 cycles AmberFF99 force field with fixed ligands (distant dependent dielectric

constant 4, steepest descent method), (2) subset minimization of the ligand and a receptor region 6 Å around using the combined protein-ligand force field MMFF64 (distant dependent dielectric constant 1, Powell method) up to an RMS gradient of 0.05 kcal $mole^{-1}$ $Å^{-1}$), (3) AmberFF99 force field with fixed ligands (distant dependent dielectric constant 4, Powell method, final RMS gradient 0.01 kcal $mole^{-1}$ $Å^{-1}$). Range constraints were occasionally applied between $Asp155^{3.32}$ and the protonated nitrogen of the ligands, additionally for cpd. **231** between $Ser159^{3.36}$ and the 2-OCH3 group, and for cpds. 5OH-**201** and **231** between $Ser239^{5.43}$ and the 5-OH and 5-OCH3 group, respectively.

5.3.5 3D QSAR Approaches: CoMFA and CoMSiA

A common structure-based alignment of the whole series was obtained by adjustment of the conformations according to the template of the respective structural class (cpds. **169**, 5OH-**201**, **231**), followed by minimizations with the template forcing method (multifit in Sybyl 7.3). CoMFA (Cramer et al., 1988b) and CoMSIA (Klebe et al., 1994) approaches were performed with the QSAR module of Sybyl 7.3. The grid size was set to 2.0 Å. In CoMFA, the steric and electrostatic fields were calculated using the default probe atom, $C.3^{+}$, and cutoff of the energies at 30 kcal/mole. In CoMSIA, the steric, electrostatic, hydrophobic, and hydrogen bond donor and acceptor fields, based on interactions of the molecules with a common probe atom (radius 1 Å, charge +1, hydrophobicity +1, H bond donor and acceptor properties +1), were considered with an attenuation factor α of 0.3.

For correlation of pEC_{50} values with the CoMFA and CoMSIA field variables, Partial Least Square (PLS) models (Wold et al., 1984) were generated by the QSAR module of Sybyl 7.3. Different cross-validation variants (Cramer et al., 1988a), leave-one-out and leave-ten-out (10 runs), were applied to obtain predictive models and to determine the optimal number of components according to the lowest standard error of prediction (s_{PRESS}).

5.4 Results and Discussion

5.4.1 Fragment Regression Analysis

"Additivity models" based on indicator variables and calculated by Free-Wilson analysis or FRA are well suited preliminary tools to obtain concise, easily interpretable QSAR results. To a certain degree, these approaches also check the coherence of the biological data and the congenerity of the series and allow the recognition of outliers. For the present FRA of pEC_{50} and log K* values, 2-phenethylamine was defined as basic structure whose contribution is represented by the intercept of the regression equation. The series has been simplified in a general structure shown in Figure 5.6.

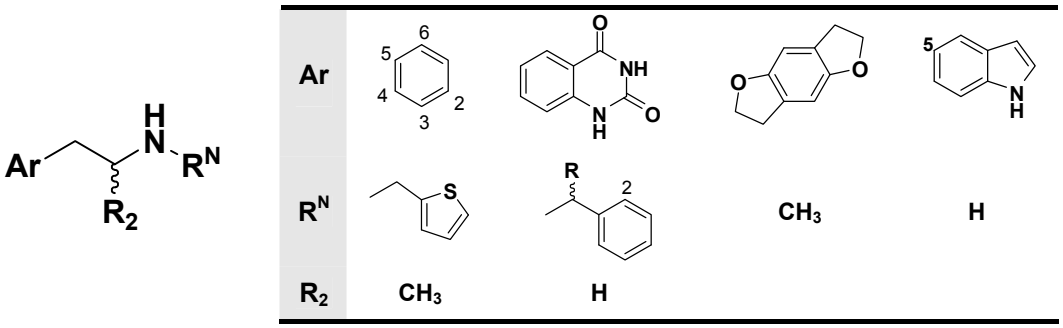

Figure 5.6: Basic structure, fragmentation and main fragments

The results are shown in Table 5.2. The FRA of pEC_{50} explains 95.7 % of the data variance. The high correlation is also due to the large range of pEC_{50} values. The residual standard deviation of 0.49 is of acceptable size compared to the experimental error. The basic phenethylamine with a contribution of only 3.45 provides a scaffold for activity enhancing substitutions and modifications. The larger aromatic systems (indole, quinazolinedione) increase pEC_{50} by ca. 1 log unit. The striking and nearly additive effect of methoxy substituents at the indole (5-OMe) and the phenyl moiety is congruent with the high contribution of the benzodifuran moiety. It can be suggested that at least one oxygen atom is involved in a polar interaction with the receptor.

The second striking result is the large contribution of lipophilic substituents like halogens and CF_3 in *para* position of phenethylamine derivatives (1.9 to 2.9 pEC_{50} units), indicating fit to a specific hydrophobic site.

Table 5.2: Results of the fragment regression analysis, FRA, of pEC_{50} and log K*

Pos.	Fragment	pEC_{50}		log K*	
		increment	95% conf.int.[1]	increment	95% conf.int.[1]
Intercept (basic structure)		3.45	±1.62 ***	-0.07	±0.66
Ar	Phenyl [2]	0		0	
	Indolyl	1.36	±1.46 *	0.19	±0.60
	Quinazolinedione	0.94	±1.61	0.25	±0.66
	Benzodifuranyl	1.89	±1.60 **	-0.16	±0.66
	2OMe	0.97	±1.14 *	-0.01	±0.47
	3OMe	0.64	±1.13	0.05	±0.46
	4OMe	0.77	±0.74 **	0.26	±0.30 *
	5OMe	0.79	±0.70 **	0.12	±0.29
	6OMe	1.61	±1.16 ***	0.08	±0.48
	2Br	1.29	±1.85	-0.07	±0.76
	3Br	1.57	±1.85 *	0.17	±0.76
	4Br	2.44	±0.81 ***	0.08	±0.33
	4I	2.93	±0.85 ***	0.09	±0.35
	$4CF_3$	1.91	±1.01 ***	-0.05	±0.42
R^2	H [2]	0		0	
	Me	-0.61	±0.67 *	-0.05	±0.27
R^N	H [2]	0		0	
	Benzyl	1.14	±0.83 ***	-0.56	±0.34 ***
	CH_2-thiophenyl	1.08	±1.19 *	-0.74	±0.49 ***
	2OH	0.89	±0.74 **	0.23	±0.31
	2OMe	0.74	±0.73 **	0.24	±0.30 *
	2OEt	0.31	±0.95	-0.05	±0.39
	2Me	-0.02	±1.23	-0.18	±0.50
	2Cl	-0.46	±1.23	-0.38	±0.50
	2Br	-0.49	±1.23	-0.35	±0.50
	$2NH_2$	-0.49	±1.23	0.44	±0.50 *
	(R)-Me	-1.41	±0.72 ***	-0.40	±0.30 ***
	(S)-Me	-0.38	±0.65	-0.18	±0.27
	N-Me	-2.12	±1.14 ***	-0.24	±0.47
		r	0.978	**r**	0.869
		r^2	0.957	**r^2**	0.755
		s	0.492	**s**	0.202
		F	20.64 ***	**F**	2.84 ***

[1] Significance levels for t-tests of the increments: * >90%, ** >95%, *** >99%. [2] Fragment belonging to the basic structure (contribution included in the intercept).

On average, methyl groups in α-position of the ethyl side chain decrease activity. However, the effect of α-Me depends on R^N: if one considers the pEC_{50} values and residuals, it becomes obvious that the methyl branch is favourable in primary amines and unfavourable in secondary benzylamines. This different behaviour may be simply due to a potential interaction of the α-Me group with the receptor which is not possible in the case of a bulky R^N moiety because of restricted degrees of freedom for fit. A methyl group as part of a tertiary amine strongly lowers activity.

It is well known that aralkyl groups as R^N substituents lead to high affinity of agonists and antagonists for many biogenic amine receptors. Corresponding to this quite general rule, secondary benzylamines are more than one pEC_{50} unit more active at the r5-HT_{2A}R than their NH_2 analogs. An *ortho*-OH or -OMe substituent at the phenyl ring further increases activity, so that the contribution of 2-OMe- or 2-OH-benzyl groups approaches 2 log units. The effect of other *ortho* substituents is not significant. It may be suggested that the oxygen is involved in a polar interaction with the receptor. Among the stereoisomeric methylbenzyl groups, the *S* isomer is equiactive compared to benzyl, whereas the *R* configuration leads to reduction of the activity by nearly 1.5 pEC_{50} units.

There is no real outlier in the FRA of pEC_{50} even when the weak criterion abs(residual) > 2s is applied. However, eight compounds cannot be validated because of unique substituents (residuals of 0). Three of the four largest residuals are due to the different α-Me effect (see above). The fourth "outlier“ is the "simple" 2,5-dimethoxyphenethylamine, whose activity is by 0.8 pEC_{50} units lower than calculated.

The analysis of log K* should provide some detailed information about structure-efficacy relationships on a scale which closely represents the free energy of receptor activation. However, this approach suffers from the low standard deviation of the dependent variable (range of log K* from -0.91 to 0.39, s = 0.29). The FRA model explains 75% of the variance.

Therefore, conclusions from the analysis are restricted to some more pronounced effects. The contribution of 2-phenethylamine as basic structure is about zero corresponding to an intrinsic activity of 50%. Larger aromatic systems (indole, quinazolinedione) and methoxy substituents (except 2-OMe) only slightly increase log K*. No contribution is significantly different from zero at the 95% level. It seems that all arylethylamine moieties except those with a benzodifuranyl group are

approximately equipotent in their ability to induce the transition from the inactive to the active receptor state. In the present series of partial agonists, appropriate substitution can improve this potential by only 0.3 log K* units.

Strikingly, log K* is significantly reduced in the case of the secondary amines. The same groups (benzyl, CH_2-2-thiophenyl) which strongly increase pEC_{50} reduce the intrinsic activity. This effect may be slightly counterbalanced by *ortho* benzyl substituents (OH, OMe, NH_2), indicating the role of polar interactions at this position also for receptor activation. On the other hand, *ortho*-halogen substitution is unfavourable. Generally, the gain in affinity by the bulky benzyl group is accompanied by a loss of the ability to activate the receptor, possibly due to reduced flexibility of the complex.

All these results and suggestions have been used, together with informations from the mutagenesis data, for the derivation of the putative human and rat 5-HT_{2A}R binding site and have been confirmed with the docking studies (see also Chapter 4).

5.4.2 Comparison between 5-HT_{2A}R models derived from β_2AR and from bovine rhodopsin

Needless to say that the differences between the crystal structures of bovine rhodopsin and the β_2 adrenoceptor mentioned above are also found in the corresponding models. The degree of homology between the 5-HT_{2A}R and the β_2AR is much higher than between the 5-HT_{2A}R and rhodopsin (32.2% vs 19%), and also the ligands of the two biogenic amine GPCRs are mutually similar, but different to retinal. Thus, the β_2AR should be a more suitable template for 5-HT_{2A}R and, in particular, ligand binding site models than rhodopsin.

In both the β_2AR and the rhodopsin based models of the 5-HT_{2A}R the packing of the seven TM helices is conserved. The secondary structure of the receptor is composed of seven TM domains (TM1-TM7) connected by three intracellular (I1-I3) and three extracellular loops (E1-E3), a truncated N-termius and the helical portion (H8) of the C-terminal domain. The conformations of the E2 loops differ depending on the template (Figure 5.7). E2 is constrained by a disulfide bridge between Cys148 and Cys272 in both models, but inserted into the membrane bilayer only in the case of the model derived from rhodopsin. In the β_2AR based model the E2 conformation is

more open towards the extracellular side so that the ligand may easily intrude into the binding site. The E2 loop of the β_2AR contains a small α-helix that is probably not present in the 5-HT_{2A}R. The length of this loop in the β_2AR and the 5-HT_{2A}R differs by 4 amino acids (22 and 18 residues, respectively). Moreover, the β_2AR shows a second, intra-E2 disulfide bond between Cys184 and Cys190 which stabilizes the helical conformation. Together these differences argue against corresponding α-helices in both biogenic amine GPCRs.

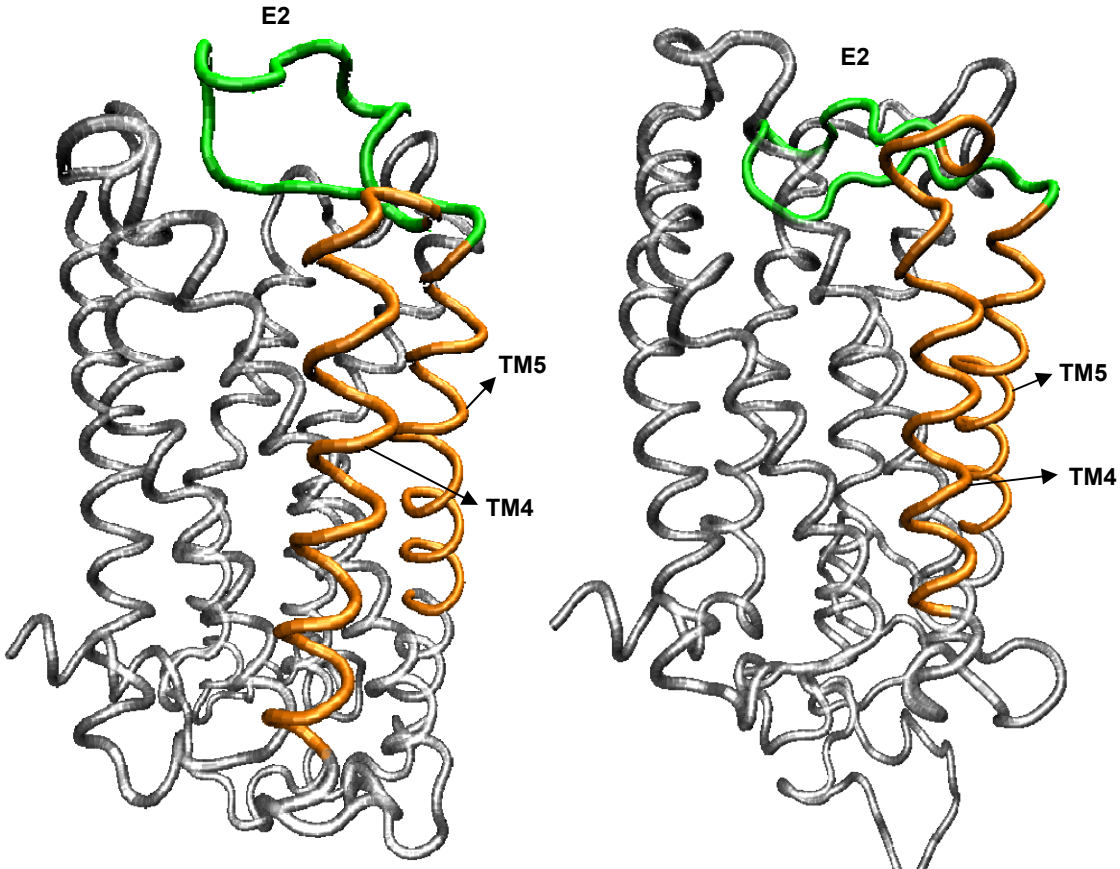

Figure 5.7: Side view of the 5-HT2AR models derived from the β_2AR (left) and bovine rhodopsin (right) crystal structures. In orange are shown TMs 4 and 5 connected by E2 (green).

The rhodopsin crystal structure and the models derived from it contain a number of interhelical contacts that are predicted to stabilize the TM domains in the inactive state of the receptor and that presumably play a functional role in the receptor activation (see Chapter 4). In the β_2AR based model, most of these contacts are not present (see Table 5.3).

Table 5.3: Comparison of interhelical interactions in the 5-HT_{2A}R models derived from bovine rhodopsin and β_2AR crystal structures

Domain	Residues	Min. distance (Å)*	
		5-$HT_{2A}R^1$	5-$HT_{2A}R^2$
TM1-TM3	$Asn92^{1.50}$ - $Asp120^{2.50}$	2.45	4.20
TM3	$Arg173^{3.50}$ - $Asp172^{3.49}$	2.11	2.37
TM3-TM6	$Arg173^{3.50}$ - $Glu318^{6.30}$	1.95	9.10
TM7-TM2	$Asn376^{7.49}$ - $Asp120^{2.50}$	2.04	5.10
TM7	$Asn376^{7.49}$ - $Ser373^{7.46}$	3.65	7.16

1 Model derived from bovine rhodopsin
2 Model derived from β_2AR
* Distance between the nearest heavy atoms of interacting residues

As already mentioned, the long distance between $Arg173^{3.50}$ and $Glu318^{6.30}$ is probably artificial due to the T4L adduct in the β_2AR template. However, typical interactions suggested to be responsible for the inactive state in analogy to rhodopsin are replaced by other contacts, some of them mediated by water molecules. E.g., $Asn92^{1.50}$ interacts *via* water with $Asn376^{7.49}$ and directly with $Ser373^{7.46}$, $Thr88^{1.46}$ and $Ile96^{1.54}$; $Asp120^{2.50}$ interacts with $Asn376^{7.49}$, $Gly124^{2.54}$ and *via* a water molecule with $Ser372^{7.45}$; $Asn376^{7.49}$ interacts with $Tyr380^{7.53}$, and $Ser373^{7.46}$ with $Tyr370^{7.43}$ supposed to be involved in ligand binding.

Also the open conformation of E2 is stabilized by a network of polar interactions. The side chain of Ser119 interacts with the side chain of Asp232, the side chain of Asp218 with the side chain of Lys223, and the backbone of Phe222 with the side chain of Lys220 and with the backbone of Ser226.

Looking at the binding site of the two receptor models (Figure 5.8) there are no significant differences. The position of the residues is similar in both models, but the binding site of the β_2AR based model is slightly shifted to the left due to the different position of some TM domains, in particular TM3 and TM5. Therefore the binding mode of the ligands should largely correspond to that suggested from 5-HT_{2A}R-partial agonist complexes based on the rhodopsin template (see Chapter 4).

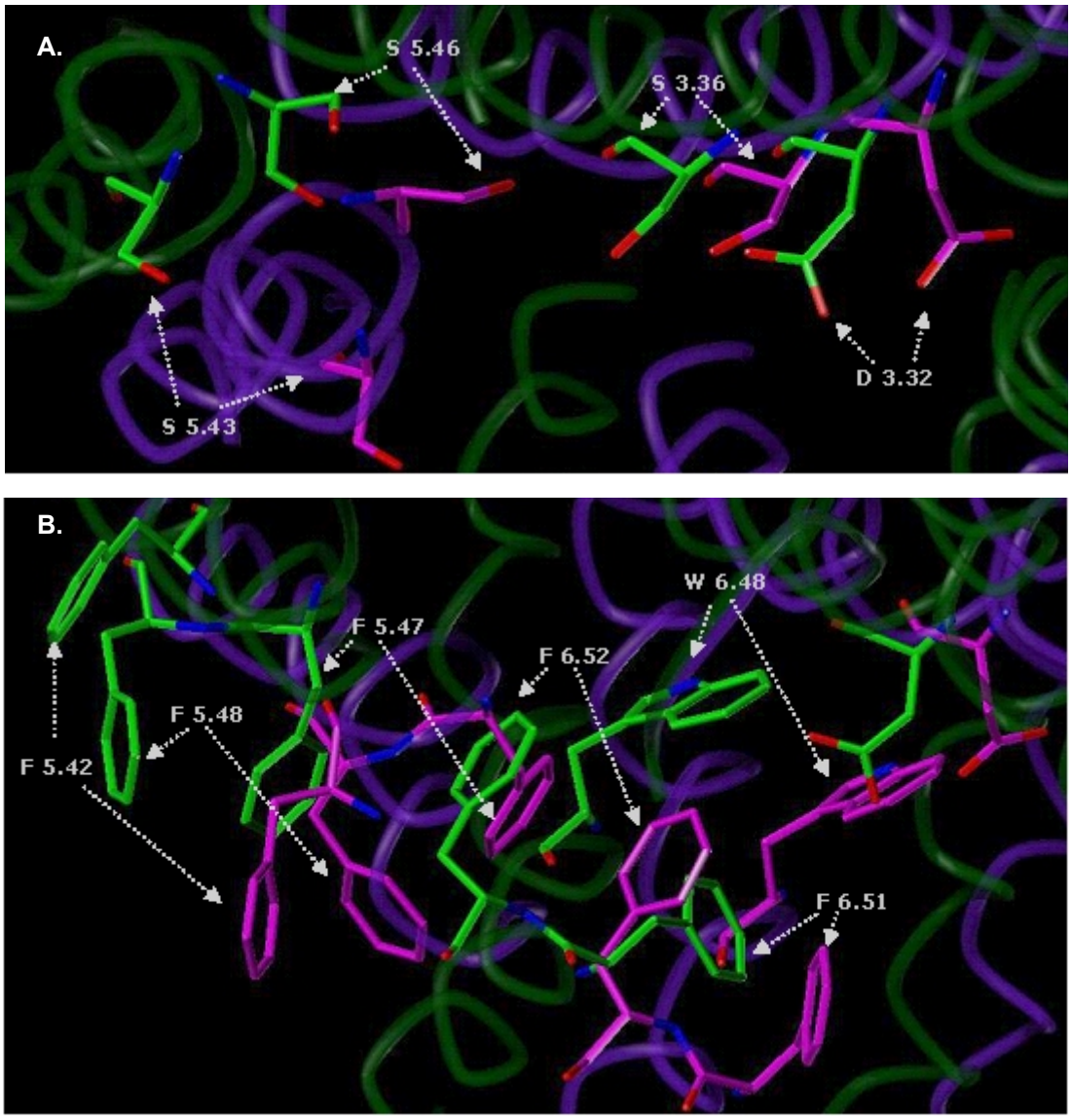

Figure 5.8: Binding site superposition of the h5-HT_{2A}R models derived from β_2AR (green) and from bovine rhodopsin (magenta). **A.** Representation of the residues involved in polar interactions with the ligands. **B.** Representation of the two hydrophobic pockets involved in interactions with aromatic moieties of the ligands.

5.4.3 Docking of representative partial agonists

As representative 5-HT_{2A}R partial agonists of the arylethylamine series the compounds 5OH-**201** (indole), **231** (methoxybenzene) and **169** (quinazolinedione) were selected (see Figure 5.5). Without consideration of the 5-hydroxy group added to cpd. **201**, the contributions of the three aryl fragments to pEC_{50} differ by only ca. 0.8 orders of magnitude (see Table 5.2). Furthermore, the effects of a 5-methoxy group at the aryl moiety and of a benzyl group as R^N is similar in each structural

class. Therefore an overlapping binding mode of the different partial agonists is likely which can be derived from the docking of the three ligands into the 5-HT_{2A}R model. Figure 5.9 shows the complexes of the r5-HT_{2A}R with the representative compounds 5OH-**201**, **231** and **169**, respectively, after energy optimization.

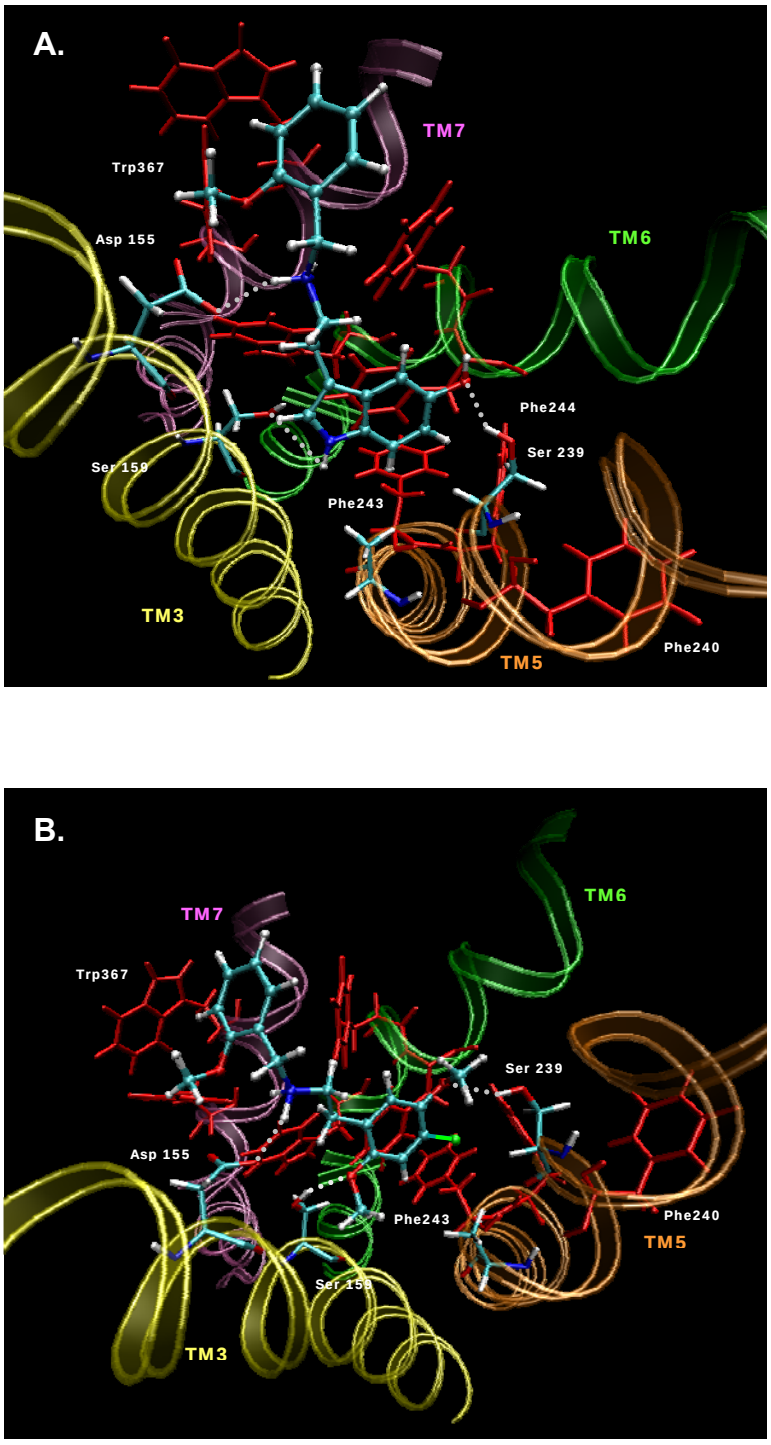

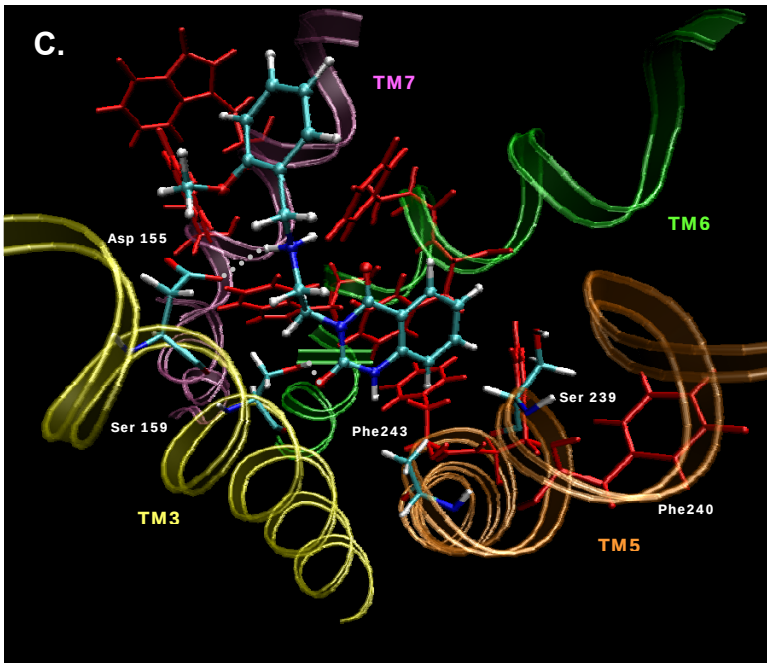

Figure 5.9: View of the r5-HT_{2A}R model from the extracellular side, in complex with cpds. 5OH-**201** (**A**), **231** (**B**) and **169** (**C**). The putative agonist binding site (C atoms of amino acids in cyan and red, respectively) and the three α helices (TM3 in green, TM5 in orange and TM6 in yellow) are shown. The amino acids in red represent hydrophobic pockets interacting with the ligands. The white dotted lines represent specific polar interactions.

In accord with the general analogy of the binding sites (see Figure 5.8), the important interactions of the three compounds with the β_2AR based r5-HT_{2A}R model are similar to those suggested from the receptor model derived from bovine rhodopsin (for detailed discussion, see Chapter 4), and can be summarized as follows:

- The arylethylamine moieties interact with three sites: (1) $Asp155^{3.32}$ forming a salt bridge with the cationic amine, (2) a hydrophobic pocket comprising $Phe243^{5.47}$, $Phe244^{5.48}$ and $Phe340^{6.52}$, as well as (3) $Ser159^{3.36}$ and $Ser239^{5.43}$ as possible H bond acceptors or donors.
- Strongly potency increasing halogen substituents in *para*-position of dimethoxy-phenyl compounds (cpd **231**, Figure 5.9 B) and the phenyl moiety of quinazolinedione derivates (cpd.**169**, Figure 5.9 C) project onto the hydrophobic pocket formed by $Phe243^{5.47}$ and $Phe244^{5.48}$.
- $Ser159^{3.36}$ may interact with the indole NH, one of the the quinazolinedione oxygens and with the 2-OMe group of dimethoxyphenyl compounds. In the h5-HT_{2A}R, $Ala242^{5.46}$ of the rat species is mutated into $Ser242^{5.46}$ which is possibly involved in H bonds with these groups, too.

- 5-OH and 5-OMe substituted indoles and 2,5-dimethoxyphenethyl compounds are able to form H bonds with Ser239$^{5.43}$. Thus, bidentate polar interactions of aryl moieties are possible in the case of these derivatives, whereas quinazolinediones probably form only one H bond.
- The benzyl substituent (R^N) interacts with a second hydrophobic pocket consisting of aromatic residues around Phe339$^{6.51}$ (Trp367$^{7.40}$ and Tyr370$^{7.43}$).
- Since an oxygen in *ortho*-position of the benzyl group (2-OH, 2-OMe) further enhances activity, an additional interaction with a hydrogen donor, possibly via water, may be suggested. In contrast to the models based on rhodopsin, Asn343$^{6.55}$ is too far away from these substituents for direct interaction.

5.4.4 3D-QSAR models

CoMFA and CoMSIA techniques were used to study quantitative structure-activity relationships of the 5-HT_{2A}R partial agonists at the three dimensional level. The pEC_{50} values were used as the dependent variable. The most crucial step in 3D QSAR approaches is to generate an alignment that represents the active conformation of the compounds. Most reliable is a structure-based alignment, using the three compounds in the conformations obtained from the docking studies as templates (Figure 5.10).

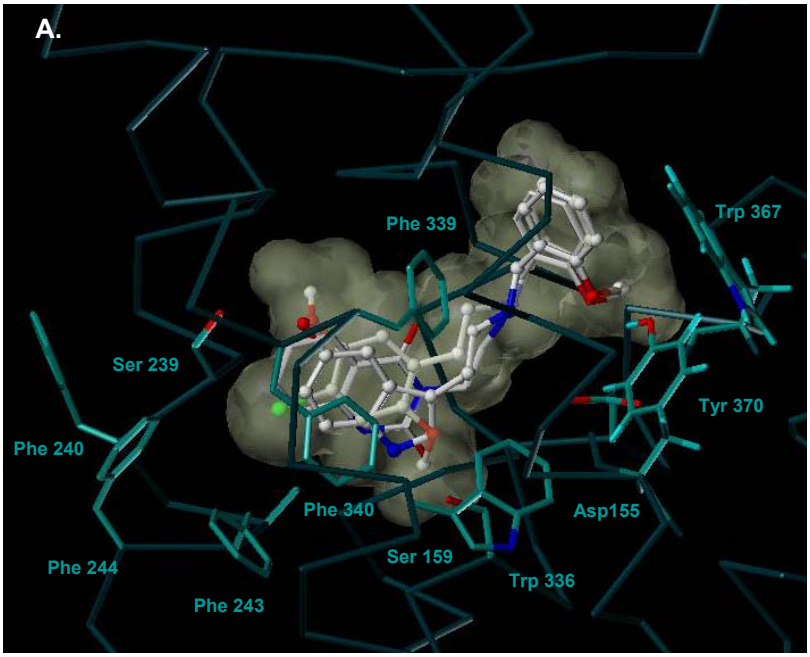

B.

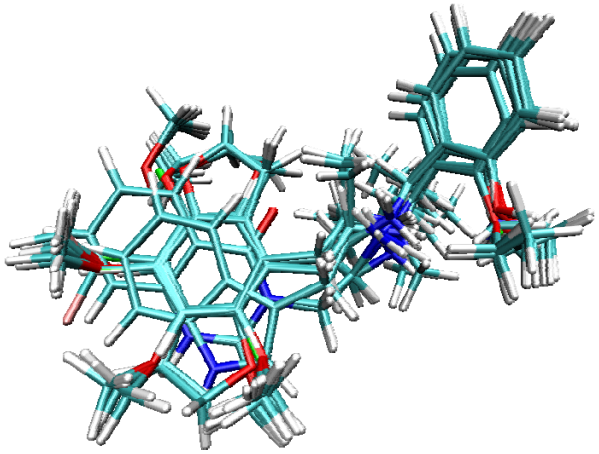

Figure 5.10: A. Binding conformation and alignment of compounds **169**, 5OH-**201** and **231**; **B.** Superposition of all compounds used in 3D QSAR analysis

Figure 5.10 also shows the resulting alignment of all compounds from Table 5.1 (except **181** because of the unique thiophenyl group) used for the 3D QSAR approaches.

The results of the PLS analyses of the dependence of pEC_{50} on the field variables from CoMFA and CoMSIA are summarized in Table 5.4.

Table 5.4: CoMFA and CoMSIA results

Analysis	Fields	Leave-one-out			Leave-ten-out			Final model		
		q^2	s_{PRESS}	PCs	q^2	s_{PRESS}	PCs	r^2	s	PCs
CoMFA	*SE*	0.716	0.922	4	0.700-0.788	0.890-1.043	4-10	0.858	0.651	4
CoMSIA	*SEHA*	0.807	0.752	3	0.763-0.809	0.767-0.957	3 (4)	0.873	0.610	3

Field contributions: **CoMFA** *S* : 0.80, *E*: 0.20. **CoMSIA** *S*: 0.16, *E*: 0.19, *H*: 0.47, *A*: 0.18

Fields: S – steric, E – electrostatic, H – hydrophobic, A – H bond acceptor

The CoMFA model, based on steric and electrostatic field variables, resulted in a cross-validated q^2 of 0.716 at the first minimum of s_{PRESS}, indicating an optimal number of four principal components (PCs). However, there was a second, even lower s_{PRESS} minimum at 10 PCs. Whereas the leave-ten-out cross validation generally confirmed the good predictivity of the model, the optimal number of PCs varied from 4 to 10. Using a large number of PCs increases the complexity and adds more details, but enhances the risk of "explaining noise" by low-variance PCs. It appears that the higher PCs depend on the least potent compounds (pEC_{50} < 5) since omission of these derivatives consistently led to three-component models.

Possibly the low activity of some 5-HT_{2A}R partial agonists is additionally due to other reasons than weak affinity (reasons that rely on the in-vitro organ assay). It is therefore appropriate to stop the inclusion of PCs at the most trusted number, i.e., four, even if some "compound specific" effects on the potency are not contained in the non-crossvalidated model. The final PLS analysis with four PCs explains 86% of the data variance, corresponding to a residual error of 0.651. This model is mainly based on the steric interactions of the ligands with the r5-HT_{2A}R, the contribution of the electrostatic field amounts to only 20%.

CoMSIA approaches considered the steric, electrostatic, hydrophobic, H-bond acceptor and H-bond donor fields. The latter one was excluded in the final models because of the marginal contribution to the explained data variance. Leave-one-out crossvalidation resulted in a slightly better predictive power than with CoMFA (q^2 0.807 vs. 0.716), and the optimal number of PCs was reduced to three. Also in this case, the leave-ten-out approaches were quite consistent. In contrast to CoMFA, the number of PCs varied only between three and four. The final PLS model accounts for 87% of the data variance (residual error 0.610). The contribution of the electrostatic field is about the same as in CoMFA. However, the steric effects representing 80% of the CoMFA model are now partitioned into a main, hydrophobic fraction (47%) and additional H-bond acceptor and "pure" steric components (ca. 18%).

An advantage of CoMFA and CoMSIA is the possibility to visualise the field effects on the biological activity as 3D contour plots. This graphical representation is helpful to identify the regions where structural modifications can affect the potency of the compounds. Moreover, structure-based alignments enable to project the contour plots onto the underlying receptor model, suggesting which ligand-receptor interactions account for the QSAR. Thus, the following CoMFA and CoMSIA plots are drawn inside the putative r5-HT_{2A}R binding site, taking the models with the three representative compounds as reference (cp. Figs. 5.9 and 5.10). .

The isocontour plots of the steric and electrostatic field contributions obtained from CoMFA are drawn together with exemplary ligands and the active site of the r5-HT_{2A}R in Figure 5.11. These maps show regions where differences in molecular fields are associated with differences in the biological activity.

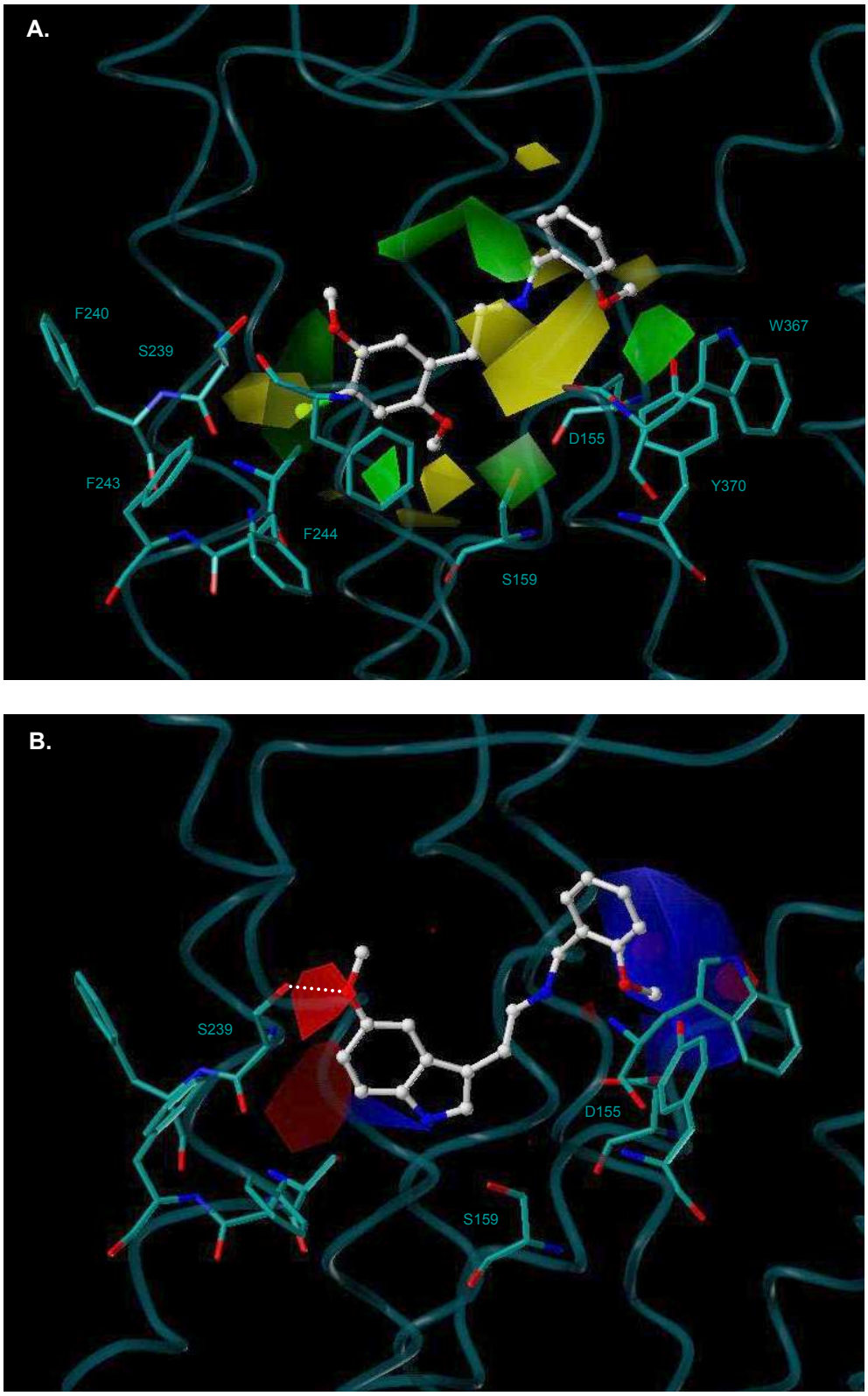

Figure 5.11: CoMFA contour maps projected into the r5-HT_{2A}R binding site. **A.** Contribution of the steric field, docking of cpd. **231**: green – bulk increases potency, yellow – bulk decreases potency.. **B.** Contribution of the electrostatic field, docking of cpd. **206**: red – negative charge increases potency, blue – positive charge increases potency.

In Figure 5.11 **A.**, the 2,5-dimethoxyphenyl derivative **231** is displayed. The green and yellow regions around the halogen substituent in *para* position of the phenyl ring point into the pocket of mainly aromatic amino acids in TM5. This pocket is narrowed and may optimally interact with *p*-Br and *p*-I substituents. The introduction of a benzyl substituent at the protonated nitrogen significantly increases the activity. This effect is reproduced by the green regions close to the benzyl moiety. The yellow contours along the alkylamine chain probably reflect the largely unfavourable influence of methyl branches and the potency differences between *(R)*- and *(S)*-methylbenzyl derivatives (distomers and eutomers, respectively)..

In Figure 5.11 **B.**, the electrostatic contour map is displayed together with the indole **206**. The red contour close to the 5-methoxy group indicates that a negative charge is favourable in this position, suggesting a H bond with $Ser239^{5.43}$ as modeled in the docking studies. The blue region around the indolic nitrogen is in agreement with its role as H bond donor, probably for $Ser159^{3.36}$. However, the arrangement of the blue and red contours below the indole moiety do not correspond to interactions of quinazolinedione derivatives with this residue. The contributions of indole and quinazolinedione fragments to pEC_{50} are similar (see FRA results), so that in both cases one H bond with the r5-HT_{2A}R can be assumed. It will be shown below that the separation of electrostatic and H bond acceptor fields in CoMSIA is better suited to predict structural effects in more detail. The small red contours at the benzyl group indicate the favourable influence of 2-hydroxy or 2-methoxy substituents. That positive charges around the benzyl moiety increase the potency (blue region) might be due to electron-withdrawing effects of those groups.

The isocontour plots of the steric, electrostatic, hydrophobic and H-bond acceptor field contributions resulting from CoMSIA are drawn together with representative ligands and the active site of the r5-HT_{2A}R in Figures 5.12 – 5.15. The effects of the steric fields on pEC_{50} (Fig. 5.12) largely correspond to the CoMFA results in spite of the much lower overall contribution to the model (16% *vs.* 80% in CoMFA). The green regions around the benzyl and the aryl moieties indicate optimal fit into the binding site with some degrees of freedom for larger rings or substituents in 6-position of phenethylamines.

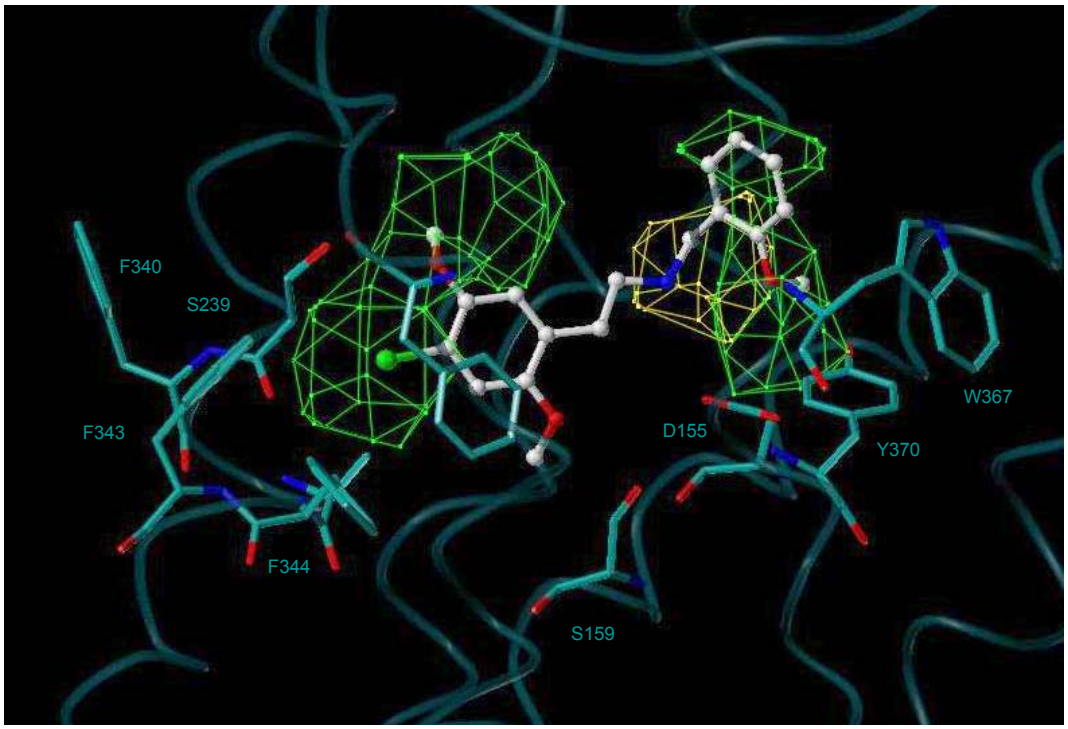

Figure 5.12: CoMSIA contour map of the steric field contribution projected into the r5-HT_{2A}R binding site, docking of cpd. **231**: green – bulk increases potency, yellow – bulk decreases potency.

The contributions of the electrostatic fields to pEC_{50} (Fig. 5.13) are more distinct than in the case of the CoMFA approach. The favourable effect of negative charges around the aryl moiety corresponds to the increase in potency caused by methoxy and halogen substituents in 2-, 4-, 5- and 6-position of phenethylamines and by the oxygens of quinazolinediones. Accordingly, the CoMSIA model suggests the role of $Ser159^{3.36}$ and $Ser239^{5.43}$ as H bond donors. However, the blue region close to the indole nitrogen, present in the electrostatic field contributions from CoMFA (see Fig. 5.11) and assumed to reflect an H bond with $Ser159^{3.36}$ as acceptor, is missing. At the benzyl moiety, the negative charge of, in particular, 2-hydroxy and -methoxy substituents is favourable.

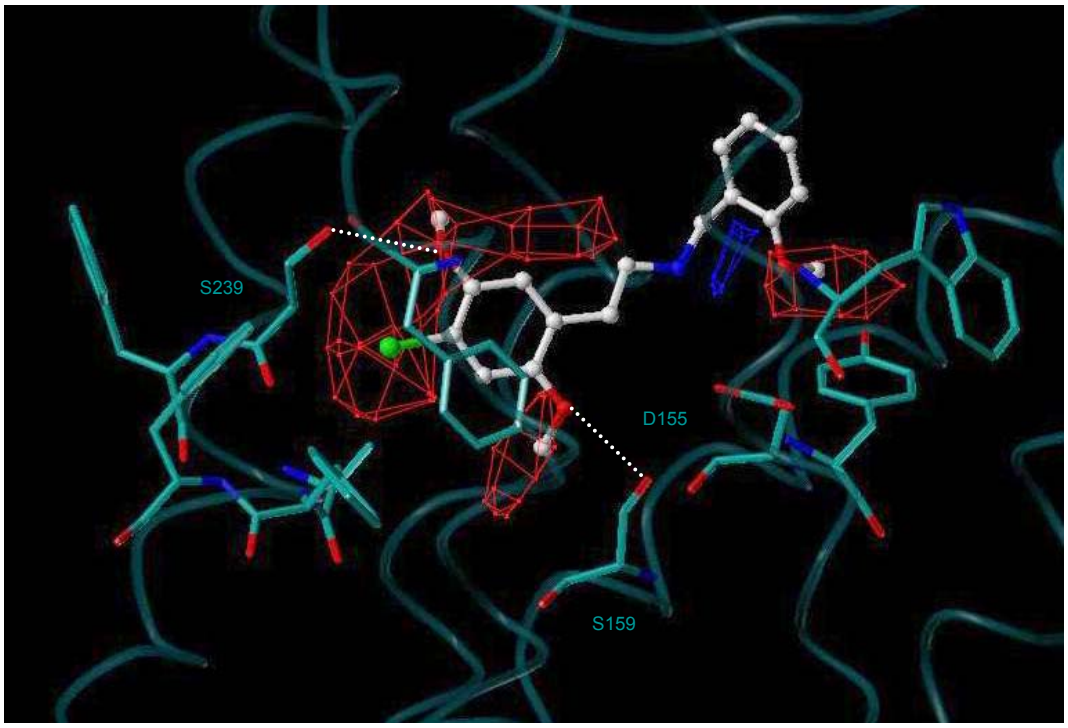

Figure 5.13: CoMSIA contour map of the electrostatic field contribution projected into the r5-HT_{2A}R binding site, docking of cpd. **231**: red – negative charge increases potency, blue – positive charge increases potency.

In some respects, the contributions of the hydrophobic (Fig. 5.14) and the steric fields to pEC_{50} complement one another. Taking into account that the overall contribution of hydrophobicity predominates in CoMSIA (47% *vs.* 16% of the steric fields), the effect of, e.g., halogen substituents in *para* position of phenethylamines is mainly of lipophilic nature, emphasizing that interaction with a hydrophobic pocket formed by $Phe243^{5.47}$, $Phe244^{5.48}$ and $Phe340^{6.52}$ is possible. In other positions of the phenyl ring and in corresponding regions of quinazolinediones, polar groups whose contributions are also represented by the electrostatic fields are favourable (red contours in Fig. 5.14). The role of a benzyl group for high potency is reflected by hydrophobicity, too. 2-substituents at this moiety are surrounded by a "polar" region, again indicating that electronic effects predominate in this position.

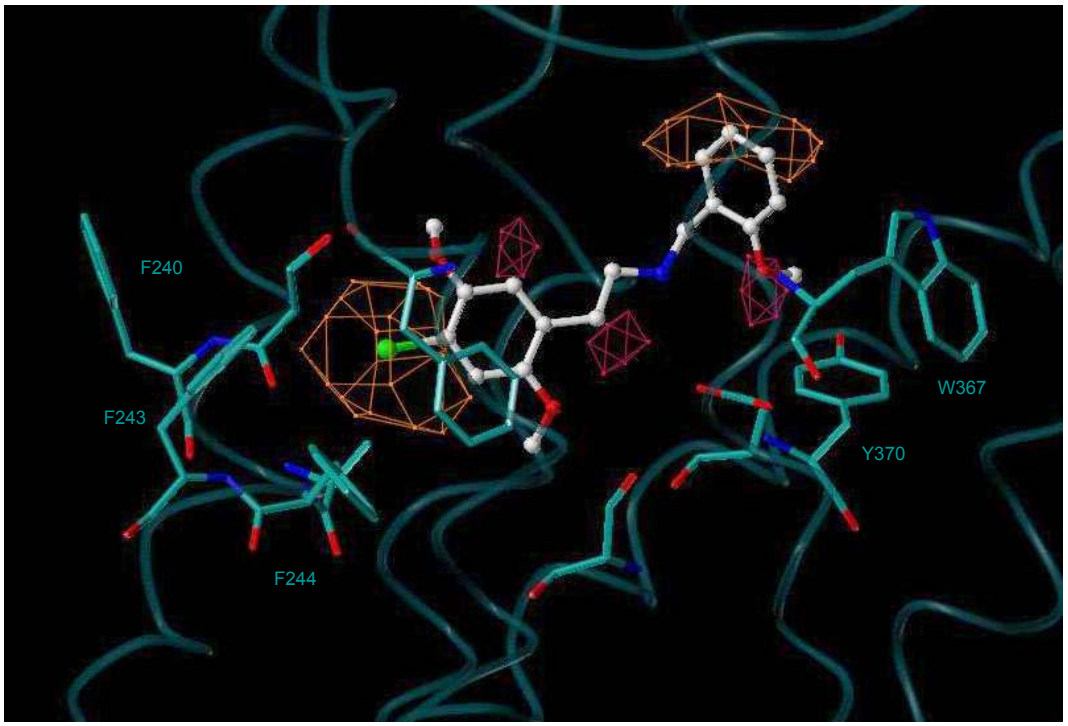

Figure 5.14: CoMSIA contour map of the hydrophobic field contribution projected into the r5-HT_{2A}R binding site, docking of cpd. **231**: orange – hydrophobic groups increase potency, red – hydrophobic groups decrease potency.

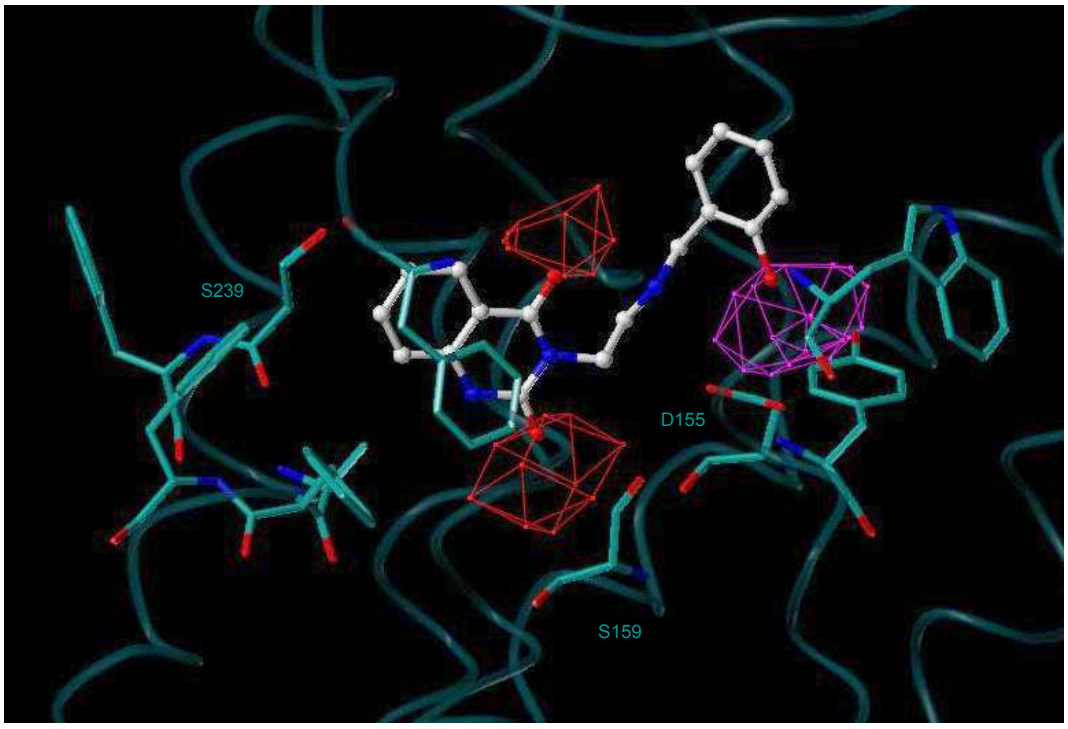

Figure 5.15: CoMSIA contour map of the H-bond acceptor field contribution projected into the r5-HT_{2A}R binding site, docking of cpd. **169**: magenta – H-bond acceptor groups increase potency, red – H-bond acceptor groups decrease potency.

The contributions of the H-bond acceptor fields to pEC_{50} (Fig. 5.15) must be analyzed together with the electrostatic efffects (Fig. 5.13). The magenta contour surrounding the methoxy substituents in *ortho*-position of the benzyl group again indicates the capability of this group to form an H bond with the receptor (possibly via a water molecule). However, this effect is in parallel with the potency increasing influence of a negative charge in the electrostatic field contributions so that the nature of the interaction is in question. On the other hand, the red contours at the aryl moiety, corresponding to unfavourable effects of H bond acceptor properties just in the case of the quinazolinedione oxygens, seem to counterbalance the role of negative charges in this region (see Fig. 5.13). Thus, the effects of the aryl systems on r5-HT_{2A}R agonistic activity are quite subtle, and the different field contributions cannot be simply separated into definite modes of interaction.

5.5 Conclusions

In this study, two 3D QSAR approaches, CoMFA and CoMSIA, have been used to predict the partial agonistic activity of a series of 50 5-HT_{2A}R ligands. The set contains three different structural classes of compounds and presents a large variability of the pharmacological data. The recent crystal structure of the human β_2AR has been used to generate 5-HT_{2A}R models by homology modeling. Based on in-vitro mutagenesis data and on a preliminary fragment regression analysis of the partial agonistic potency, docking studies of representative ligands have led to the identification of putative bioactive conformations, to suggestions about important interactions with amino acids of the binding site and to a structure-based alignment of the whole series. The models derived from the 3D QSAR approaches are compatible with the docking studies and indicate which effects account for the activity of the compounds considered.

5.6 References

Ballesteros, J. A., A. D. Jensen, G. Liapakis, S. G. Rasmussen, L. Shi, U. Gether, and J. A. Javitch, 2001, Activation of the beta 2-adrenergic receptor involves disruption of an ionic lock between the cytoplasmic ends of transmembrane segments 3 and 6: *J Biol Chem*, v. **276**: p. 29171-7.

Cherezov, V., D. M. Rosenbaum, M. A. Hanson, S. G. Rasmussen, F. S. Thian, T. S. Kobilka, H. J. Choi, P. Kuhn, W. I. Weis, B. K. Kobilka, and R. C. Stevens, 2007, High-resolution crystal structure of an engineered human beta2-adrenergic G protein-coupled receptor: *Science*, v. **318**: p. 1258-65.

Choudhary, M. S., S. Craigo, and B. L. Roth, 1993, A single point mutation (Phe340-->Leu340) of a conserved phenylalanine abolishes 4-[125I]iodo-(2,5-dimethoxy)phenylisopropylamine and [3H]mesulergine but not [3H]ketanserin binding to 5-hydroxytryptamine2 receptors: *Mol Pharmacol*, v. **43**: p. 755-61.

Choudhary, M. S., N. Sachs, A. Uluer, R. A. Glennon, R. B. Westkaemper, and B. L. Roth, 1995, Differential ergoline and ergopeptine binding to 5-hydroxytryptamine2A receptors: ergolines require an aromatic residue at position 340 for high affinity binding: *Mol Pharmacol*, v. **47**: p. 450-7.

Costanzi, S., S. Vincenzetti, G. Cristalli, and A. Vita, 2006, Human cytidine deaminase: a three-dimensional homology model of a tetrameric metallo-enzyme inferred from the crystal structure of a distantly related dimeric homologue: *J Mol Graph Model*, v. **25**: p. 10-6.

Cramer, I., R.D., J. D. Buce, and D. E. Petterson, 1988a, Crossvalidation, bootstrapping, and Partial Least Squares compared with multiple regression in conventional QSAR studies: *Quant. Struct.-Act. Relat.*, v. **7**: p. 18-25.

Cramer, I., R.D., D. E. Patterson, and J. D. Buce, 1988b, Comparative Molecular Field Analysis (CoMFA): Effect of Shape on Binding of Steroids to Carrier Protein: *J. Am. Chem. Soc.*, v. **110**: p. 5959-5967.

Elz, S., T. Kläß, U. Warnke, and H. H. Pertz, 2002, Developpement of highly potent partial agonists and chiral antagonists as tool for the stsudy of 5-HT2A-receptor mediated function: *Naunyn-Schmiedeberg's Arch. Pharmacol*, v. **365**: p. R29.

Heim, R., H. H. Pertz, I. Walther, and S. Elz, 1998, Congeners of 3-(2-Benzylaminoethyl)-2,4-quinazolindione: partial agonists for rat vascular 5-HT2A receptors: *Naunyn-Schmiedeberg's Arch. Pharmacol*, v. **358**: p. R105.

Heim, R., H. H. Pertz, M. Zabel, and S. Elz, 2002, Stereoselective synthesis, absolute configuration and 5-HT_{2A} agonism of chiral 2-methoxybenzylamines: *Arch. Pharm. Pharm. Med. Chem.*, v. **335**: p. 82.

Hubbell, W. L., C. Altenbach, C. M. Hubbell, and H. G. Khorana, 2003, Rhodopsin structure, dynamics, and activation: a perspective from crystallography, site-directed spin labeling, sulfhydryl reactivity, and disulfide cross-linking: *Adv Protein Chem*, v. **63**: p. 243-90.

Johnson, M. P., R. J. Loncharich, M. Baez, and D. L. Nelson, 1994, Species variations in transmembrane region V of the 5-hydroxytryptamine type 2A receptor alter the structure-activity relationship of certain ergolines and tryptamines: *Mol Pharmacol*, v. **45**: p. 277-86.

Kjelsberg, M. A., S. Cotecchia, J. Ostrowski, M. G. Caron, and R. J. Lefkowitz, 1992, Constitutive activation of the alpha 1B-adrenergic receptor by all amino acid substitutions at a single site. Evidence for a region which constrains receptor activation: *J Biol Chem*, v. **267**: p. 1430-3.

Klebe, G., U. Abraham, and T. Mietzner, 1994, Molecular similarity indices in a comparative analysis (CoMSIA) of drug molecules to correlate and predict their biological activity: *J Med Chem*, v. **37**: p. 4130-46.

Lefkowitz, R. J., S. Cotecchia, P. Samama, and T. Costa, 1993, Constitutive activity of receptors coupled to guanine nucleotide regulatory proteins: *Trends Pharmacol Sci*, v. **14**: p. 303-7.

Luthy, R., J. U. Bowie, and D. Eisenberg, 1992, Assessment of protein models with three-dimensional profiles: *Nature*, v. **356**: p. 83-5.

Okada, T., Y. Fujiyoshi, M. Silow, J. Navarro, E. M. Landau, and Y. Shichida, 2002, Functional role of internal water molecules in rhodopsin revealed by X-ray crystallography: *Proc Natl Acad Sci U S A*, v. **99**: p. 5982-7.

Okada, T., M. Sugihara, A. N. Bondar, M. Elstner, P. Entel, and V. Buss, 2004, The retinal conformation and its environment in rhodopsin in light of a new 2.2 A crystal structure: *J Mol Biol*, v. **342**: p. 571-83.

Palczewski, K., T. Kumasaka, T. Hori, C. A. Behnke, H. Motoshima, B. A. Fox, I. Le Trong, D. C. Teller, T. Okada, R. E. Stenkamp, M. Yamamoto, and M. Miyano, 2000, Crystal structure of rhodopsin: A G protein-coupled receptor: *Science*, v. **289**: p. 739-45.

Pertz, H. H., R. Heim, and S. Elz, 2000, *N*-Benzylated Phenylethanamines are Highly Potent Partial Agonists at 5-HT_{2A} Receptors: *Arch. Pharm. Pharm. Med. Chem.*, v. **333**: p. 30.

Rasmussen, S. G., H. J. Choi, D. M. Rosenbaum, T. S. Kobilka, F. S. Thian, P. C. Edwards, M. Burghammer, V. R. Ratnala, R. Sanishvili, R. F. Fischetti, G. F. Schertler, W. I. Weis, and B. K. Kobilka, 2007, Crystal structure of the human beta2 adrenergic G-protein-coupled receptor: *Nature*, v. **450**: p. 383-7.

Ratzeburg, K., R. Heim, S. Mahboobi, J. Henatsch, H. H. Pertz, and S. Elz, 2003, Potent partial 5-HT_{2A}-receptor agonism of phenylethamines related to mescaline in the rat tail artery model: *Naunyn-Schmiedeberg's Arch. Pharmacol*, v. **367**: p. R31.

Rosenbaum, D. M., V. Cherezov, M. A. Hanson, S. G. Rasmussen, F. S. Thian, T. S. Kobilka, H. J. Choi, X. J. Yao, W. I. Weis, R. C. Stevens, and B. K. Kobilka, 2007, GPCR engineering yields high-resolution structural insights into beta2-adrenergic receptor function: *Science*, v. **318**: p. 1266-73.

Sakmar, T. P., S. T. Menon, E. P. Marin, and E. S. Awad, 2002, Rhodopsin: insights from recent structural studies: *Annu Rev Biophys Biomol Struct*, v. **31**: p. 443-84.

Salom, D., D. T. Lodowski, R. E. Stenkamp, I. Le Trong, M. Golczak, B. Jastrzebska, T. Harris, J. A. Ballesteros, and K. Palczewski, 2006, Crystal structure of a

photoactivated deprotonated intermediate of rhodopsin: *Proc Natl Acad Sci U S A*, v. **103**: p. 16123-8.

Schertler, G. F., C. Villa, and R. Henderson, 1993, Projection structure of rhodopsin: *Nature*, v. **362**: p. 770-2.

Sealfon, S. C., L. Chi, B. J. Ebersole, V. Rodic, D. Zhang, J. Ballesteros, and H. Weinstein, 1995, Related Contribution of Specific Helix 2 and 7 Residues to Conformational Activation of the Serotonin 5-HT_{2A} Receptor: *The Journal of Biological Chemistry*, v. **28**: p. 16683-16688.

Teller, D. C., T. Okada, C. A. Behnke, K. Palczewski, and R. E. Stenkamp, 2001, Advances in determination of a high-resolution three-dimensional structure of rhodopsin, a model of G-protein-coupled receptors (GPCRs): *Biochemistry*, v. **40**: p. 7761-72.

Wang, C. D., T. K. Gallaher, and J. C. Shih, 1993, Site-directed mutagenesis of the serotonin 5-hydroxytrypamine2 receptor: identification of amino acids necessary for ligand binding and receptor activation: *Mol Pharmacol*, v. **43**: p. 931-40.

Warne, T., M. J. Serrano-Vega, J. G. Baker, R. Moukhametzianov, P. C. Edwards, R. Henderson, A. G. Leslie, C. G. Tate, and G. F. Schertler, 2008, Structure of a beta(1)-adrenergic G-protein-coupled receptor: *Nature*.

Wold, S., A. Ruhe, H. Wold, and W. J. Dunn, 1984, The covariance problem in linear regression. The Partial Least Square (PLS) approach to generalized inverses: *SIAM J. Sci. Stat.*, v. **Comp. 5**: p. 735-743.

Chapter 6
Modeling of the human 5-HT_{2A} receptor in different active states and of interactions with ligands

6.1 Introduction

The binding of agonists stabilizes or induces active states of GPCRs, representing specific conformations which are recognised by heterotrimeric G-proteins through interactions with the intracellular domains. Analysis of several GPCR mutants has indicated that the transmembrane (TM) pocket close to the extracellular region forms the binding site for cationic biogenic amine ligands, while the intracellular loops mediate receptor-G-protein coupling (Strader et al., 1994). Changes in certain TM positions lead to constitutively active receptor mutants, CAMs (Robinson et al., 1992; Scheer and Cotecchia, 1997), whereas other mutations generate uncoupling mutants, UCMs, that bind agonists, but fail to activate G proteins (Monnot et al., 1996; Strader et al., 1988). Some mutations affect agonist, but not antagonist binding (Wess et al., 1991), and vice versa (Heitz et al., 1999). These findings and the observation of rigid-body motions of the TMs (Farrens et al., 1996; Resek et al., 1993) in the photoactivation process of rhodopsin suggest the presence of multiple conformational states in inactive and active GPCRs. Whereas the recent crystal structures of the human β_2-adrenoceptor provide direct information on the 3D structure of inactive GPCR states, there are still no homologous templates represen-

ting active GPCR conformations. However, conclusions can be drawn from analogies with the respective states of rhodopsin. The photochemical isomerisation of the retinylidene chromophore transfers rhodopsin, a class A GPCR, from the inactive to the active form, metharhodopsin II, through a number of photointermediates: bathorhodopsin, lumirhodopsin, metarhodopsin I, metarhodopsin $I_{380,}$ metarhodopsin Ib (Figure 6.1). The activation process comprises several steps corresponding to different states of receptor activation.

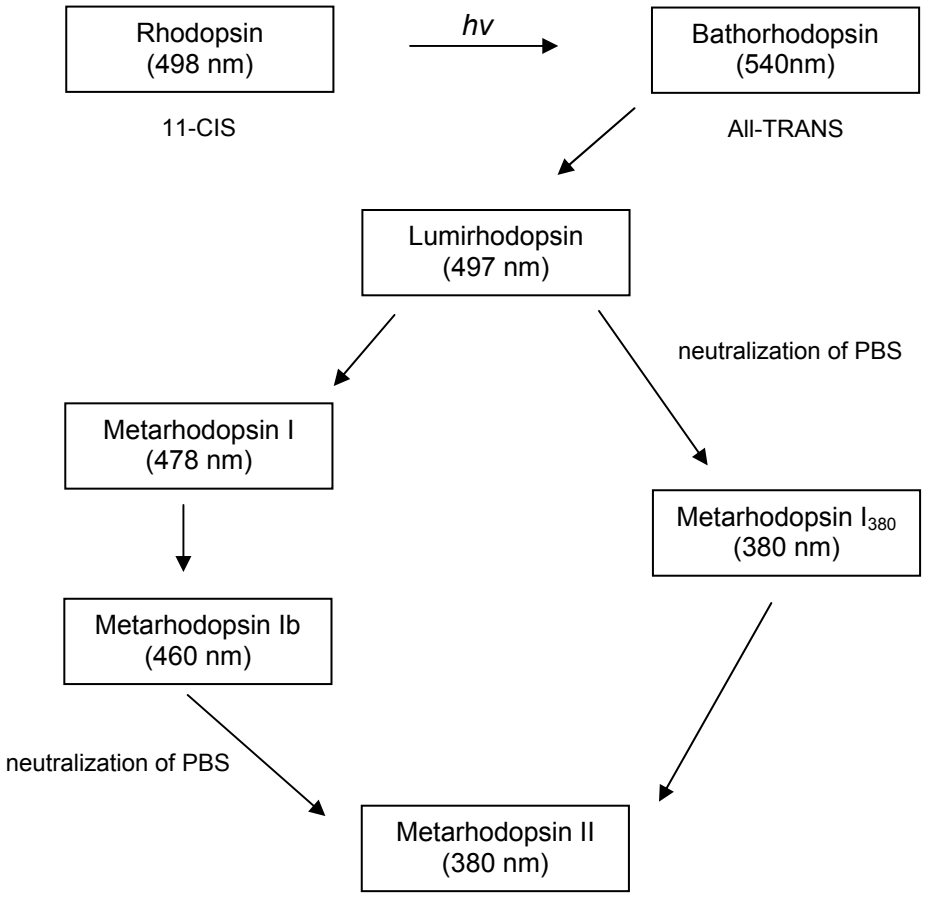

Figure 6.1: The photocascade of rhodopsin photointermediates. Rhodopsin binds the 11-cis retinylidene chromophore which isomerizes to the all-trans chromophore in bathorhodopsin. Neutralization of the Schiff base (PBS) occurs under physiological conditions during the lumirhodopsin to metarhodopsin I_{380} transition, or at low temperatures during the metarhodopsin Ib to metarodopsin II transition. The UV absorption maximum for each of the photointermediates is indicated in parenthesis.

The structural changes of the receptor photointermediates during the activation process has been suggested from FTRI (Ohkita et al., 1995), NMR (Feng et al., 2000), CD (Shichida et al., 1978; Waggoner and Stryer, 1971) mutagenesis (Struthers et al., 2000) and molecular modeling studies (Choi et al., 2002; Ishiguro,

2004; Ishiguro et al., 2003; Ishiguro et al., 2004). All these studies indicate that the arrangement of TMs 1, 2, 5 and 7 is not strongly affected by the conversion of rhodopsin to metarhodopsin II. In particular, TMs 1, 2, and 7 remain unchanged during the activation process because of the stability of an H-bond network formed by conserved residues and a hydrophobic core consisting of residues at the intracellular ends of the three TMs and in helix 8. However, TMs 3, 4 and 6 move away from their positions in the rhodopsin structure, the largest displacements occuring in the cytoplasmic face of the receptor. During photoactivation and cis-trans isomerisation of retinal, TM3 is forced outwards probably as result of steric interactions with the chromophore. This initial motion corresponds to the formation of the first, instable photointermediate, bathorhodopsin. Lumirhodopsin and metarhodopsin I_{380} result after a subsequent swing of the C-terminal end of TM3 and a following movement and partial rotation of the N-terminal part of TM4. The complete activation of the receptor, corresponding to metarhodopsin II, is caused by a counter-clockwise rotation (ca. 100°) of TM6 around the axis of its N-terminal end and a translation of TM6 towards TM3.

As described above, the motions of the transmembrane segments lead to different receptor structures with specific functions. Metarhodopsin I does not bind the G protein transducin and is thus totally inactive, whereas the subsequent intermediate, metarhodopsin Ib, binds but does not activate transducin (Sakmar, 1998; Tachibanaki et al., 1997). The photoisomerization of the retinylidene chromophore induces the motion of TM3 and TM4 and the formation of the next intermediates. The initial movement of these helices appears to be insufficient for interactions of the second intracellular loop (I2) with transducin. The structure of metarhodopsin I_{380}, photointermediate in the alternative pathway to metarhodopsin II, is suggested to be analogous to a rhodopsin mutant with higher constitutive activity than opsin (Ishiguro, 2004; Robinson et al., 1992). This mutant, although only partially active, exhibits full activity upon binding of exogenous all-*trans* retinal. Thus, the mutant structure is expected to resemble a receptor state stabilized by partial agonists, and the formation of the fully active form is thought to involve rotational motion of TM6.

Let us assume that three of the photointermediates in the rhodopsin photocascade, rhodopsin, metarhodopsin I_{380}, and metarhodopsin II, correspond to individual GPCR states, namely an inactive, a partially active, and a fully active state, representing the binding of antagonists, partial agonists and agonists, respectively (Figure 6.2). Then

it should be possible to extend the results obtained for the interaction of ligands with the inactive state of the h5-HT_{2A}R (based on rhodopsin, see Chapter 4). The aim of the present chapter is to derive homology models of partially active and fully active h5-HT_{2A}R states, to analyze their characteristic features, and to perform docking of representative partial agonists and agonists.

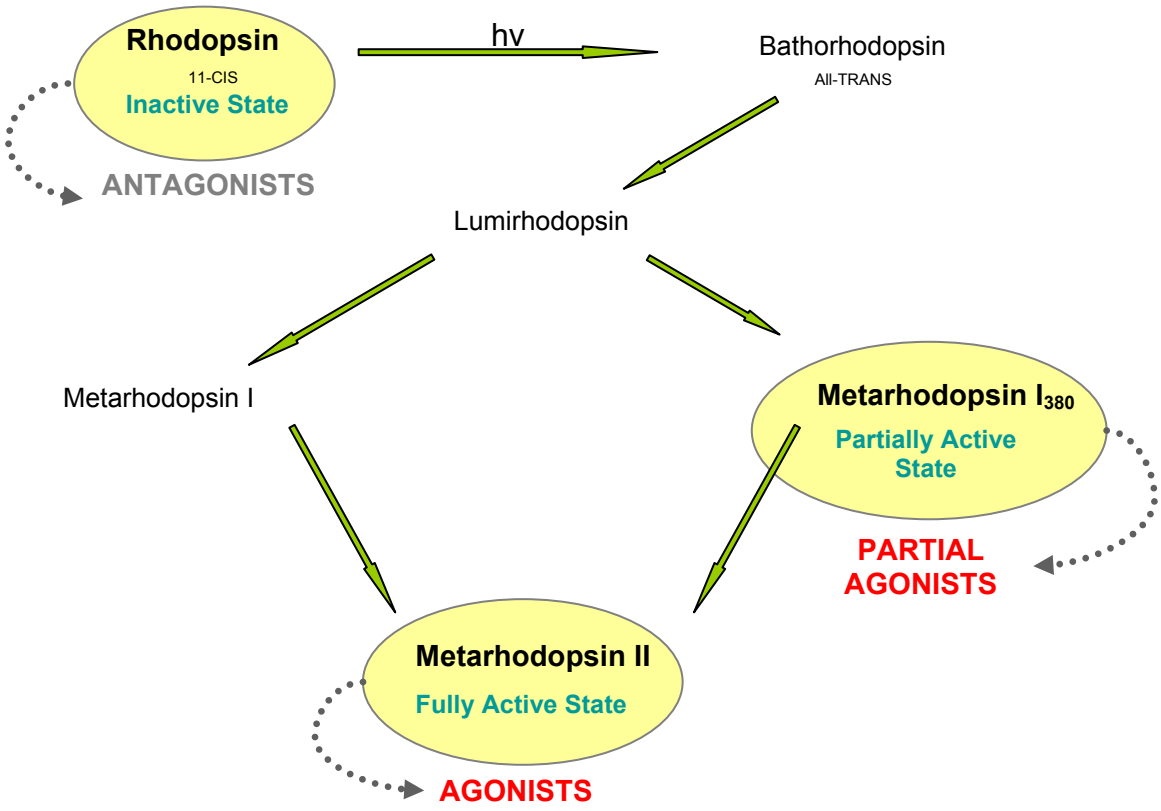

Figure 6.2: The supposed three binding states of the receptor, rhodopsin (inactive state), metarhodopsin I_{380} (partially active state), and metarhodopsin II (fully active state), involved in the binding of functionally distinct ligands, antagonists, partial agonists, and agonists respectively.

6.2 Material and methods

6.2.1 Model construction

3D models of the human 5-HT_{2A} receptor (h5-HT_{2A}R) were generated by homology modeling using the structures of bovine rhodopsin in two different states of activation as template. The structures were produced by Dr. M. Ishiguro from Suntory Institute for Bioorganic Research, Osaka, and kindly handed to our laboratory for this study (Figure 6.3).

The sequence of the bovine rhodopsin templates was mutated into the corresponding sequence of the h5-HT_{2A}R at positions without gaps and deletions using the same alignment as obtained from the Fugue approach in Chapter 4 (Figure 6.4). The remaining intracellular and extracellular loops (E2, I2, I3) were filled by the Biopolymer loop search facility in Sybyl 7.3 (Tripos, St. Luis, MO) with appropriate segments from a binary protein database based on PDB structures. Side chains and hydrogens were added using the Biopolymer package of Sybyl 7.3. The models were relaxed first with steepest descent minimization using the Amber FF99 force field, Amber FF99 charges and a distant dependent dielectric constant of 4, until the RMS gradient approaches 0.5 kcal $mole^{-1}$ $Å^{-1}$. This initial optimization was followed by a Powell minimization (end RMS gradient 0.01 kcal $mole^{-1}$ $Å^{-1}$). The energy minimizations were carried out with fixed backbones to avoid large movements of the TM domain (see below). To verify the integrity of the structures, the optimized receptor models were submitted to 3D-Verify and Procheck (Luthy et al., 1992).

Since the N-terminal and the C-terminal segments of the h5-HT_{2A}R are by 39 and 37 residues, respectively, longer than the corresponding parts of bovine rhodopsin, and since the degree of homology is very low in these regions, the modeling of the termini is highly speculative. Therefore, the first 70 and the last 71 residues were not considered in the construction of the models.

As reference of the inactive state, the h5-HT_{2A}R model derived from the crystal structure of bovine rhodopsin (1F88) was used (see Chapter 4).

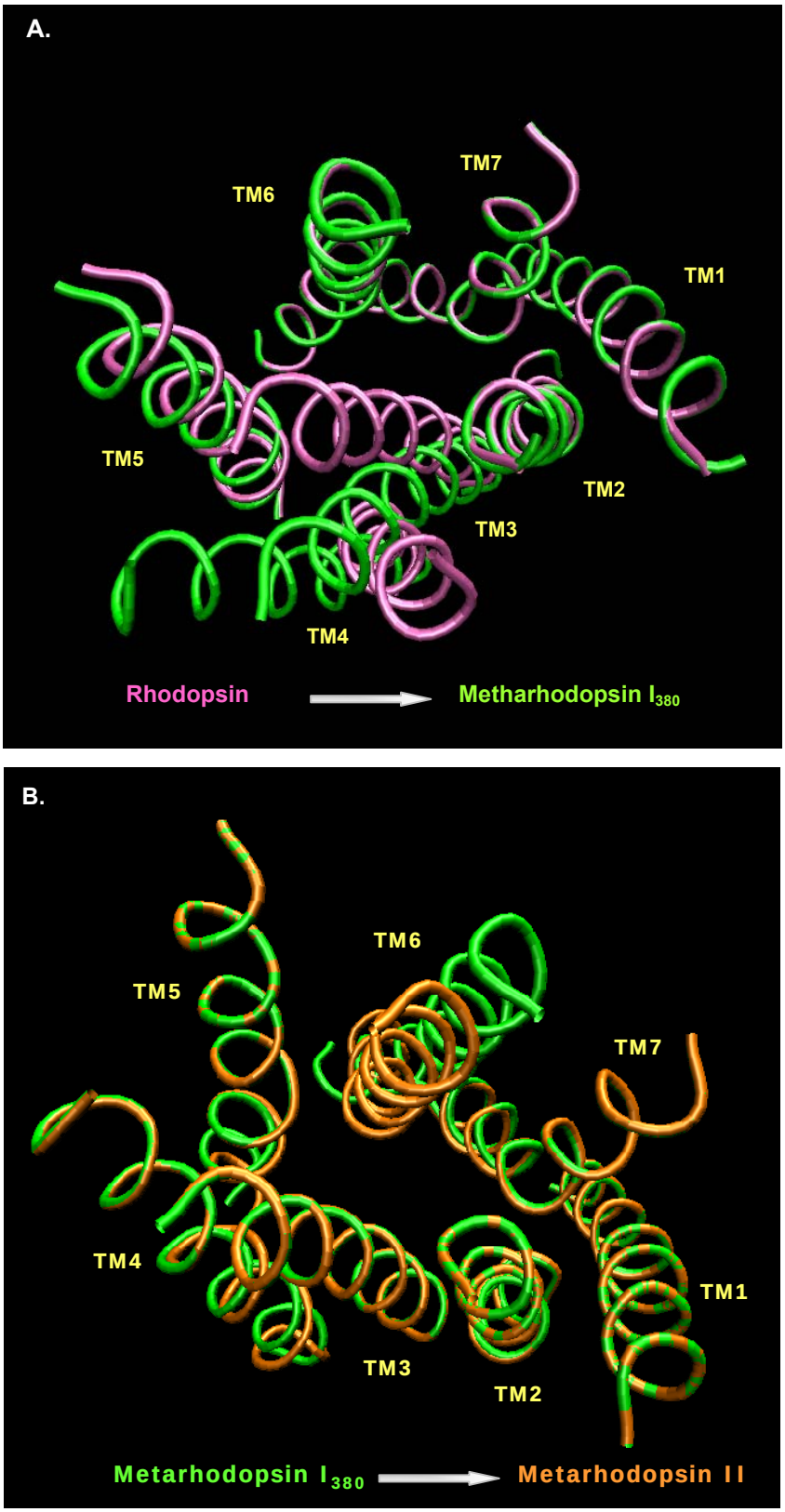

Figure 6.3: Three dimensional models of bovine rhodopsin in the three states of activation. Views are from the intracellular site. **A.** Transition from rhodopsin, inactive state (purple), represented by the crystal structure 1F88, to metarhodopsin I_{380}, partially active state (green). **B.** Transition from partially active state (green) to fully active state (orange) represented by metarhodopsin II.

```
                        10        20        30        40        50
Rho                 mnGtegpnfyVP--------fsnktgvVrsPFeapQyyLae---------
h5-HT2A             MDILCEENTSLSSTTNSLMQLNDDTRLYSNDFNSGEANTSDAFNWTVDSE

                        60        70        80        90        100
Rho                 --------------------pwqFsmlAayMflLImlGfpiNflTlyVTv
h5-HT2A             NRTNLSCEGCLSPSCLSLLHLQEKNWSALLTAVVIILTIAGNILVIMAVS

                        110       120       130       140       150
Rho                 qHkkLrtplNyILlnLAvADlfMVfgGFtTTLyTSlhGy-FvfgptGCnl
h5-HT2A             LEKKLQNATNYFLMSLAIADMLLGFLVMPVSMLTILYGYRWPLPSKLCAV

                        160       170       180       190       200
Rho                 EGffATLGGEIaLWSLvvLAieRyvvVckpmsnfrf-genhaimgvafTw
h5-HT2A             WIYLDVLFSTASIMHLCAISLDRYVAIQNPIHHSRFNSRTKAFLKIIAVW

                        210       220       230       240       250
Rho                 vmAlaCAapPlvgwSrYIPEGMQCSÇGIDYYTpheetnNesFViyMfvvH
h5-HT2A             TISVGISMPIPVFGLQDDSKVFKEGS--------CLLADDNFVLIGSFVS

                        260       270       280       290       300
Rho                 fiiPlivIffcygqLvftvkeaaa-------------------------
h5-HT2A             FFIPLTIMVITYFLTIKSLQKEATLCVSDLGTRAKLASFSFLPQSSLSSE

                        310       320       330       340       350
Rho                 --------------qqqesattqkaekevTrMViiMviAFliCWlpYAgv
h5-HT2A             KLFQRSIHREPGSYTGRRTMQSISNEQKACKVLGIVFFLFVVMWCPFFIT

                        360       370       380       390       400
Rho                 AfyIfthqg---sdFgpifMTipAFfAKtSAVYNPvIYimMnkqFrNCmv
h5-HT2A             NIMAVICKESCNEDVIGALLNVFVWIGYLSSAVNPLVYTLFNKTYRSAFS

                        410       420       430       440       450
Rho                 Ttlccgknplgd-------------------------------------
h5-HT2A             RYIQCQYKENKKPLQLILVNTIPALAYKSSQLQMGQKKNSKQDAKTTDND

                        460       470
Rho                 -------deasttVsktetsqvapa
h5-HT2A             CSMVALGKQHSEEASKDNSDGVNEKVSCV
```

Figure 6.4: Sequence alignment of bovine rhodopsin (Rho) with the human 5-HT$_{2A}$ receptor derived from the Fugue online server. The amino acids in bold represent the sequences corresponding to the α helices in both receptors.

6.2.2 Docking of 5-HT_{2A} receptor agonists and partial agonists

Compounds showing different pharmacological profiles, an agonist (5-HT) and a partial agonist (cpd. **169**), have been docked into the binding site of the models representing the active receptor states.. Cpd. **169** belongs to the large series of 5-HT_{2A}R ligands analysed Chapter 5. The ligands are shown in Figure 6.5.

The structures were constructed using Sybyl 7.3. All molecules were assumed to be protonated under physiological conditions. Amber FF99 atom types and Gasteiger-Hückel charges were assigned to the ligands. The bioactive conformations were derived from the analysis of the binding site of the r5-HT_{2A}R model generated with the Fugue/Orchestrar approach (see Chapter 4).

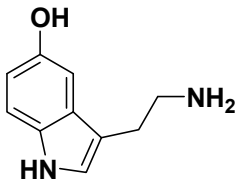

5-HT

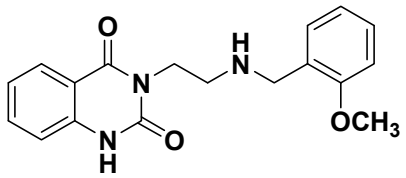

Cpd. 169

Figure 6.5: Compounds docked into the binding site of 5-HT_{2A} receptor models. 5-HT represents full agonists (pEC_{50} = 7.00, E_{max} = 100%), and cpd. **169** partial agonists (pEC_{50} = 6.58, E_{max} = 49%).

5-HT was docked into the binding site of the fully active form of the h5-HT_{2A}R model based on the metarhodopsin II template, and the partial agonist (cpd. **169**) into the partially active species of the receptor derived from metarhodopsin I_{380}.

The complexes were optimized using the Amber FF99 force field and agggregates,. first constraining the whole and then only the TM backbone to avoid strong movements of the relative positions of the seven TM helices. Preliminary studies have indicated that such displacements occur without using constraints. Figure 6.6 compares the starting structure of the fully active receptor with the model after a few steps of energy minimization without aggregates. There are significant changes in the spatial positions of the TM domains, especially close to the extracellular loops. This immoderate effect which is probably due to the more or less arbitrary modeling of E2 and E3 by loop searches should not strongly predetermine the resulting structure. The same result has been obtained for the partially active 5-HT_{2A}R model..

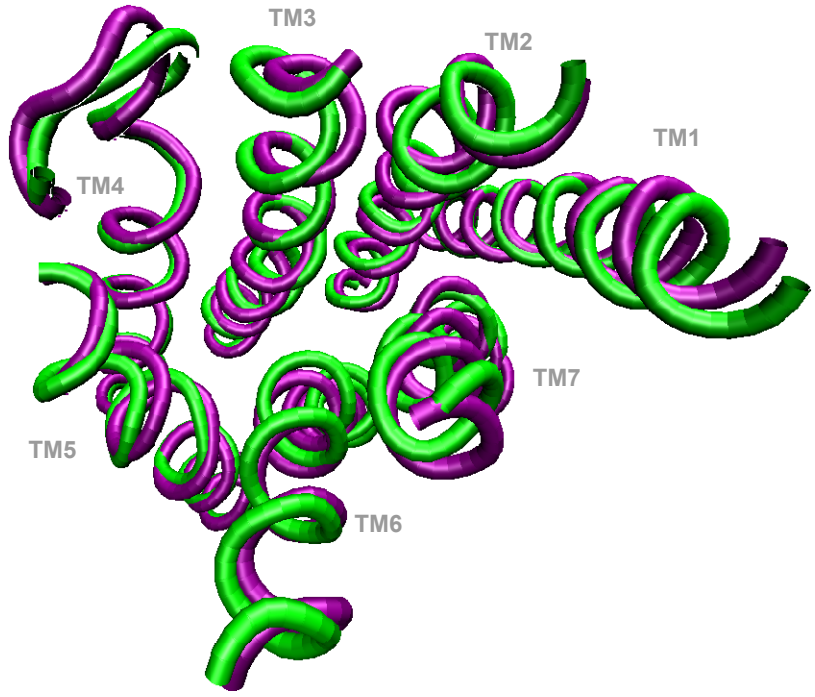

Figure 6.6: Comparison of the seven TM domain of the starting structure of the active state 5-HT_{2A}R model (green) with the receptor after some steps of minimization without aggregates (magenta). View from the extracellular side

6.3 Results

6.3.1 Comparison of h5-HT_{2A}R models in different states

The packing of the TM domain in the h5-HT_{2A}R model based on the rhodopsin crystal structure shows the typical interactions characterizing the stabilization of the inactive state of biogenic amine GPCRs and bovine rhodopsin (Figure 6.7).

The model suggests that the inactive state is stabilized by several interactions that are supposed to be broken during the activation process:

- a salt bridge formed by two highly conserved amino acids, $Arg173^{3.50}$ (DRY consensus motif in TM3) and $Glu318^{6.30}$ (cytoplasmic part of TM6),
- a hydrogen bond network mediating interactions between TM1 ($Asn72^{1.50}$), TM2 ($Asp120^{2.50}$) and TM7 ($Asn376^{7.49}$),
- a disulfide bridge between $Cys148^{3.25}$ and $Cys227^{E2.15}$ causing that E2 is partially inserted into the transmembrane part, the only interaction that is maintained during the activation,
- a network of intraloop H bonds stabilizing the course of E2, e.g., the backbone of $Lys220^{E2.8}$ is linked with the backbone of $Glu224^{E2.12}$, $Ser226^{E2.14}$, and $Gly225^{E2.13}$, the backbone of $Asp218^{E2.6}$ with the backbone of $Leu228^{E2.16}$, the

backbone of Asn233$^{E2.21}$ with the backbone of Ile237$^{5.41}$, and the backbone of Asp231$^{E2.19}$ with the backbone of Val235$^{5.39}$ (Table 6.1).

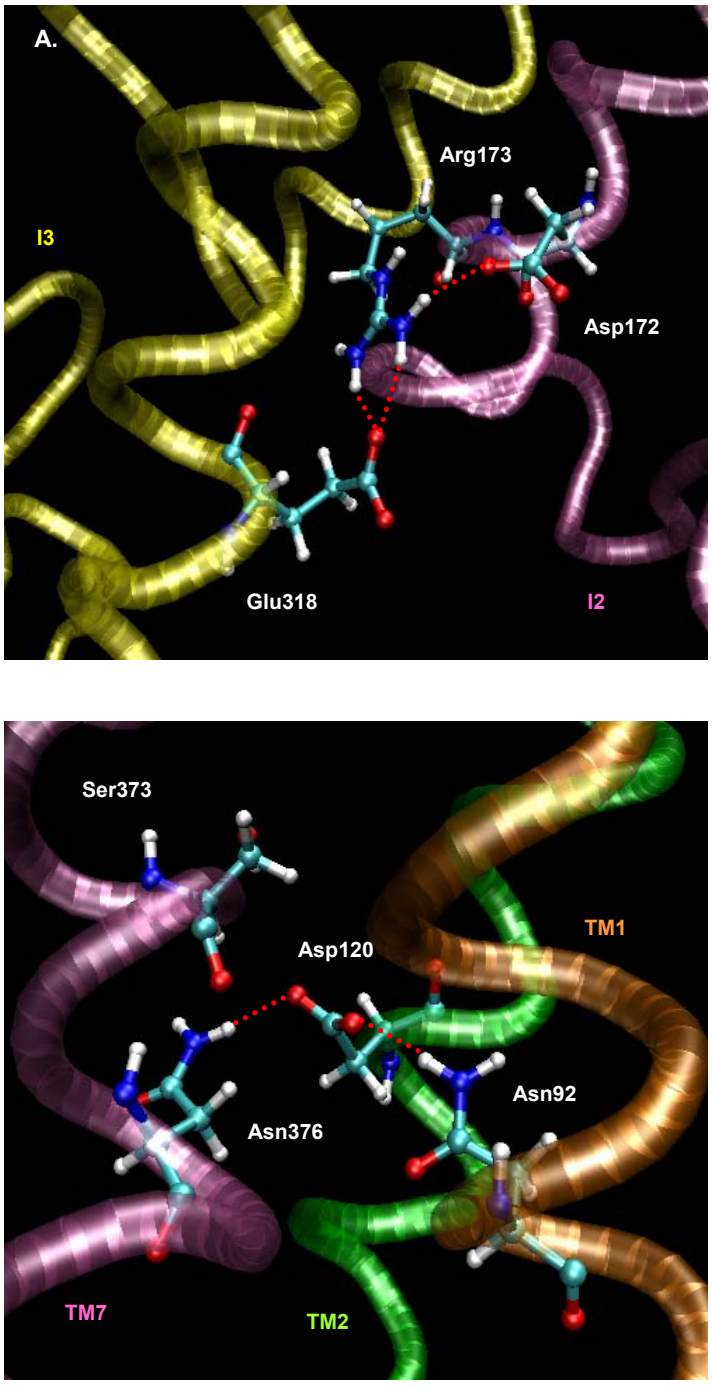

Figure 6.7: Interactions stabilizing the inactive state of the h5-HT_{2A}R. A. Hydrogen bond network between two amino acids belonging to the DRY sequence (Asp172$^{3.49}$ and Arg173$^{3.50}$) and Glu318$^{6.30}$. B. Polar interaction between TM1 (Asn92$^{1.50}$), TM2 (Asp120$^{2.50}$) and TM7 (Asn376$^{7.49}$). The red dotted lines represent the interaction between residues.

Table 6.1: Conserved intramolecular interactions of the inactive h5-HT_{2A}R state

Domain	Residues	Min. distance (Å)*
TM3	Arg173$^{3.50}$ - Asp172$^{3.49}$	2.11
TM3-TM6	Arg173$^{3.50}$ - Glu318$^{6.30}$	1.95
TM7-TM2	Asn376$^{7.49}$ - Asp120$^{2.50}$	2.04
TM7	Asn376$^{7.49}$ - Ser373$^{7.46}$	3.65
E2-TM5	Glu216$^{E2.4}$ - Asp231$^{5.35}$	2.05
E2	Glu216$^{E2.4}$ - Asp218$^{E2.6}$	2.26
E2	Glu216$^{E2.4}$ - Leu229$^{E2.17}$	1.98
E2	Glu224$^{E2.12}$ - Lys223$^{E2.11}$	2.03

*Distance between the nearest heavy atoms of interacting residues

In the partially active state model, characterized by a lower number of stabilizing H bonds, these interactions are not present. The movement of TM3 and TM4 unlocks the salt bridge between Arg173$^{3.50}$ (DRY motif) and Glu318$^{6.30}$ (I3-TM6 intersection). Also the hydrogen bond network between TM1 (Asn72$^{1.50}$), TM2 (Asp120$^{2.50}$) and TM7 (Asn376$^{7.49}$) is broken (Figure 6.8).

Different movements of TM4 (large) and TM5 (small) in their extracellular parts are responsible for a conformational change of the second extracellular loop (E2). As described for bovine rhodopsin, E2 is partially inserted into the TM domain. This insertion is not present in the partially active state (metarhodopsin I_{380}). Furthermore, rhodopsin in the dark state and the h5-HT_{2A}R model derived from this template contain a β-sheet in E2 that is not present in the partially active structures. The second extracellular loop is stabilized in its new conformation by a network of intraloop H bonds, e.g. the side chain of Lys220$^{E2.8}$ is linked with the backbone of Asp231$^{E2.19}$ and the backbone of Leu228$^{E2.16}$, the backbone of Ser219$^{E2.7}$ with the backbone of Leu228$^{E2.16}$ and the backbone of Lys223$^{E2.11}$. However, the recent crystal structures of the β_2-adrenoceptor in its inactive state (Cherezov et al., 2007; Rasmussen et al., 2007) do not confirm the "cap-like" function of E2 but indicate a more open conformation allowing easy access of ligands into the TM region (see Chapter 5). Therefore, it cannot be concluded that similar conformational changes of E2 like suggested in the case of rhodopsin do also play a role for the activation of biogenic amine GPCRs.

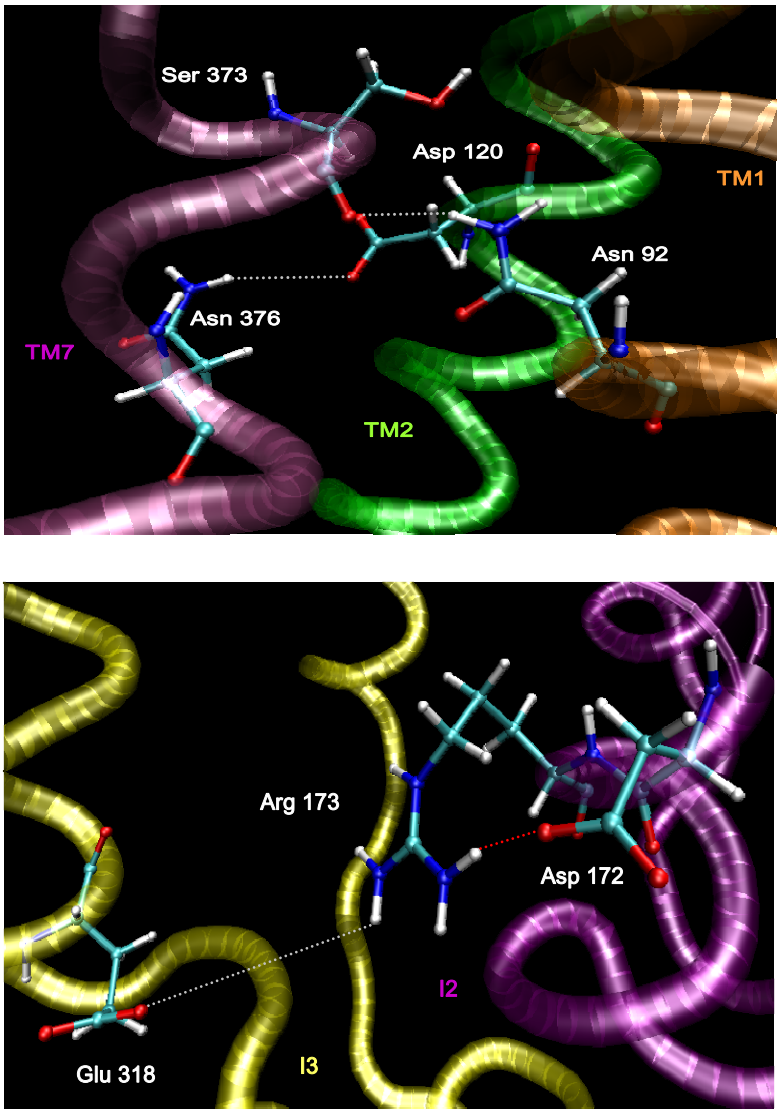

Figure 6.8: Characteristic regions of the partially active state of the h5-HT_{2A}R deviating from the inactive state. Interactions only present in the inactive state – gray dotted lines. The H-bond between Asp172 and Arg173 (red dotted line) is conserved in the partially active state.

The last conformational change during the receptor activation is a rotational motion of TM6 (see Introduction). In the h5-HT_{2A}R model of the fully active state, this movement allows a small rearrangement of the helical segments and the intra- and extracellular loops compared to the partially active state. In particular, the E2 loop is again inserted into the TM domain and stabilized in this position by a network of intraloop H-bond, e.g. the side chain of $Lys223^{E2.11}$ is linked with the side chain of $Asp218^{E2.6}$ and the backbone of $Ser2.19^{E2.8}$, the backbone of $Glu224^{E2.12}$ with the backbone of $Lys220^{E2.8}$. Once more, this rearrangement of E2 seems to be important

for rhodopsin activation, but is rather questionable in the case of the h5-HT_{2A}R (see above).

With respect to the putative binding site of the three h5-HT_{2A}R models, an analysis of the amino acids interacting with ligands indicates similar binding modes of agonists, partial agonists and antagonists. Residues such as Asp155$^{3.32}$ and Ser159$^{3.36}$ in TM3, Ser239$^{5.43}$ and Ser242$^{5.46}$ in TM5 as well as Tyr370$^{7.43}$ and Trp367$^{7.40}$ in TM7 are similarly oriented in different activation states (Figure 6.9). However, two important residues, Phe339$^{6.51}$ and Phe340$^{6.52}$, show another orientation in the fully active model compared to the models of the inactive and the partially active state. This difference is due to the counter-clockwise rotation of TM6 by approximately 100° around the axis of the N-terminal TM6 moiety.

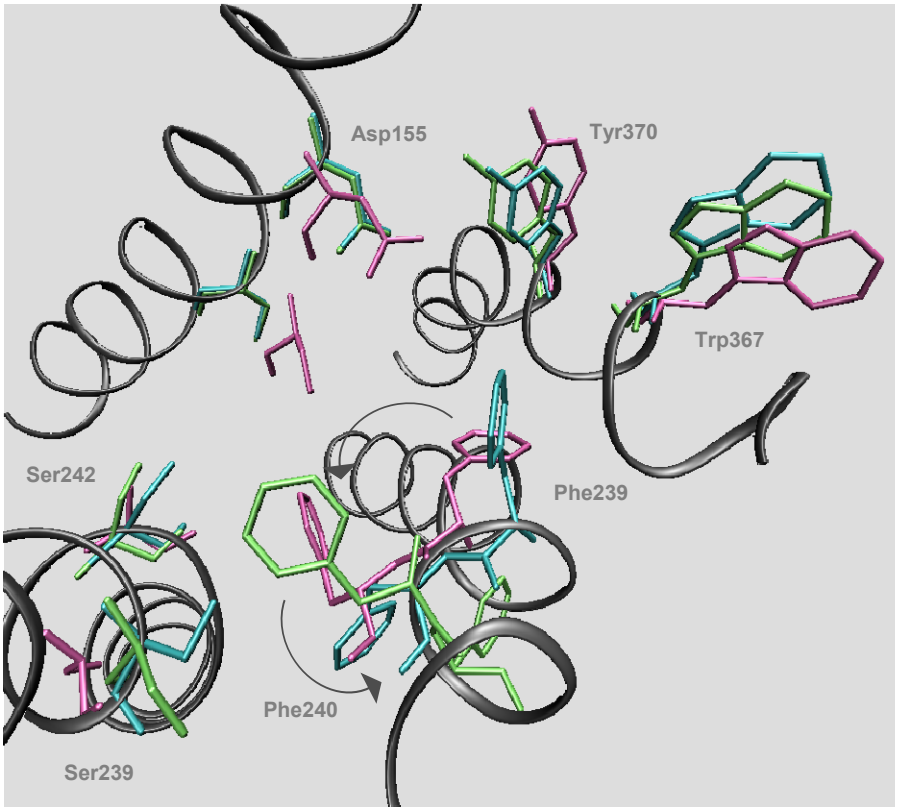

Figure 6.9: Aligned ligand binding sites of the three h5-HT_{2A}R models. Important amino acids are drawn in different colours: inactive state – pink, partially active state – cyan, fully active state – green The silver ribbon represents the TM helices in the fully active state, and the arrows indicate the rotation of TM6.

6.3.2 Analysis of the fully active h5-HT_{2A}R model in complex with 5-HT

5-HT was docked into the binding site of the fully active form of the h5-HT_{2A}R model derived from metharhodopsin II. Most positions correspond to the 5-HT docking mode published previously (Ishiguro et al., 2004). The cationic amine moiety of the unsubstituted indole derivatives forms an ionic interaction with Asp155$^{3.32}$ and an H bond with Ser159$^{3.36}$ (Almaula et al., 1996; Wang et al., 1993). Considering all interactions important for the activity of 5-HT, the fit is optimal if a folded conformation of the ethylamine side chain is assumed (see Figure 6.10). By contrast, compounds with a substituent at the cationic amine moiety rather adopt extended side chain geometries to enable interactions with hydrophobic residues in TM6 and TM7. The indole group was suggested to form H bonds with the two serines Ser239$^{5.43}$ (5-OH substituent) and Ser242$^{5.46}$ (indole NH) in TM5. Amino acids in these two positions are known to be involved in the interaction with neurotransmitters in various GPCRs. However, as discussed in Chapters 4 and 5, H bonds of the indole NH to the side chains of Ser159$^{3.36}$ or Thr160$^{3.37}$ may also be possible since Ser242$^{5.46}$ is mutated into Ala in the rat 5-HT_{2A}R. An interaction of the indole NH with the backbone oxygen of Met335$^{6.47}$, as proposed by Ishiguro et al. (2004), appears to be rather uncommon, but cannot be excluded.

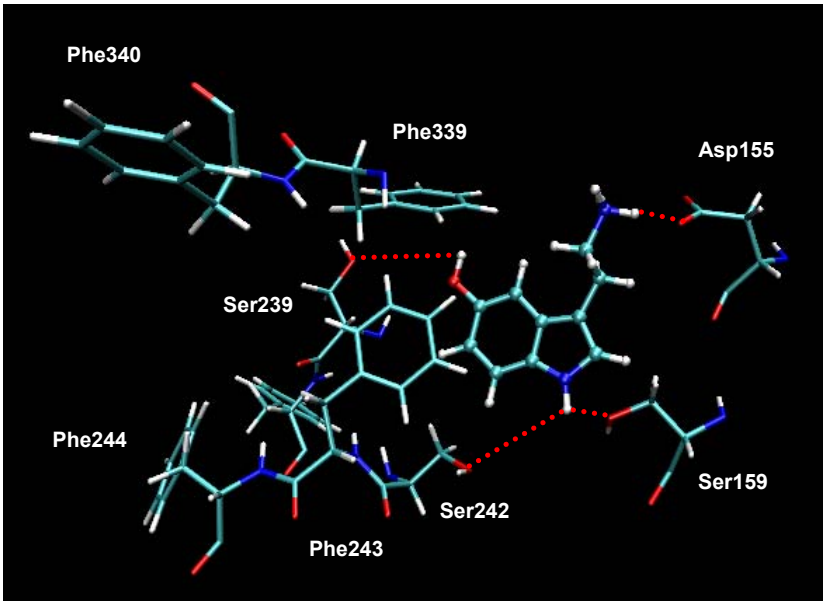

Figure 6.10: Docking of 5-HT into the binding site of the fully active h5-HT_{2A}R model. Ligand – balls and sticks, amino acids interacting with 5-HT – sticks only. The red dotted lines represent the polar interactions between 5-HT and residues.

After energy optimization the key interactions between 5-HT and residues in TM3 were retained, indicated by the short distances between the charged nitrogen and Asp155$^{3.32}$ (2.49 Å) and Ser159$^{3.36}$ (2.36 Å), respectively. Remarkably, the indole ring is parallel aligned with the side chain of Phe339$^{6.51}$ indicating optimal $\pi-\pi$ interaction. This contact is obviously due to the 100° rotation of TM6 in the fully active state and replaces the corresponding interaction with Phe340$^{6.52}$ suggested from docking of indole derivatives into the inactive state models and from results with Phe340$^{6.52}$Leu mutants (Choudhary et al., 1993; Roth et al., 1997) (see Chapters 4 and 5). For biogenic amine GPCRs it is assumed that the effect of agonists on the so called "toggle switch" (Cys335$^{6.47}$, Trp336$^{6.48}$ and Phe340$^{6.52}$ in the case of the 5-HT_{2A}R) modulates the proline kink in TM6 (Cherezov et al., 2007; Rosenbaum et al., 2007) as precondition for the 100° rotation and, by this, activation of the receptor. Insofar, the model in Figure 6.10 could indeed reflect an agonist-bound active GPCR state although Phe339$^{6.51}$Leu mutants do not markedly reduce binding and efficacy of 5-HT (Choudhary et al., 1993; Roth et al., 1997). The distances of the 5-OH group of 5-HT and Ser239$^{5.43}$, and of the indole nitrogen and Ser242$^{5.46}$ are in the range of 3-3.5 Å after constrained energy optimization. I.e., the interactions of 5-HT with the suggested key residues in TM5 are possibly weaker in the fully active than in the inactive state.

6.3.3 Analysis of the partially active h5-HT_{2A}R model in complex with a partial agonist

A quinazolinedione derivative (cpd. **169**, see Chapters 4 and 5), a partial agonist at 5-HT_{2A} receptors, was docked into the binding site of the partially active 5-HT_{2A}R model based on metarhodopsin I_{380}. The docking pose of the quinazolinedione moiety was suggested to be similar to that of the indole moiety in 5-HT. The benzyl substituent at the charged nitrogen was assumed to interact with a hydrophobic pocket of aromatic residues in TM3, TM6 and TM7 (see Chapter 4). This implies that the ethylamine chain adopts an extended conformation. According to the hypothesis derived previously (see Chapter 4), the secondary amino group was positioned in proximity to the conserved Asp155$^{3.32}$ in TM3, one of the oxygens and the nitrogen of the quinazolinedione ring close to Ser159$^{3.36}$ and Ser242$^{5.46}$, respectively, and the

second oxygen close to Asn343$^{6.55}$. A hydrophobic pocket of aromatic residues in TM5 (Phe240$^{5.44}$, Phe243$^{5.47}$ and Phe244$^{5.48}$) and TM6 (Phe340$^{6.52}$) accomodates the quinazolinedione moiety. The benzyl substituent is fitted into a second hydrophobic pocket, consisting of residues in TM3 (Trp151$^{3.28}$), TM6 (Trp336$^{6.48}$ and Phe339$^{6.51}$), and TM7 (Trp367$^{7.40}$ and Tyr370$^{7.43}$).

In the energy optimized model (Figure 6.11), Asp155$^{3.32}$ is the only residue that interacts with the charged nitrogen. Ser159$^{3.36}$ is too far away to act as H acceptor and is involved in another interaction with one of the oxygens of the quinazolinedione group.

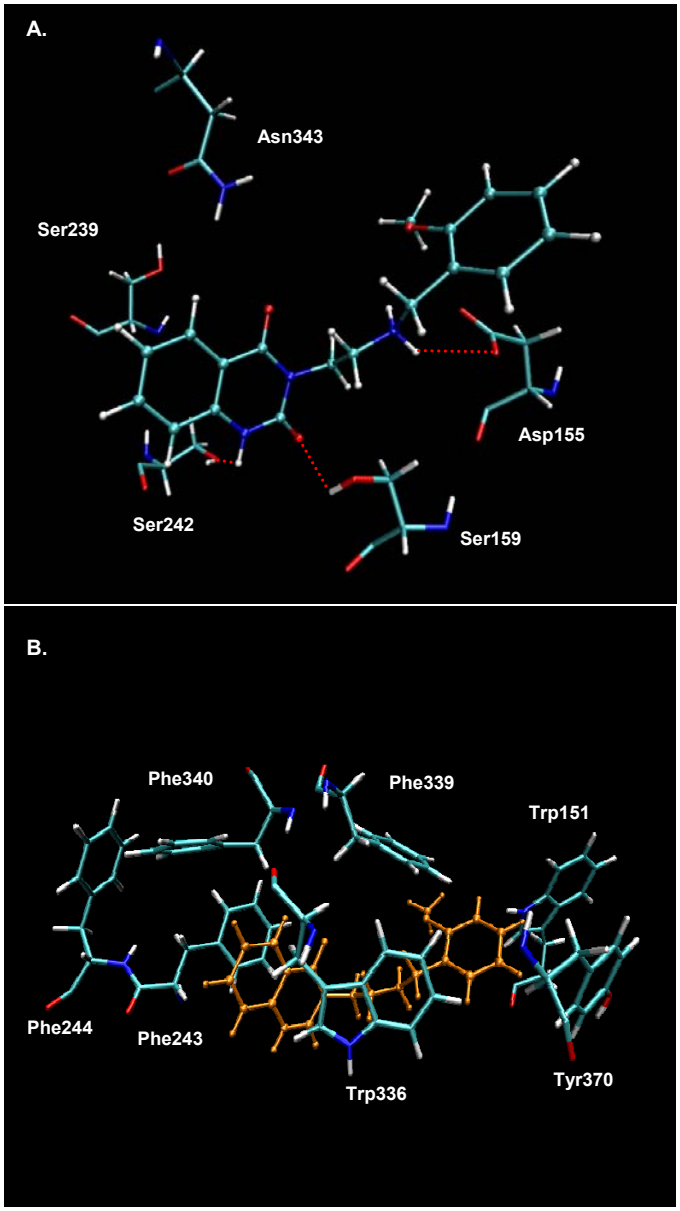

Figure 6.11: Docking of cpd **169** into the binding site of the partially active h5-HT_{2A}R model. Ligand – balls and sticks, amino acids interacting with 5-HT – sticks only. **A**. Polar interactions between 5-HT and residues (red dotted lines). **B**. Hydrophobic pockets surrounding the ligand (orange).

The interaction between the partial agonist and TM3 in the optimized conformation does not include only the residues Asp155$^{3.32}$ and Ser159$^{3.36}$, but also a hydrophobic residue, Tyr151$^{3.28}$, positioned close to the benzyl substituent of the ligand which also interacts with aromatic residues in TM6 and TM7 (see above). The last step in the activation process is the rotation of TM6, leading to the different position of Phe339$^{6.51}$ and Phe340$^{6.52}$ in the partially and the fully active state, respectively. These amino acids are involved in the interaction with the agonist (5-HT) and partial agonist (cpd. **169**), but in a different way. In the fully active model, 5-HT interacts via the indole moiety with Phe339$^{6.51}$, but Phe340$^{6.52}$ does not approach the ligand. By contrast, the partially active model indicates interactions of Phe339$^{6.51}$ with the benzyl and of Phe340$^{6.52}$ with the quinazolinedione group. Probably the tight fit of the benzyl moiety into a hydrophobic pocket containing key residues in TM6 impedes the complete receptor activation due to inhibiting the rotation of this helix. I.e, the activation energy is higher in the case of partial agonists like cpd. **169**, and the equilibrium between the partially and the fully active state is shifted to the former one. The quinazolinedione moiety interacts with TM5 also in the partially active model. The conserved Ser242$^{5.46}$ is involved in an H bond with one of the oxygens. Moreover, a pocket of hydrophobic residues in TM5 (Phe243$^{5.47}$, Phe244$^{5.48}$) and TM6 (Phe340$^{6.52}$) inserts the quinazolinedione group. In comparison with the docking mode suggested for cpd. **169** at the model of the inactive state relying on the crystal structure of bovine rhodopsin (see Chapter 4), the interaction pattern is quite similar irrespective of the different positions of TMs 3, 4 and 5. In particular, interactions with the hydrophobic pocket formed by residues in TMs 5 and 6 are generally retained. This is rather achieved by a global translation and rotation of the ligand together with TMs 3 and 5 than by a major conformational change. The quinazolinedione moiety is strongly shifted (ca. 5 Å), whereas the benzylamine position differs only by about 1.5Å when the fixed domains of both models, TMs 1, 2 and 7, are aligned.

6.4 Conclusions

Models of the h5-HT_{2A}R in different activation states suggest conformational differences and important collective changes of TM domains during the activation process. These models also help in understanding the different interactions of typical agonists and partial agonists with a largely common binding site. The analysis of the putative receptor-ligand interactions has shown that:

- The different 5-HT_{2A}R states are similar with respect to the amino acids interacting with ligands, but show individual topologies of the binding sites due to TM movements. The interconversion of states may be accompanied by co-translations and rotations of the ligands.
- Rather weak interactions with residues in TM5 of the fully active 5-HT_{2A}R state are possibly one of the reasons for the low activity of 5-HT.
- The binding site of the partially active 5-HT_{2A}R model accomodates the partial agonist **169** by polar and hydrophobic interactions. Probably the tight fit of the benzyl substituent into a hydrophobic pocket containing key residues in TM6 impedes the complete receptor activation due to inhibiting the rotation of this helix

Generally, the inhibition of collective TM moves may be a common principle by which partial agonists and antagonists "act" unlike agonists. Interactions with additional binding sites lead to stabilized, more rigid conformational states of the complex requiring high activation energies to convert into other states. In particular, more or less stabilization of the "toggle switch region" in TM6 will determine the efficacy of a ligand. High affinity of a partial agonist or antagonist is therefore at the expense of its ability to activate a receptor.

Although the present results on h5-HT_{2A}R states and their interactions with ligands are only derived from putative models of rhodopsin states, general insights into possible activation modes of GPCRs have been obtained which may help in deriving refined models on the base of experimental receptor structures.

6.5 References

Almaula, N., B. J. Ebersole, D. Zhang, H. Weinstein, and S. C. Sealfon, 1996, Mapping the binding site pocket of the serotonin 5-Hydroxytryptamine2A receptor. Ser3.36(159) provides a second interaction site for the protonated amine of serotonin but not of lysergic acid diethylamide or bufotenin: *J Biol Chem*, v. **271**: p. 14672-5.

Cherezov, V., D. M. Rosenbaum, M. A. Hanson, S. G. Rasmussen, F. S. Thian, T. S. Kobilka, H. J. Choi, P. Kuhn, W. I. Weis, B. K. Kobilka, and R. C. Stevens, 2007, High-resolution crystal structure of an engineered human beta2-adrenergic G protein-coupled receptor: *Science*, v. **318**: p. 1258-65.

Choi, G., J. Landin, J. F. Galan, R. R. Birge, A. D. Albert, and P. L. Yeagle, 2002, Structural studies of metarhodopsin II, the activated form of the G-protein coupled receptor, rhodopsin: *Biochemistry*, v. **41**: p. 7318-24.

Choudhary, M. S., S. Craigo, and B. L. Roth, 1993, A single point mutation (Phe340-->Leu340) of a conserved phenylalanine abolishes 4-[125I]iodo-(2,5-dimethoxy)phenylisopropylamine and [3H]mesulergine but not [3H]ketanserin binding to 5-hydroxytryptamine2 receptors: *Mol Pharmacol*, v. **43**: p. 755-61.

Farrens, D. L., C. Altenbach, K. Yang, W. L. Hubbell, and H. G. Khorana, 1996, Requirement of rigid-body motion of transmembrane helices for light activation of rhodopsin: *Science*, v. **274**: p. 768-70.

Feng, X., P. J. Verdegem, M. Eden, D. Sandstrom, Y. K. Lee, P. H. Bovee-Geurts, W. J. de Grip, J. Lugtenburg, H. J. de Groot, and M. H. Levitt, 2000, Determination of a molecular torsional angle in the metarhodopsin-I photointermediate of rhodopsin by double-quantum solid-state NMR: *J Biomol NMR*, v. **16**: p. 1-8.

Heitz, F., J. A. Holzwarth, J. P. Gies, R. M. Pruss, S. Trumpp-Kallmeyer, M. F. Hibert, and C. Guenet, 1999, Site-directed mutagenesis of the putative human muscarinic M2 receptor binding site: *Eur J Pharmacol*, v. **380**: p. 183-95.

Ishiguro, M., 2004, Ligand-binding modes in cationic biogenic amine receptors: *Chembiochem*, v. **5**: p. 1210-9.

Ishiguro, M., T. Hirano, and Y. Oyama, 2003, Modelling of photointermediates suggests a mechanism of the flip of the beta-ionone moiety of the retinylidene chromophore in the rhodopsin photocascade: *Chembiochem*, v. **4**: p. 228-31.

Ishiguro, M., Y. Oyama, and T. Hirano, 2004, Structural models of the photointermediates in the rhodopsin photocascade, lumirhodopsin, metarhodopsin I, and metarhodopsin II: *Chembiochem*, v. **5**: p. 298-310.

Luthy, R., J. U. Bowie, and D. Eisenberg, 1992, Assessment of protein models with three-dimensional profiles: *Nature*, v. **356**: p. 83-5.

Monnot, C., C. Bihoreau, S. Conchon, K. M. Curnow, P. Corvol, and E. Clauser, 1996, Polar residues in the transmembrane domains of the type 1 angiotensin II receptor are required for binding and coupling. Reconstitution of the binding site by co-expression of two deficient mutants: *J Biol Chem*, v. **271**: p. 1507-13.

Ohkita, Y. J., J. Sasaki, A. Maeda, T. Yoshizawa, M. Groesbeek, P. Verdegem, and J. Lugtenburg, 1995, Changes in structure of the chromophore in the photochemical process of bovine rhodopsin as revealed by FTIR spectroscopy for hydrogen out-of-plane vibrations: *Biophys Chem*, v. **56**: p. 71-8.

Rasmussen, S. G., H. J. Choi, D. M. Rosenbaum, T. S. Kobilka, F. S. Thian, P. C. Edwards, M. Burghammer, V. R. Ratnala, R. Sanishvili, R. F. Fischetti, G. F. Schertler, W. I. Weis, and B. K. Kobilka, 2007, Crystal structure of the human beta2 adrenergic G-protein-coupled receptor: *Nature*, v. **450**: p. 383-7.

Resek, J. F., Z. T. Farahbakhsh, W. L. Hubbell, and H. G. Khorana, 1993, Formation of the meta II photointermediate is accompanied by conformational changes in the cytoplasmic surface of rhodopsin: *Biochemistry*, v. **32**: p. 12025-32.

Robinson, P. R., G. B. Cohen, E. A. Zhukovsky, and D. D. Oprian, 1992, Constitutively active mutants of rhodopsin: *Neuron*, v. **9**: p. 719-25.

Rosenbaum, D. M., V. Cherezov, M. A. Hanson, S. G. Rasmussen, F. S. Thian, T. S. Kobilka, H. J. Choi, X. J. Yao, W. I. Weis, R. C. Stevens, and B. K. Kobilka, 2007, GPCR engineering yields high-resolution structural insights into beta2-adrenergic receptor function: *Science*, v. **318**: p. 1266-73.

Roth, B. L., M. Shoham, M. S. Choudhary, and N. Khan, 1997, Identification of conserved aromatic residues essential for agonist binding and second messenger production at 5-hydroxytryptamine2A receptors: *Mol Pharmacol*, v. **52**: p. 259-66.

Sakmar, T. P., 1998, Rhodopsin: a prototypical G protein-coupled receptor: *Prog Nucleic Acid Res Mol Biol*, v. **59**: p. 1-34.

Scheer, A., and S. Cotecchia, 1997, Constitutively active G protein-coupled receptors: potential mechanisms of receptor activation: *J Recept Signal Transduct Res*, v. **17**: p. 57-73.

Shichida, Y., F. Tokunaga, and T. Yoshizawa, 1978, Circular dichroism of squid rhodopsin and its intermediates: *Biochim Biophys Acta*, v. **504**: p. 413-30.

Strader, C. D., T. M. Fong, M. R. Tota, D. Underwood, and R. A. Dixon, 1994, Structure and function of G protein-coupled receptors: *Annu Rev Biochem*, v. **63**: p. 101-32.

Strader, C. D., I. S. Sigal, M. R. Candelore, E. Rands, W. S. Hill, and R. A. Dixon, 1988, Conserved aspartic acid residues 79 and 113 of the beta-adrenergic receptor have different roles in receptor function: *J Biol Chem*, v. **263**: p. 10267-71.

Struthers, M., H. Yu, and D. D. Oprian, 2000, G protein-coupled receptor activation: analysis of a highly constrained, "straitjacketed" rhodopsin: *Biochemistry*, v. **39**: p. 7938-42.

Tachibanaki, S., H. Imai, T. Mizukami, T. Okada, Y. Imamoto, T. Matsuda, Y. Fukada, A. Terakita, and Y. Shichida, 1997, Presence of two rhodopsin intermediates responsible for transducin activation: *Biochemistry*, v. **36**: p. 14173-80.

Waggoner, A. S., and L. Stryer, 1971, Induced optical activity of the metarhodopsins: *Biochemistry*, v. **10**: p. 3250-4.

Wang, C. D., T. K. Gallaher, and J. C. Shih, 1993, Site-directed mutagenesis of the serotonin 5-hydroxytrypamine2 receptor: identification of amino acids necessary for ligand binding and receptor activation: *Mol Pharmacol*, v. **43**: p. 931-40.

Wess, J., D. Gdula, and M. R. Brann, 1991, Site-directed mutagenesis of the m3 muscarinic receptor: identification of a series of threonine and tyrosine residues involved in agonist but not antagonist binding: *Embo J*, v. **10**: p. 3729-34.

Chapter 7
Summary

The 5-HT_{2A} receptor (5-HT_{2A}R) is a biogenic amine receptor that belongs to the class A of G protein coupled receptors. It is characterized by a low affinity for serotonin (5-HT) and for other primary amines. Introduction of an *ortho*-methoxybenzyl substituent at the amine nitrogen increases the partial agonistic activity by a factor of 40 to 1400 compared with 5-HT.

The present study was to analyse the QSAR of a series of 51 5-HT_{2A}R partial agonistic arylethylamines, tested in vascular *in-vitro* assays on rats, at a structure-based level and to suggest ligand binding sites. The compounds belong to three different structural classes, (1) indoles, (2) methoxybenzenes (including benzo-difurans as cyclic analogs) and (3) quinazolinediones. Following a hierarchical strategy, different methods have been applied which all contribute to the investigation of ligand-receptor interactions: fragment regression analysis (FRA), receptor modeling, docking studies and 3D QSAR approaches (comparative molecular field analysis, CoMFA, and comparative molecular similarity index analysis, CoMSIA).

An initial FRA indicated that methoxy substituents at indole and phenyl derivatives increase the activity and may be involved in polar interactions with the 5-HT_{2A}R. The large contribution of lipophilic substituents in *p* position of phenethylamines suggests fit to a specific hydrophobic pocket. Secondary benzylamines are more than one order of magnitude more active than their NH_2 analogs. An *ortho*-OH or -OMe substituent at the benzyl moiety further increases activity.

Homology models of the human and rat 5-HT_{2A}R were generated using the crystal structure of bovine rhodopsin and of the β_2-adrenoceptor as templates. The derivation of the putative binding sites for the arylethylamines was based on the results from FRA and on mutagenesis data. Both templates led to 5-HT_{2A}R models with similar topology of the binding pocket within the transmembrane domains TM3,

TM5, TM6 and TM7. Docking studies with representative members of the three structural classes of partial agonists suggested that the aryl moieties and particularly *para*-substituents in phenyl derivatives fit into a hydrophobic pocket formed by Phe243$^{5.47}$, Phe244$^{5.48}$ and Phe340$^{6.52}$. The 5-methoxy substituents in indole and phenyl compounds form H bonds with Ser239$^{5.43}$. In each case, an additional H bond with Ser159$^{3.36}$ may be assumed. The cationic amine interacts with the conserved Asp155$^{3.32}$. The benzyl group of secondary arylethylamines is inserted into another hydrophobic pocket formed by Phe339$^{6.51}$, Trp367$^{7.40}$ and Tyr370$^{7.43}$. In this region, the docking poses depend on the template used for model generation, leading to different interactions especially of *ortho*- substituents.

The docking studies with the β_2-adrenoceptor based rat 5-HT$_{2A}$R model provided templates for a structure-based alignment of the whole series which was used in 3D QSAR analyses of the partial agonistic activity. Both approaches, CoMFA and CoMSIA, led to highly predictive models with low complexity (cross-validated q^2 of 0.72 and 0.81 at 4 and 3 components, respectively). The results were largely compatible with the binding site and confirm the docking studies and the suggested ligand-receptor interactions. Steric and hydrophobic field effects on the potency indicate a hydrophobic pocket around the aryl moiety and near the *para* position of phenyl derivatives and account for the increased activity of secondary benzylamines. The effects of electrostatic and H-bond acceptor fields suggest a favourable influence of negative charges around the aryl moiety, corresponding to the increase in potency caused by methoxy substituents in 2-, 4-, 5- and 6-position of phenethylamines and by the quinazolinedione oxygens. This is in accord with the role of Ser159$^{3.36}$ and Ser239$^{5.43}$ as H bond donors. At the benzyl moiety, the negative charge and the acceptor potential of, in particular, 2-hydroxy and -methoxy substituents is of advantage.

Partial and full agonists stabilize or induce active receptor states not reflected by the existing crystal structures. Based on models of different rhodopsin states, a homology modeling and ligand docking study on corresponding 5-HT$_{2A}$R states suggested to be specific to agonist and partial agonist binding, respectively, was performed. The models indicate collective conformational changes of TM domains during activation. The different 5-HT$_{2A}$R states are similar with respect to the amino acids interacting with the arylethylamines, but show individual topologies of the binding sites. The interconversion of states by TM movements may be accompanied by co-translations

and rotations of the ligands. In the case of the secondary amines considered, the tight fit of the benzyl substituent into a hydrophobic pocket containing key residues in TM6 probably impedes the complete receptor activation due to inhibiting the rotation of this helix. High affinity of a partial agonist is therefore often at the expense of its ability to fully activate a receptor.

Chapter 8
Appendix

8.1 Abbreviations

3D	three-dimensional
5HT	5-hydroxytryptamine, serotonin
5-HTR	serotonergic receptor, 5-HT receptor
CNS	central nervous system
CoMFA	comparative molecular field analysis
CoMSIA	comparative molecular similarity index analysis
DAG	diacylglycerol
DOB	1-(4-bromo-2,5-dimethoxyphenyl)-isopropylamine
DOI	1-(4-iodo-2,5-dimethoxyphenyl)-isopropylamine
DMT	dimethyltryptamine
E1, E2, E3	1^{st}, 2^{nd}, and 3^{rd} extracellular loop of G protein coupled receptors
EC_{50}	agonist concentration inducing 50% of the maximum effect
ER	endoplasmatic reticulum
FRA	fragment regression analysis
G_{α}	α-subunit of G proteins
$G_{\beta\gamma}$	heterodimer formed by β and γ subunits of G proteins
GDP	guanosine diphosphate
GPCR	G protein coupled receptor
GTP	guanosine threephosphate
h5-HT_{2A}R	human serotonergic 2A receptor
I1, I2, I3	1^{st}, 2^{nd}, and 3^{rd} intracellular loop of G protein coupled receptors

IP_3	Inositolthreephosphate
LSD	Lysergic acid diethylamide
PC	principal component
PDB	protein data bank
PKC	protein kinase C
PLC	phospholipase C
PLS	partial least squares
QSAR	quantitative structure-activity relationships
r5-HT_{2A}R	rat serotonergic 2A receptor
RMSD	root mean square deviation
SAR	structure-activity relationships
TM	transmembrane domain of G protein coupled receptors

8.2 List of publications

Silva, M.E., Elz, S., Dove, S., Theoretical studies of the interactions of partial agonists with the 5-HT_{2A} receptor, 5th joint Meeting on Medicinal Chemistry, Portoroz, Slovenia, June 17-21, 2007

Silva, M.E., Elz, S., Dove, S., Theoretical studies of the interactions of partial agonists with the 5-HT_{2A} receptor, 3rd Summer school Medicinal chemistry, University of Regensburg, Germany, September 25-27, 2006.

Silva, M.E., Elz, S., Dove, S., Theoretical studies of the interactions of partial agonists with the 5-HT_{2A} receptor, The 16th European Symposium on Quantitative Structure-Activity Relationship & Molecular Modelling, Mediterranean Sea, Italy, September 10-17, 2006

Silva, M.E., Dove, S., Wenzel-Seifert, K., Seifert, R., Elz, S., Theoretical studies of the interactions of partial agonists with the 5-HT_{2A} receptor, poster contribution in occasion of the evaluation of the Research Training Group (Graduiertenkolleg, GRK) 760 of the Deutsche Forschungsgemeinschaft, University of Regensburg, Germany, January 10, 2006.

Pedretti, A., Silva, M. E., Villa, L., Vistoli, G. 2004. Binding site analysis of full-length α_{1a} adrenergic receptor using homology modelling and molecular docking. *Biochemical and Biophysical Research Communications* 319: 493-500.

A manuscript on the 5-HT_{2A} receptor modeling and the QSAR studies is in preparation (to be submitted 2008 to J. Comp. Aid. Mol. Des.).

Erklärung

Ich erkläre hiermit an Eides statt, dass ich die vorliegende Arbeit ohne unzulässige Hilfe Dritter und ohne Benutzung anderer als der angegebenen Hilfsmittel angefertigt habe; die aus anderen Quellen direkt oder indirekt übernommenen Daten und Konzepte sind unter Angabe des Literaturzitats gekennzeichnet.

Regensburg, im Juli 2008

(Maria Elena Silva)

Acknowledgements

I would like to thank Prof. Dr. Stefan Dove, who offered me the chance to perform my PhD in Germany, giving me an interesting research project, and supported its development at any time.

I thank all the professors of the Graduietenkilleg GRK 760 Research Training Group and in particular Prof. Dr. Sigurd Elz for the collaboration, Prof. Dr. Armin Buschauer and Prof. Dr. Oliver Reiser for supporting my research work.

I am thankful to Dr. Alessandro Pedretti and Dr. Giulio Vistoli (Universitá degli Studi di Milano), for the continuous actualization of VEGA ZZ and for their precious help with computational techniques.

A special thanks to Prof. Dr. Masaji Ishiguro (Niigata University of Pharmacy and Applied Life Sciences), who provided me the coordinates files of the rhodopsin photointermediates models.

I am grateful to my PhD colleagues and in particular to Dr. Hendrik Preuß, for the scientific discussions, his constant support, and for the nice time spent in the “lab”.

For the financial support, I am grateful to the Deutsche Forschungsgemeinschaft (DFG) and to the DAAD (international Quality Network Medicinal Chemistry).

I would like also to thank all the people who had an important role in my life in Regensburg:

Gerhard, for his friendship, his constant presence, for the nice evenings spent learning Italian and German, watching movies and drinking a lot a beer; Christian for his sympathy and the nice time spent in our flat.; Edith, Ralf, Stefan, Hendrik, Martin, Anja for the crazy party and the great beer weekend; all the “multikulti” friends and in particular Sebastien for the good and fanny discussions, and Mahesh for the tasty Indian dinners we had together.

At the end I would like to thanks the Italian faction in Regensburg and In Italy:

La Pupona (Noemi) per la sua amicizia, per avermi aiutata quando era necessario, per le belle serate C&F, e per le grandi risate; Lo zio Franz (Francesco) per aver avuto sempre una buona parola, per la sua simpatia e per le buone cene italiane; Lo sciupafemmine (Valerio) per le belle chiacchierate durante le nostre pausette, per tutta la musica e i film e per la sua simpatia; Marina e Gianluca per la loro amicizia anche a distanza.

Mio fratello Alessandro per avermi dato il buon esempio e avermi aiutata ad andare avanti.

I miei genitori Rita e Luigi per il loro aiuto incondizionato, per avermi dato anche questa volta una grande possibilitá e avermi fatta diventare grande fino ad arrivare fino a qui.

E soprattutto vorrei ringraziare El mio Amorino (Pancho) per la pazienza, i buoni consigli, l'incoraggiamento ogni volta che ne ho avuto bisogno, per avermi ascoltata e capita con amore, per essere stato presente in ogni momento e per Tutto.